



universität  
wien

# MASTERARBEIT / MASTER'S THESIS

Titel der Masterarbeit / Title of the Master's Thesis

**“Development of a PCR based Method for the  
Differentiation of Vaccinium Species using High  
Resolution Melting (HRM)”**

verfasst von / submitted by

**Alexandra Wanka, BSc**

angestrebter akademischer Grad / in partial fulfilment of the requirements for the degree of  
**Master of Science (MSc)**

Wien, 2019 / Vienna 2019

Studienkennzahl lt. Studienblatt /  
degree programme code as it appears on  
the student record sheet:

A 066 862

Studienrichtung lt. Studienblatt /  
degree programme as it appears on  
the student record sheet:

Masterstudium Chemie UG2002

Betreut von / Supervisor:

Prof. Mag. Dr. Margit Cichna-Markl



## **Acknowledgment**

I want to thank Prof. Mag. Dr. Margit Cichna-Markl for supervising this thesis. .

I also want to thank the working group, namely Katja, Maria, Mariusz, Steffi and especially Doris, Georg and Andi. Their constant support made the time working on my thesis a time I will always fondly remember.

Of course I want to thank my parents who endured my years of studying hardly without questioning which enabled me to follow my own way.

Last but not least I full heartedly want to thank Kerstin Mayerhofer, who accompanied me not only during my studies but also as my partner in life. Without her constant support, both academic and emotional, I would not have been able to make it this far.





## Table of contents

1	Introduction .....	2
1.1	Food fraud and adulteration .....	2
1.2	The <i>Vaccinium</i> genus .....	3
1.2.1	<i>Vaccinium macrocarpon</i> – American cranberry .....	7
1.2.2	<i>Vaccinium oxycoccos</i> – European cranberry .....	8
1.2.3	<i>Vaccinium vitis-idaea</i> – lingonberry .....	9
1.3	DNA barcoding .....	10
1.3.1	MatK .....	11
1.3.2	ITS .....	11
2	Aims .....	14
3	Theoretical part .....	16
3.1	DNA extraction .....	16
3.2	Determination of the DNA concentration using spectrophotometric and fluorometric measurements .....	17
3.3	Polymerase chain reaction .....	19
3.3.1	DNA .....	19
3.3.2	PCR .....	21
3.3.3	Primer design .....	25
3.3.4	Real-time PCR .....	26
3.3.5	High resolution melting analysis .....	29
3.4	Agarose gel electrophoresis .....	31
4	Experimental part .....	34
4.1	Working with DNA .....	34
4.2	Samples .....	34
4.3	DNA extraction with QiAamp®DNA Mini and Blood Mini Kit .....	35
4.3.1	DNA extraction protocol with polyvinylpyrrolidone (PVP) .....	35
4.4	Determination of DNA concentration and purity .....	36
4.4.1	Spectrophotometric measurements .....	36
4.4.2	Fluorometric measurements .....	36
4.5	PCR/HRM .....	37
4.5.1	Primer Design .....	38

4.5.2	PCR and HRM .....	40
4.5.3	Optimization of PCR conditions.....	41
4.5.4	Analysis .....	42
4.6	Gel electrophoresis.....	43
4.6.1	Preparation .....	43
4.6.2	Gel analysis .....	43
5	Results and Discussion .....	44
5.1	DNA extraction.....	44
5.2	Spectrophotometric and fluorometric measurements.....	44
5.3	Differentiation of the berry species in the MatK Region .....	44
5.4	Multiplexing approaches and the CP12 barcoding region.....	52
5.5	Differentiation of the Vaccinium species in the ITS regions .....	63
5.6	Optimization and Validation.....	66
5.6.1	Matrices .....	67
5.6.2	Spiking experiments .....	70
5.6.3	Robustness – Testing QuantStudio 5 and MeltDoctor™ chemistry .....	89
5.7	Detection of adulteration.....	91
5.7.1	Herbarium samples and fresh plant samples .....	91
5.7.2	Products labelled as containing lingonberry.....	95
5.7.3	Products labelled as containing European Cranberry .....	97
5.7.4	Products labelled as containing (American) Cranberry .....	99
6	Conclusion.....	110
7	Appendix.....	112
7.1	Abbreviations.....	112
7.2	Abstract.....	113
7.3	Zusammenfassung .....	114
7.4	List of tables.....	116
7.5	List of figures .....	117
7.6	Equipment.....	125
7.6.1	Chemicals and kits.....	125
7.7.2.	Equipment/Instruments.....	125
7.7.3.	Expendables/Consumables.....	126
7.7.4.	Software.....	126

7.7	Sample-list .....	127
7.7.1	Samples.....	127
7.7.2	Concentration and purity of the DNA extracts of the positive controls, herbarium samples, and commercial food samples .....	131
7.7.3	Concentration and purity of the Matrix-components DNA extracts .....	134
7.8	References .....	136



# 1 Introduction

“Let food be thy medicine and medicine be thy food.”

— Hippocrates

Food plays an essential role in the life of every human being, every animal, and plant. It provides nutrients and energy sustaining growth and maintenance. In an economy that grows more and more conscious about how and most importantly what people eat catchphrases like “healthy lifestyle” and “superfoods” gain attention. And berries, with their highly favoured ingredients like anthocyanins and polyphenols are an easy solution for supplementing a well-balanced diet.

As long as the label promises health benefits, most consumers will not take any effort in scrutinizing these claims. Instead, they trust in the validity of the manufacturers’ health claims and the correct labelling of every product they consume. These habits are justified as manufacturers are forced by law to do so.

This is where the need for analytical methods dealing with this complex variety of problems becomes apparent. An approach, that closes the gap between raising customer demands and awareness on the one hand and the need to verify the correct implementation of legal regulations for labelling on the other hand, are DNA based methods.

## 1.1 Food fraud and adulteration

As food is that essential, many aspects of food production and more importantly food safety are embedded in national law and European law as well. Nevertheless, food fraud is far from being a symptom of modern times. Even in ancient Rome and Athens, there were laws regulating and prohibiting the adulteration of wine with colours and flavours [1]. Germany and France passed statutes concerning food control in the thirteenth century while in England legislation regarding adulteration of human food was passed by Henry III. (1207-1272). [2]

Current legislation in Europe also deals with potential fraud and the need for clear declaration and authenticity. The Austrian Lebensmittelsicherheits- und Verbraucherschutzgesetz (LMSVG) clearly regulates that it is prohibited to put foodstuff into circulation that

- is harmful to health and therefore not safe for human consumption or
- is adulterated or lowered in value without this circumstance being clearly and generally comprehensible [3]

This law, that became effective in 2006, aims to protect consumers and customers not only from the intake of unsafe food. It also strictly prevents any tempering concerning marketing and promoting food containing misleading information. This aspect of food safety gains more and more momentum. Especially on the field of premium foodstuff, customers demand clear and proper labelling.

In recent years many scandals linked to food fraud and adulteration were reported in the media. In 1985 the “anti-freeze scandal” occurred, when wine was adulterated with ethylene glycol. This substance is used as an ingredient of e.g. anti-freeze [4] and was used to make the wine taste sweeter [5]. The ethylene was added to wines by a small number of Austrian winemakers, for the purpose of personal financial gain [6]. In 2008 the Chinese milk scandal caused a somewhat *éclat* as Chinese milk manufacturers added melamine to their products in order to feign a higher protein content [7,8]. Apart from that being blunt fraud it also posed a major health risk and forced authorities to react [7,9–11]. But in Europe too, there were food scandals in their own right like the 2013 horsemeat scandal. This didn’t affect public health but not everyone is fine with eating horsemeat when the label says it is beef [12–14]. This scandal caused uproar throughout Europe. The quality of raw material, whether it be plant or animal based, is central to food production [15] because of the nutritional value and taste [16,17]. Edible plants are a necessity in human diet, so a lot of scientific effort is directed in food safety of plants, especially traceability, and taxonomic studies [18–22].

## 1.2 The *Vaccinium* genus

Three members of the *Vaccinium* genus that produce red coloured fruit, are *V. macrocarpon*, the American cranberry, *V. oxycoccos*, the European cranberry, and *V. vitis-idaea*, the lingonberry. Many species of the *Vaccinium* genus are integrated in the human diet. As food supply chains have become global the risks have emerged [23]. One of these risks being economically motivated adulteration (EMA) [24]. Cheaper fruits, or imitations of more exclusive fruits used in products is relatively recent [25,26], but common [27–29].

*Vaccinium macrocarpon* can be an adulterant itself, namely in *Punica granatum* (pomegranate) juices [30] and, together with *Vaccinium vitis-idaea*, in *Vaccinium myrtillus* (bilberry) products [31].

The *Vaccinium* genus of the *Ericaceae* family is widespread with more than 450 species [32]. It is fairly common in Europe and North America, and was first described by Carl Linnaeus in the eighteenth century. The name *Vaccinium* derives from Latin and was originally used for bilberry.<sup>1</sup>

---

<sup>1</sup> However it is not the same root as *vaccinum*, meaning regarding cows [33]

Table 1-1 gives an overview of the location of the *Vaccinium* genus amidst the tree of life.

**Table 1-1:** Scientific classification of the *Vaccinium* genus

Scientific classification		The <i>Vaccinium</i> genus consists of many species (such as blueberries, lingonberries, bilberries and cranberries) and, as a large genus, is taxonomically complex. The evolutionary relationships within the genus have been debated intensively [34]. Many of these species are consumed for their phytonutrients, especially potent antioxidants. Most of these plants are perennial shrubs, producing richly coloured berries that have been gathered from the wild by indigenous people wherever they could be found [35].
Kingdom:	Plantae	
Clade:	Angiosperms	
Clade:	Eudicots	
Clade:	Asterids	
Order:	Ericales	
Family:	Ericaceae	
Tribe:	Vaccinieae	
Genus:	<i>Vaccinium</i>	

berries that have been gathered from the wild by indigenous people wherever they could be found [35].

The *Vaccinium* species investigated in the course of this research were

- *V. macrocarpon* (VM) or American cranberry
- *V. oxycoccos* (VO) or European cranberry and
- *V. vitis-idaea* (VV) or lingonberry

Regarding the colour of the fruit, the leaves and the habit all three species look somewhat alike as can be seen in Figure 1-1.



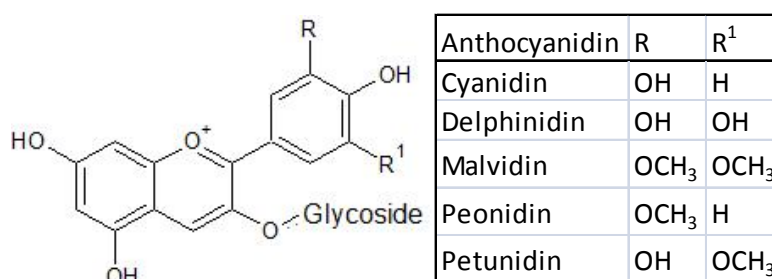
**Figure 1-1:** Comparison of the fruits of *V. macrocarpon* (left), *V. oxycoccos* (middle), and *V. vitis-idaea* (right) [36–38]

Whereas the binomial nomenclature usually used in scientific/botanical context is very clear and straight forward the trivial names of these species can lead to confusion (see Table 1-2).

**Table 1-2:** Summary of the three *Vaccinium* species and their English and German synonyms

Binomial nomenclature	English	German
<i>Vaccinium macrocarpon</i>	American cranberry, large cranberry, bearberry	großfrüchtige Moosbeere, Kranbeere, Kraanbeere, Cranberry, Kulturpreiselbeere
<i>Vaccinium oxycoccos</i>	small cranberry, European cranberry, bog cranberry, swamp cranberry, cranberry*	gewöhnliche Moosbeere
<i>Vaccinium vitis-idaea</i>	lingonberry, partridgeberry, cowberry, foxberry	Preiselbeere
*in Britain		

Health promoting and therapeutic properties are attributed to the entire genus and thus being intensely investigated [39]. Especially anthocyanins, that are shown in Figure 1-2, proanthocyanins and flavonols are attributed a positive effect on the human health [40–42]. The anthocyanines concentration in American cranberries ranges from 0.2 to 3.6 mg/g [43,44] with cyanidin and peonidin being the most abundant anthocyanidines [39]<sup>2</sup>. In addition, trace amounts of delphinidin, petunidin, and malvidin have also been found [45]. These phytochemicals are rapidly produced during ripening and are typically found only in peel tissue [46]. Also, the fruits contain high levels of pectin [47,48].

**Figure 1-2:** Structure of anthocyanidines (left) and common anthocyanines found in fruits of the *Vaccinium* genus [49]

In the past, a number of research projects dealt with the genetics and the bioactive compounds of various *Vaccinium* species (see Table 1-3). For instance, Fajardo *et al.* [50] used 12 single sequence repeats (SSR) which were established by Zhu *et al.* [51] to assess the genetic diversity of cranberry cultivars. Mislabelled samples were observed as well as cranberry cultivar subclone variants, but overall a differentiation between well established

<sup>2</sup> Anthocyanines are the sugar containing counterpart of anthocyanidines.



cultivars was possible using different SSR loci. Bassil [52] too, used SSR to assess the genetic diversity of *Vaccinium* species. These studies used DNA barcoding solely for the purpose of genetic and taxonomic studies.

Kylli *et al.* studied *Vaccinium vitis-idaea* and *Vaccinium microcarpon* (although named “European cranberry” in this study) by identifying their respective proanthocyanidins using ultra performance liquid chromatography (UPLC) and liquid chromatography mass spectrometry (LC-MS) with a focus to the antimicrobial and anti-inflammatory effects of the proanthocyanidins [53].

Jungfer *et al.* [54] compared the procyanidin profiles of *V. macrocarpon*, *V. oxycoccos*, and *V. vitis-idaea* with regards to authenticity. Concentrations of selected procyanidins were evaluated using ultrahigh-performance liquid chromatography coupled to a triple-quadrupole mass spectrometer. Although some differences could be shown by means of phytochemical profiling, only the berries of each species were tested. No foodstuff was investigated.

In 2010 Jaakola *et al.* [55] approached the authenticity question using DNA barcoding with subsequent high resolution melting. Berries from different genera (*Ericaceae*, *Crossulariaceae*, and *Rosaceae*) were tested using different DNA barcoding regions (ITS, trnL-F, and rpl36-ps8). Within the ITS region the differentiation between *V. vitis-idaea* and other *Vaccinium* species was possible. But *V. macrocarpon* and *V. oxycoccos* were not investigated in this study. Neither were commercial food products.

**Table 1-3:** Previous research concerning *Vaccinium* species in the context of differentiation

Aim	Method	Reference
Discrimination of American Cranberry Cultivars and Assessment of Clonal Heterogeneity Using Microsatellite Markers	PCR, SSR genotyping	Fajardo <i>et al.</i> 2013 [50]
Novel approaches based on DNA barcoding and high-resolution melting of amplicons for authenticity analyses of berry species	PCR, HRM	Jaakola <i>et al.</i> 2010 [55]
Assessing genetic diversity of wild southeastern North American <i>Vaccinium</i> species using microsatellite markers	SSR marker analysis	Bassil 2017 [52]
Comparing Procyanidins in Selected <i>Vaccinium</i> Species by UHPLC MS2 with Regard to Authenticity and Health Effects	UHPLC-MSMS	Jungfer <i>et al.</i> 2012 [54]
Lingonberry ( <i>Vaccinium vitis-idaea</i> ) and European Cranberry ( <i>Vaccinium microcarpon</i> ) Proanthocyanidins: Isolation, Identification, and Bioactivities	UPLC and LC-MS	Kylli <i>et al.</i> 2011 [53]

Concluding, the examples given show that research has been done regarding the taxonomical relationship between the species of the *Vaccinium* genus. The phytochemicals in different *Vaccinium* species have also been investigated with regards to differentiation and authentication. Up to now, DNA based methods have not yet been evaluated to differentiate between *V. macrocarpon*, *V. oxycoccus*, and *V. vitis-idaea* in raw material and processed foodstuff.

### **1.2.1 *Vaccinium macrocarpon* – American cranberry**

The American cranberry, *Vaccinium macrocarpon* (VM), is native to north-east and north central USA and Canada, at latitudes about 39° in the northern hemisphere [56], where it has been cultivated for commercial use and become a major industry. Cranberries were first cultivated in Massachusetts in the 1800s and the cranberry industry has grown ever since [57]. Nowadays, the cultivation centers around Wisconsin, New Jersey, and Massachusetts, in the US, as well as in British Columbia in Canada [58,59]. As the name “macrocarpon” suggests the American cranberry produces rather large fruit in comparison to other species of the genus. *V. macrocarpon* is a low growing shrub that forms a dense spreading mat. It has large seed as well as large leaves. The genome is diploid [60] with a chromosome number of 12. The American cranberry is most closely related to the diploid form of *V. oxycoccus* (VO) [61]. The fruit, that ripens in a period between late September and November is tart in taste, and has a red skin with white flesh. The inside of the fruit bears four hollow spaces for the seeds. This fact is used for the so called “wet-harvesting” of cranberries as they float on water (see Figure 1-3). As fresh fruit is astringent, most of the harvest is processed into juice and other products [62].



**Figure 1-3:** Wet harvesting Cranberries (left), and a cross section of a cranberry (right) showing the aerated cavities causing the cranberries to float [63,64]

Cranberry fruits have been consumed by humans for centuries [59]. As American cranberries are native to North America they were used in folk medicine by the natives for stomach ailments, liver problems, and blood disorders [65]. Nowadays cranberries are associated with the holidays of Thanksgiving and Christmas, when cranberry sauce is traditionally served in the US. As the health promoting properties of plants gained more and more popularity, the consumption of cranberry products increased. In addition, cranberries are highly prized for their medicinal and nutritional attributes [66]. Especially phytochemicals with antioxidant effects are the subject of diverse studies. A variety of health claims was investigated or has been investigated:

- American cranberries may benefit oral health [67–69]
- evidence of cardioprotection by *Vaccinium* fruit [70,71]
- indication of cancer chemoprevention [39,72]
- support of urinary tract health [73,74]

However, the European Food Safety Authority (EFSA) could not conclude, that a cause and effect relationship could be established considering the claim of prevention of urinary tract infections upon consuming cranberry and lingonberry products [75,76]. The claim that the consumption of cranberries and products thereof has a positive effect on the “heart health” and that cranberries act as “protectors of our gums” the EFSA deems non-specific [77].

### **1.2.2 *Vaccinium oxycoccos* – European cranberry**

Like other *Vaccinium* species the European cranberry is an evergreen woody shrub, albeit smaller in habit with leathery dark leaves (see Figure 1-4). The species name „oxycoccos“ derives from the sour taste of the fruit produced [78]. This *Vaccinium* species is highly adapted for cold weather [60]. The species mainly consists of hexaploid and tetraploid populations but there are some pentaploid populations in Sweden and the Czech Republic. The less common diploid varieties are usually treated as a different species, *V. macrocarpon*, respectively [79,80].



**Figure 1-4:** Comparison between the leaves of VM (left) and VO (right) showing the different size and shape [81].

However, their natural habitat lies often within national parks, and since the berries are small (smaller than *V. macrocarpon* fruit) and the fruit is sparse, it is economically uninteresting to harvest them commercially [56].

In the United States products derived from *Vaccinium oxycoccos* (European cranberry) can legally be labelled as cranberry [82].

### 1.2.3 *Vaccinium vitis-idaea* – lingonberry

The lingonberry, *V. vitis-idaea* (VV), is named after the Swedish *lingon* deriving from the Norse term for heather. The specific part of the binominal name *vitis-idaea* originates from the Latin “vitis” meaning vine and “idaeus” meaning from Mount Ida. Like the other species of the *Vaccinium* genus the lingonberry forms dense clonal colonies of evergreen shrub with leaves that are oval with a wavy margin [83]. The diploid plants ( $2n=24$ ) have a resistance to bacterial fruit rot [60] and there is the theory, that lingonberries are sort of a cranberry-blueberry intermediate [84]. This species is widespread in the north of Europe and north Russia but also thrives in northern Italy, the Caucasus, and the Balkans [60]. *Vaccinium vitis-idaea* tolerates temperatures up to  $-40^{\circ}\text{C}$  and prefers acidic soils [85]. In Europe as well as in northern America lingonberry is commercially harvested and turned into juices, jam and wines as well as consumed as raw fruit for its finer flavour than American cranberries.

Especially in Europe there is a long history of using lingonberries for their medicinal and health promoting properties such as in the treatment of rheumatism or wounds [60]. Recently also the antioxidant components of the phytochemicals produced are the subject of studies investigating their role in cancer treatment [86].

### 1.3 DNA barcoding

DNA barcoding in general refers to a method using orthologous genetic markers to identify and assign organisms to a particular species. Orthologous in this context means that genes have been separated by a genetic event creating a new species while usually retaining the same function. In terms of taxonomy DNA barcoding is primarily used to assign unknown samples to a pre-existing classification [87]. DNA barcoding is a useful tool capable of answering more than one question. The “Barcode of Life Initiative”, launched by an international consortium, tried to summarize the applications of DNA barcoding as follows:

- (i) enabling species identification, including any life stage or fragment
- (ii) facilitating species discoveries based on cluster analyses of gene sequences
- (iii) promoting development of handheld DNA sequencing technology that can be applied in the field for biodiversity inventories and
- (iv) providing insight into the diversity of life. [88]

The challenging part of DNA barcoding is finding the suitable locus. A prerequisite for each barcoding locus is a variable sequence that differs from species to species – or even from cultivar to cultivar – encased by conserved regions. The purpose of finding conserved regions is to design universal primers to bind in these regions. The variable parts are the key point in terms of differentiating and identifying species.

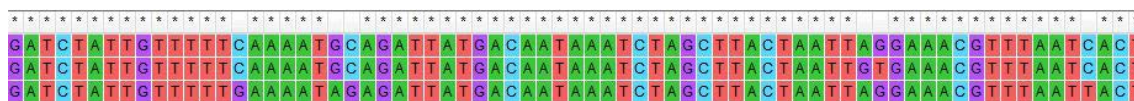


**Figure 1-5:** Alignment of a DNA section of *V. macrocarpon* (U61316.2) above, *V. oxycoccus* (LC168883.1) in the middle, and *V. vitis idaea* (AF382819.1) below. Conserved loci are denoted with an asterisk.

Figure 1-5 shows an alignment of a segment of the *matK* region for VM, VO and VV. Each asterisk in the first row depicts a congruence concerning the DNA sequence. These sections are conserved. Within these sections there are some bases that differ in between species –

identified by the absence of the asterisk. These subtle differences in the genome are used to analyse and distinguish different species.

Nowadays a variety of barcoding regions is used, depending on the analytical problem. For animals and other eukaryotes the mitochondrial gene COX1 (Cytochrome oxidase I) is commonly used as a barcoding region [89]. In plants, four primary barcodes are used:

- (i) rbcL (Ribulose-1,5-bisphosphate carboxylase/oxygenase),
- (ii) MatK (Maturase K),
- (iii) trnH-psbA, and
- (iv) ITS1 and ITS2 (Internal transcribed spacer) [90]

MatK and both ITS regions being the ones investigated within this research. In addition, the chloroplastic region CP12, coding for the Calvin cycle protein 12, was taken into consideration for suitable barcodes, too.

After finding a suitable locus, PCR is performed and the PCR product is analysed by e.g. sequencing or high resolution melting analysis.

### 1.3.1 *MatK*

MatK (maturase K) is a plant gene located in the plastid and encoding for an intron maturase, which is a protein involved in splicing introns thus maturing a protein to its bioactive form [91,92]. The MatK region has been frequently used in e.g. plant phylogenetic analysis due to its small size and highly conserved flanks [11] (see Figure 1-6).

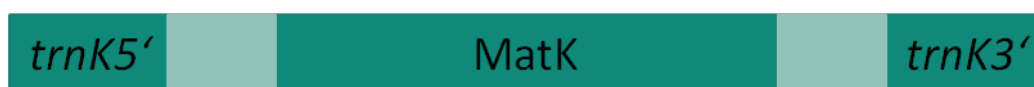


**Figure 1-6:** Scheme of the MatK region and its surroundings, adapted from [93]

However, a major drawback using the MatK region is the low amplification rate [94].

### 1.3.2 *ITS*

Other interesting and widely used barcoding regions are the ITS (internal transcribed spacer) regions. An internal transcribed spacer is a sequence in-between the genes coding for ribosomal RNA (rRNA). This particular RNA is the main constituent (about 60%) of the ribosome with the other 40% being protein. Ribosomes are essential for the biosynthesis of proteins; they consist of a small and a large subunit each.

In this context a spacer is a DNA sequence that is in the first step transcribed correctly but then cleaved. The benefit of using ITS as a barcoding region is the fact that it frequently mutates. Additionally, there are multiple copies per genome making it less prone to false negative results [95]. A schematic representation of the ribosomes and the rRNA can be seen in Figure 1-7.

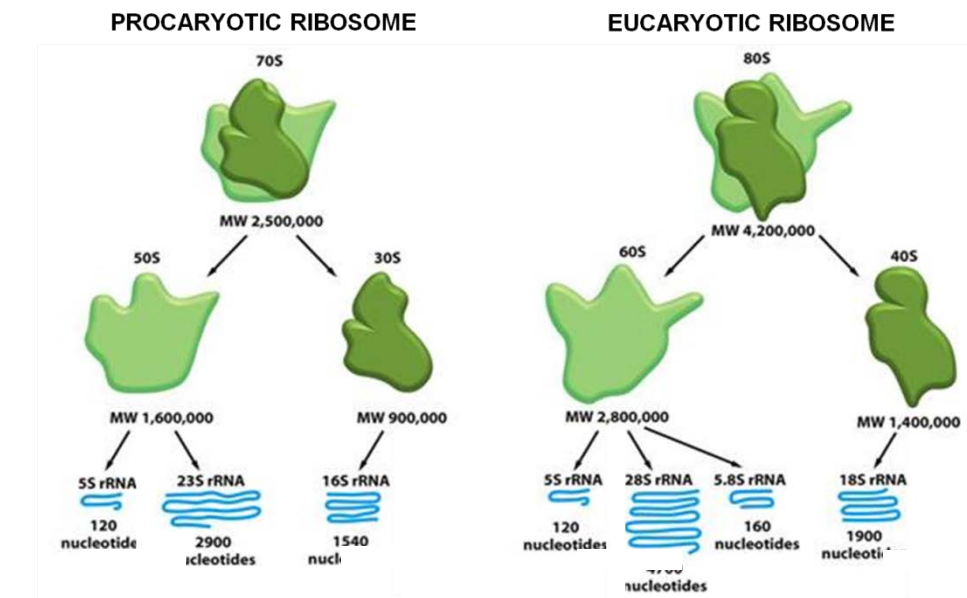


**Figure 1-7:** Prokaryotic and eukaryotic ribosomes in comparison, and the subunits they are comprised of, modified from [96]

In phylogenetics, rRNA sequences are used for working out evolutionary relationships among organisms because they are of ancient origin. As mentioned above and also can be seen in Figure 1-7 prokaryotic and eukaryotic ribosomes consist of different subunits. In eukaryotes the small subunit is the 18S rRNA whereas the large subunit contains 3 different rRNA species. In mammals, these are the 5S, 5.8S, and 28S rRNA, and in plants the 25S rRNA. The denomination “S” stands for Svedberg unit and reflects the size of the respective rRNA and its sedimentation rate. The 28S/25S, 18S and 5.8S rRNAs are all encoded by a single transcription unit and separated by two internal transcribed spacers (ITS).



**Figure 1-8:** Scheme of the arrangement of the ITS region, modified from [97]

Figure 1-8 shows the position of the ITS regions within the rRNA genes for eukaryotes. Within the scope of this research both ITS regions were investigated, but none of the external transcribed spacer (ETS) regions.



## 2 Aims

As a healthy and aware lifestyle becomes more and more important, so do the quality and the ingredients of the products consumed. Berries of the *Vaccinium* genus, namely *Vaccinium macrocarpon* (American cranberry), *Vaccinium oxycoccos* (European cranberry), and *Vaccinium vitis-idaea* (lingonberry) are a part of a healthy diet and lifestyle. This trend certainly tempts producers to replace the highly sought-after berries with cheaper or easier to come by alternatives or bluntly substituting one berry species with another. Prior research partly used polyphenol profiling in order to investigate food fraud, but DNA based methods like DNA barcoding were used, too. Especially PCR with subsequent HRM DNA barcoding previously showed to be not only capable of detecting food fraud, but also allows for the differentiation between different species.

The aim of this research was the development of a DNA barcoding based method to differentiate between three *Vaccinium* species, *V. macrocarpon* (American cranberry), *V. oxycoccos* (European cranberry), and *V. vitis-idaea* (lingonberry), reflecting the regulations and instructions of the LMSVG, as it demands correct labelling. The first goal was to find appropriate DNA barcoding regions and to design primer sets that are capable of differentiating between the three *Vaccinium* species. The DNA barcoding regions investigated were MatK, CP12, and both ITS regions. For each primer set the PCR conditions were optimized. The selectivity was analysed by looking into cross reactions with other commonly used food ingredients. Additionally, the limit of detection (LOD) was investigated using binary mixtures.

Another goal was to examine the application of the developed method to commercially available products. Prior to testing, DNA had to be extracted in sufficient amount and quality from highly processed foodstuff including supplements, jams, juices, dairy products, chocolates, and tea.



### **3 Theoretical part**

#### **3.1 DNA extraction**

When working with DNA there is a certain need to purify the sample prior to subjecting it to further experiments. Plants contain a high level of polyphenolic compounds and polysaccharides [98]. These compounds have been identified as polymerase chain reaction inhibitors, thus depletion thereof is mandatory [99–102]. A commonly used method is solid phase extraction (SPE). SPE is a technique for sample preparation that uses the physical and chemical properties to separate the compounds of a sample and can be used to isolate and purify the analytes of interest [103,104]. The main driving force of the separation is – much like in chromatography – the different affinities of certain compounds between the solid phase and the dissolved or suspended sample. There are many types of commercial kits available, mostly highly specialised for a small range of applications. In course of this work the QIAamp® DNA Mini and Blood Mini Kit was used. A solid phase extraction protocol usually consists of the same steps: after the preparation of the sample the DNA is bound to the solid phase of the SPE cartridge subsequently washed and finally eluted (see Figure 3-1). In the first step the DNA adsorbs selectively to the SPE material (silica) in the presence of high concentrations of chaotropic salts provided by the buffer. These salts disrupt the hydrogen-bonds thus making the denatured DNA more stable than its native structured counterpart [105,106]. With the DNA bound to the silica, unbound and interfering impurities can be washed out using the wash solutions. In the last step alkaline conditions and a low salt concentration facilitate an efficient elution from the SPE material [107]<sup>3</sup>.

---

<sup>3</sup> The binding buffer and the wash solutions are part of the commercial kit. Therefore one does not know exactly all the constituents and their concentrations, as this is a company's secret.

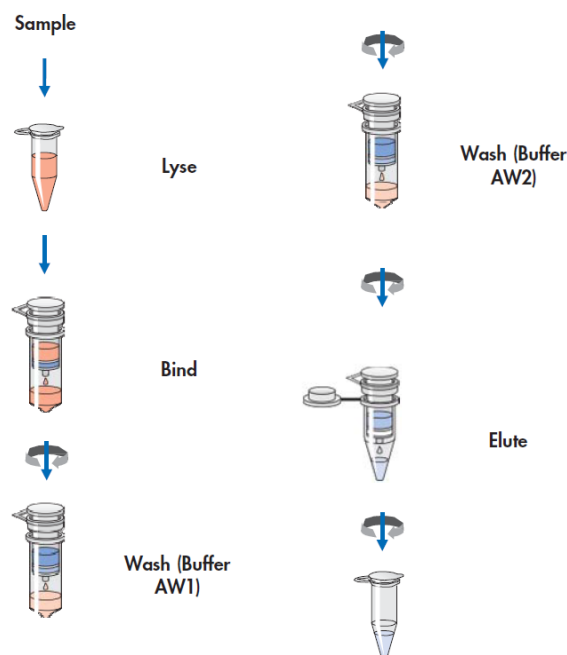


**Figure 3-1:** The steps to purify DNA via a commercial kit [108]

Although these commercial kits are designed for a specific application, they too are subject to optimization when facing a specific analytical problem. During this research polyvinylpyrrolidone (PVP) was added during sample preparation (see Figure 3-2), as it has been shown to improve DNA extract quality [109,110].

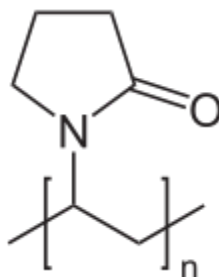


**Figure 3-2:** Structure of polyvinylpyrrolidone, a polymer made from the monomer N-vinylpyrrolidone

PVP binds to and therefore eliminates undesirable sample components like polyphenols which occur in high quantities in plants and influence subsequent analysis with regard to photometric measurement of DNA concentration [111,112].

### 3.2 Determination of the DNA concentration using spectrophotometric and fluorometric measurements

After the purification of a DNA extract and prior to subjecting it to further experiments there is a need to measure the concentration of each DNA extract. A commonly used cheap and quick method is spectrophotometric measurement. In this study the Thermo Scientific™

NanoDrop™ 2000c was used. Spectrophotometric methods are based on the Beer-Lambert law that links the light penetrating a sample to the light transmitted.

$$E_{\lambda} = \log_{10} \left( \frac{I_0}{I_1} \right) = \epsilon_{\lambda} * c * d$$

The Beer-Lambert law is given above with  $E_{\lambda}$  being the absorbance,  $I_0$  the intensity of the incident light [ $\text{Wm}^{-2}$ ],  $I_1$  the intensity of the light transmitted [ $\text{Wm}^{-2}$ ],  $\epsilon_{\lambda}$  the absorption coefficient [ $\text{m}^2\text{mol}^{-1}$ ],  $d$  path length of the beam of light through the material sample [m], and  $c$  the concentration [ $\text{molm}^{-3}$ ].

When working with DNA extraction kits the volume of the extracted DNA is usually quite low so the NanoDrop™ was designed to account for that as only 0.5 to 2  $\mu\text{L}$  of sample per measurement is sufficient. It measures at a variable wavelength ranging from 220 to 350 nm. With DNA having its maximum absorbance at 260 nm the NanoDrop™ measurement not only calculates the DNA concentration of a given sample but gives information about the purity of the sample, too. When scanning a broader range than only the vicinity of the DNA absorption maximum, proteins (with a maximum at 280 nm) and polyphenols and carbohydrate carryover (with a maximum of 230 nm) are detected as well (see Figure 3-3). Thus, based on the absorbance at 230, 260, and 280 nm, two ratios are given by the software to determine sample purity: the A260/230 ratio and the A260/280 ratio. Ideally those ratios range between 1.8 and 2.2 to indicate purity. The dynamic range of the NanoDrop™ is from 2ng/ $\mu\text{L}$ -15,000ng/ $\mu\text{L}$  with a limiting amount of sample at the pedestal of 2ng/ $\mu\text{L}$ , both for double stranded DNA.

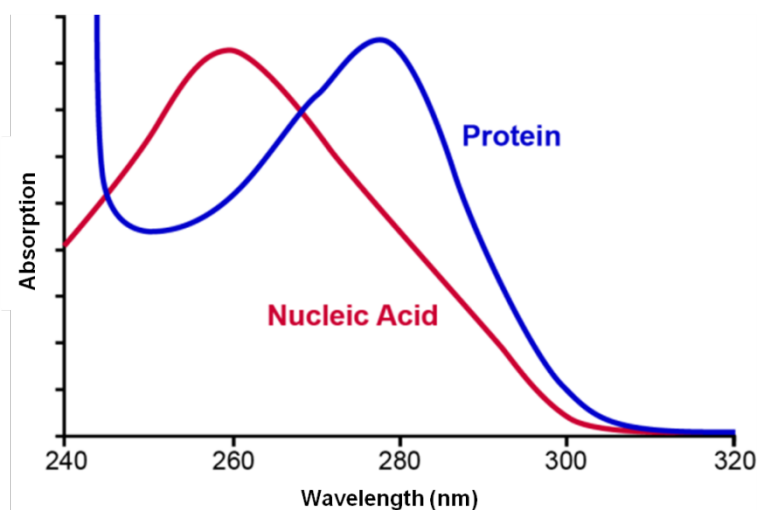


**Figure 3-3:** Depiction of an ideal result obtained by spectrophotometric measurement with an absorption maximum at 260 nm for DNA and an absorption maximum at 280 nm for proteins, modified from [113]

A current other method to determine the DNA concentration with high specificity, is to make use of albeit more expensive and complex fluorometric measurement. In this study the Qubit 2 and Qubit 3 were used. Whereas the NanoDrop<sup>TM</sup> measures the absorbance non-specifically as explained above, the Qubit system works with distinct fluorescent dyes for DNA, RNA or protein. These dyes exhibit extremely low fluorescence when not bound but emit a strong fluorescent signal upon binding to their respective targets. Based on two calibration standards provided by the kit manufacture the Qubit software calculates the concentration of the sample. The high sensitivity DNA kit for ds DNA has a quantitation range from 0.2-100ng.

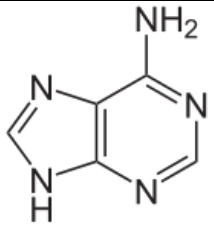
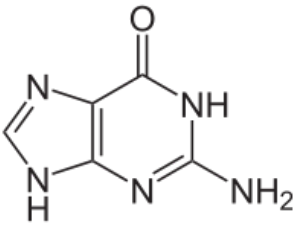
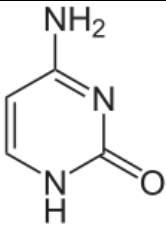
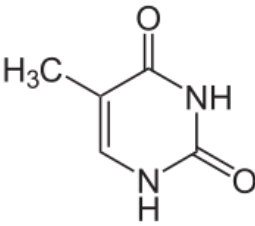
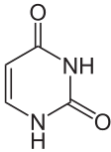
### **3.3 Polymerase chain reaction**

As the DNA sequence is unique for each species, it is gaining more and more impact as analytical target. One method used is the polymerase chain reaction (PCR), because it allows for quick (almost) exponential amplification of DNA [114–116]. To explain the principle of PCR in detail, a brief summary on DNA and its molecular structure is given first.

#### **3.3.1 DNA**

DNA consists of two strands of nucleotides with each nucleotide in turn consisting of a nucleobase, a pentose-sugar and one phosphate group. There are four bases that can be found in DNA (a fifth base is part of RNA, ribonucleic acid). The bases can be grouped into purine bases (adenine and guanine) and pyrimidine bases (cytosine and thymine, and uracil for RNA), as can be seen in Table 3-1.

**Table 3-1:** Overview over the structure of the nucleobases

purine bases	pyrimidine bases
 adenine (A)  guanine (G)	 cytosine (C)  thymine (T)  uracil (U)

Each base within the DNA superstructure is connected to the five-carbon sugar deoxyribose via a beta-glycosidic linkage. These glycosylamines, called nucleosides, are adenosine, guanosine, thymidine and cytidine. If the pentose is connected to at least one phosphate group, the resulting moiety is called nucleotide. These nucleotides play a crucial role in metabolism as the phosphate bond is used to store energy within e.g. a metabolic pathway. To form single stranded DNA (ssDNA) each nucleotide is linked to its neighbouring nucleotide via phosphodiester bonds between the third (3') and fifth (5') carbon atoms of the pentose sugar, resulting in a so called 5' end of the DNA strand with a free phosphate group and a 3' end with a free hydroxyl group.

DNA's most interesting property is the formation of double strands that is achieved due to base pairing. There are two types of base pairs: adenine (A) and thymine (T), and cytosine (C) and guanine (G). A and T share two hydrogen bonds while there are three between C and G, as can be seen in Figure 3-4. Hydrogen bonds are not covalent which means they are comparatively easy to break (e.g. by a rise in temperature) without altering the covalent backbone structure. The higher the GC-content of the DNA fragment, the higher is the temperature required to separate the two strands. This fact is used to prove the identity of DNA strands by recording high resolution melting curves (see chapter 4.5).

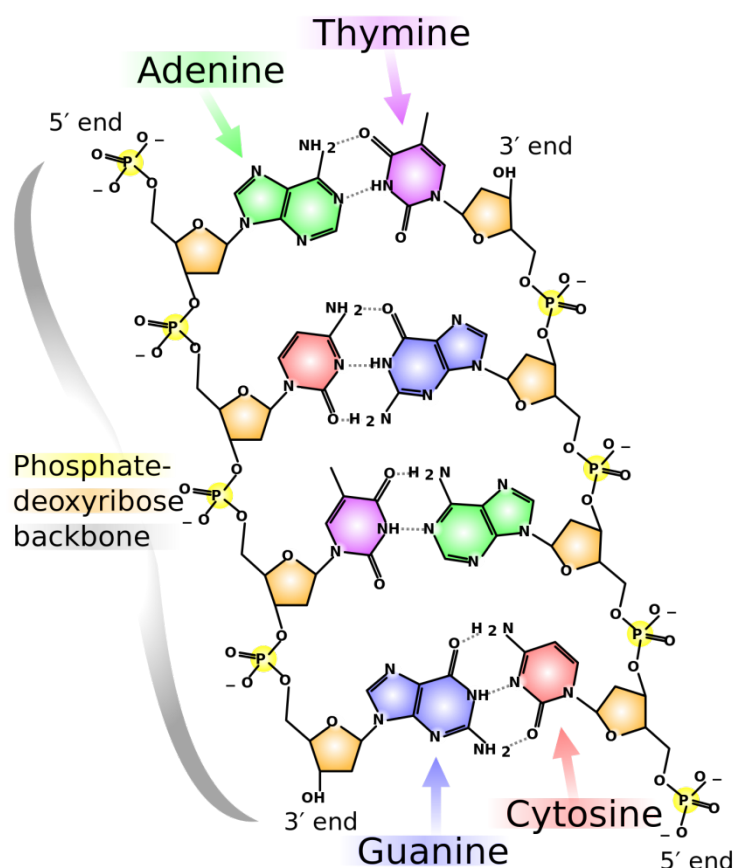


**Figure 3-4:** DNA structure and binding structures [117].

The very specific base pairing leads to two complementary strands, thus forming a double helix with the two strands running in opposite directions (antiparallel). This complex structure was first described by James Watson and Francis Crick with the help of x-ray fraction data obtained by Rosalind Franklin. This double helix, that is most commonly right-handed in nature, has around 10 basepairs (bp) per turn. The basepairs with their hydrogen bonds form planar structures just like the steps of a ladder while the phosphate and sugar backbone is directed outwards. In addition to the hydrogen bonds, pi-stacking between neighbouring bases contributes to the stability of the structure [118,119].

### 3.3.2 PCR

Polymerase chain reaction was developed in 1983 by Kary Mullis, who received a Nobel Prize for his work ten years later [120]. The goal of PCR is to amplify specific DNA regions of interest in order to obtain sufficient amounts thereof for further analysis. At first, high temperatures melt dsDNA into two strands, acting as template. An enzyme is used to build complementary strands to each of these single stranded templates thus resulting in a



doubling of DNA. So basically PCR is used to (almost exponentially) amplify a target region of DNA. PCR is usually performed in a 3 step way. These steps are

- 1) denaturation
- 2) annealing, and
- 3) elongation

as is shown in Figure 3-5.

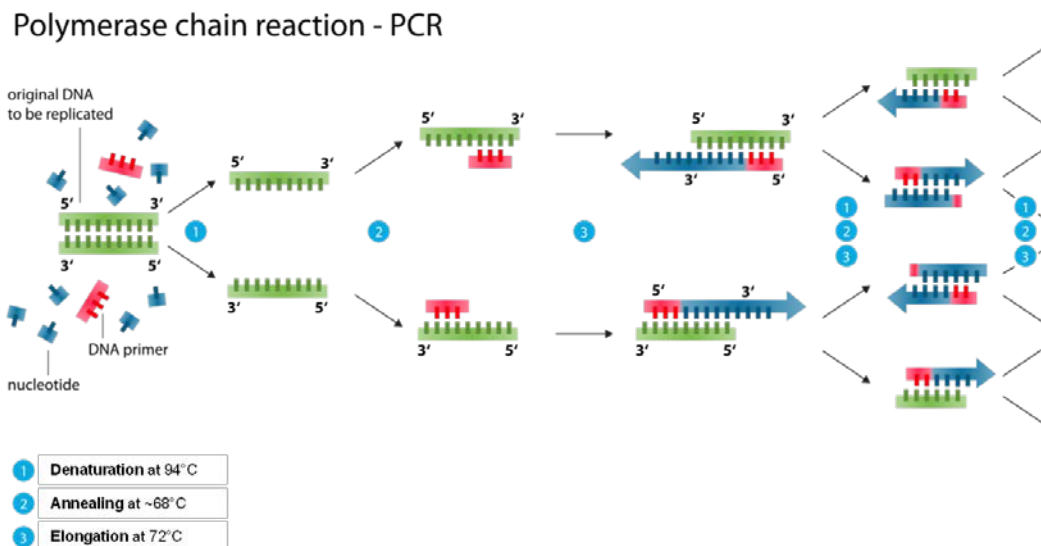


**Figure 3-5:** Scheme of a PCR cycle, modified from [121]

As a dsDNA template is used it has to be converted into ssDNA first by heating up the sample. The melting temperature of a specific DNA sequence ( $T_m$ ) is the temperature where exactly half of the template is single stranded [122]. In order to melt the whole template protocols usually use around 95°C to effectively convert all the dsDNA into single strands. This stage lasts for 20-30 seconds. Subsequently, the temperature is dropped allowing for primers – single stranded DNA sequences especially designed for each experiment (see chapter 3.3.3) – to anneal, meaning to form a short double stranded sequence. The temperature used in this step is subject to optimization as it is dependent on the primer sequence. In fact, there are two primers for each target region; often differing in the annealing temperature, thus finding the optimal temperature is challenging. But this is a key step for the procedure as the DNA formation via the polymerase enzyme depends on a free 3' end to begin assembling the complementary strand. The last step is elongation which is performed at the temperature optimum of the polymerase used, commonly at 72°C (when a Taq polymerase is used). This step ensures that the enzyme has enough time to synthesize the complementary strand. The time is dependent on the size of the target region to be amplified. The larger the amplicon the longer the elongation time is set.

These three steps together are called cycle and are repeated 25-50 times. Furthermore, these cycles are encased by two more steps, an initializing step when using a hot-start PCR (see chapter 3.3.2.2) and a final elongation to ensure complete elongation of remaining ssDNA. Lastly the final hold cools the system for an infinite time, serving as a kind of short term storage for the PCR products [119].

The first PCR reactions were done manually using differently tempered water baths and moving the reaction tubes in between them. Nowadays the whole process is highly automated. The equipment used to perform PCR is called a thermal cycler, a benchtop device that cools and heats the samples according to the protocol.

There are basically three types of thermal cyclers available. One type uses a metal block which is heated and cooled electrically. But there are so called Peltier-elements, too. These use the temperature change caused by a current running in one or the opposite direction. A third method is heating and cooling via electromagnetic radiation [123]. Furthermore there is a variety of reaction tubes to be used. One type uses a metal block holding either a reaction plate or individual reaction tubes. On the other hand there are thermal cyclers that use so called strip tubes positioned on a rotor spinning freely with the inside of the rotorspace being heated and cooled. Each of these solutions have their advantages and limitations, however this will not be further discussed.

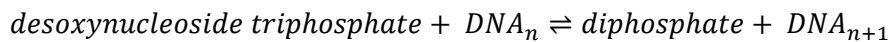
The PCR reaction itself demands for an often called Master Mix which contains all the chemicals needed – with the exception of the DNA to be amplified, the template, and the specific primers. Commercially available Master Mixes already contain the right amount of each ingredient suitable for a specific PCR protocol but everything can be purchased separately leaving room for further experimentation and optimization.

#### *3.3.2.1 Buffer*

Generally, the chemicals in the buffer ensure optimal conditions for the polymerase to work. Especially the magnesium concentration is crucial for the reaction as  $Mg^{2+}$  is a cosubstrate for the enzyme. Furthermore it builds soluble complexes with the nucleotides present in the Master Mix and stabilizes the annealing procedure. Also, there is a direct relation between  $Mg^{2+}$  concentration and the melting temperature of the amplicon as the melting temperature increases with the addition of magnesium.

#### *3.3.2.2 Polymerase*

As the name PCR suggests the enzyme used is a polymerase. A polymerase is an enzyme that synthesizes DNA from deoxyribonucleotides (dNTPs). It adds nucleotides to the 3' end of the DNA strand, thus completing the complementary strand of the template.



A prerequisite for a polymerase used during PCR is a high activity at a temperature between the annealing temperature and the temperature at which the DNA denaturation occurs [124]. One of these polymerases is the *Taq* polymerase which is named after the bacterium *Thermus aquaticus* where it was originally isolated from [125]. *T. aquaticus* is a bacterium living in hydrothermal vents under extreme conditions therefore the polymerase produced by this organism is able to withstand the high temperatures during PCR. The optimum temperature for the *Taq* polymerase is between 75-80°C, but studies showed that for the *Taq* polymerase a single enzyme can synthesize up to 1000 bp in 10 seconds at 72°C with a half-life of 40 minutes at 40°C [125,126] thus allowing to run PCR at higher temperatures than before. This fact helped to reduce the synthesis of nonspecific DNA products such as primer dimers and facilitated a higher specificity of the primers in general [127]. One downside of the *Taq* polymerase is however that it does not have a so called proof reading function like the *Pfu* polymerase derived from the microorganism *Pyrococcus furiosus*. This means that the *Pfu* enzyme not only possesses the desirable 5'-3'-polymerisation activity but also a 5'-3'-exonuclease activity [126]. This means that this enzyme checks after the incorporation of a new base if it is correct and, if it is not, removes this last base again [128] leading to a 3-4 fold lower error rate than the error rate of the *Taq* polymerase [129]. As shown above the ion concentration in the reaction tube is a factor that needs to be taken seriously. Certain salts, such as KCl, and ions like  $\text{Mg}^{2+}$  act as a promoter for the enzymatic activity of the *Taq* polymerase. However the proper  $\text{Mg}^{2+}$  concentration in term depends on the nucleoside triphosphate concentration. Yet high concentrations of the ions mentioned above have the opposite effect and inhibit the *Taq* polymerase activity [130].

To ensure that the polymerase is not active ahead of time causing unspecific amplification, a so called hot start PCR is beneficial. There are two possibilities: either the enzyme is pipetted into the reaction tube after the first denaturation step or a specific antibody is used. This antibody is reversibly bound to the polymerase thus inhibiting its activity. At higher temperatures, like the initializing step at 95°C, the antibody is cleaved off, and the enzyme is activated.

### 3.3.2.3 Nucleotides

In order to synthesize new DNA, the building blocks of DNA have to be available to the polymerase. So all four of the deoxynucleoside triphosphates (dATP, dCTP, dGTP, dTTP)

are required to be in the Master Mix in equimolar concentration usually between 0.1 and 0.3  $\mu\text{M}$  [131].

#### 3.3.2.4 *Templates*

A template can derive from many sources, like genomic DNA, plasmids or even viral DNA. This DNA however contains the target sequence that is to be amplified. When using specific primers only the target sequence gets amplified. The rest of the DNA will not be copied. The size of the amplicon is defined by the two primer binding sites adjacent to template region of interest. A major factor concerning the template is sample preparation to ensure complete removal of compounds that inhibit the PCR.

#### 3.3.2.5 *Primer*

Primers are essential for a PCR. These short ssDNA sequences bind to their complementary parts on the template DNA and allow for the polymerase to start synthesizing. To achieve good result with PCR primers have to be carefully designed.

### 3.3.3 *Primer design*

In order to obtain good results with PCR one must first design primer sets specific for the target region. Each primer set consists of a forward primer that is complementary to the upper (-) strand of the DNA (5' to 3' direction), whereas the reverse primer is complementary to the lower (+) strand. Since the synthesis of DNA is always starting from the 3' end, the 3' ends of both primers point towards each other and thus determine the length of the amplicon. Furthermore, both of the primers have to fulfil certain criteria which are important to consider during the primer design:

- length between 17 and 28 bp
- even G/C to A/T ratio
- melting temperature between 55 and 80°C
- preferably similar melting temperature
- no formation of secondary structures like hairpins especially at the 3' end
- no forming of dimers neither with itself nor with the second primer involved
- preferably no G/C at the 3' end as this facilitates mispriming
- preferably no "unusual" sequence like poly(A) [131]

The software used to design primers in course of this research was the PyroMark Assay Design 2.0 by QIAGEN. This software is able to place primers in selected areas of a DNA sequence that are a preliminary fit to the above mentioned criteria. In addition, certain parameters can be adjusted e.g. the length of the primer or segment of the DNA sequence it

is complementary to. Consecutively, the software calculates potential complementary binding sites within the selected sequence, the probability of the formation of primer dimers, and a rough estimation of the melting temperature of the respective primer. There are many equations dealing with the determination of the melting temperature of short ssDNA sequences as shown below (see Equation 3.3-1 and Equation 3.3-2).

$$T_m = 4 \times (G + C) + 2 \times (A + T)$$

**Equation 3.3-1:** Determination of the melting temperature of a primer with less than 15 bases with G, C, A and T, being the number of the respective bases [132].

$$T_m = 81.5 + 16.6(\log_{10}[J^+]) + 0.4(\%G + C) - \frac{600}{\text{Number of bases}} - 0.63(\%FA)$$

**Equation 3.3-2:** Determination of the melting temperature of a primer with 20-70 bases; with G, C, A and T, being the number of the respective bases, and J = concentration of monovalent cations, FA = formamide [132].

### 3.3.4 Real-time PCR

An enhanced setup in PCR allows for tracking of the amount of DNA formed throughout the entire reaction progress, and is therefore called real-time PCR. Fluorescent dyes such as e.g. SybrGreen are added to the reaction mixture. They are designed to intercalate non-specifically<sup>4</sup> into double stranded, but exclusively into double stranded DNA via binding to the minor groove of the double helix [116]. If these dyes are excited by short wavelength light they emit a fluorescent signal (see Figure 3-6). This is not a continuous process for during one cycle of PCR there is double stranded as well as single stranded DNA present. The fluorescent signal is only emitted, and therefore only detected, during the elongation phase.

---

<sup>4</sup> There are other methods of using real-time PCR e.g. specifically such as fluorescent probes. But as they weren't used in this study, the author refrains from giving more information about these.

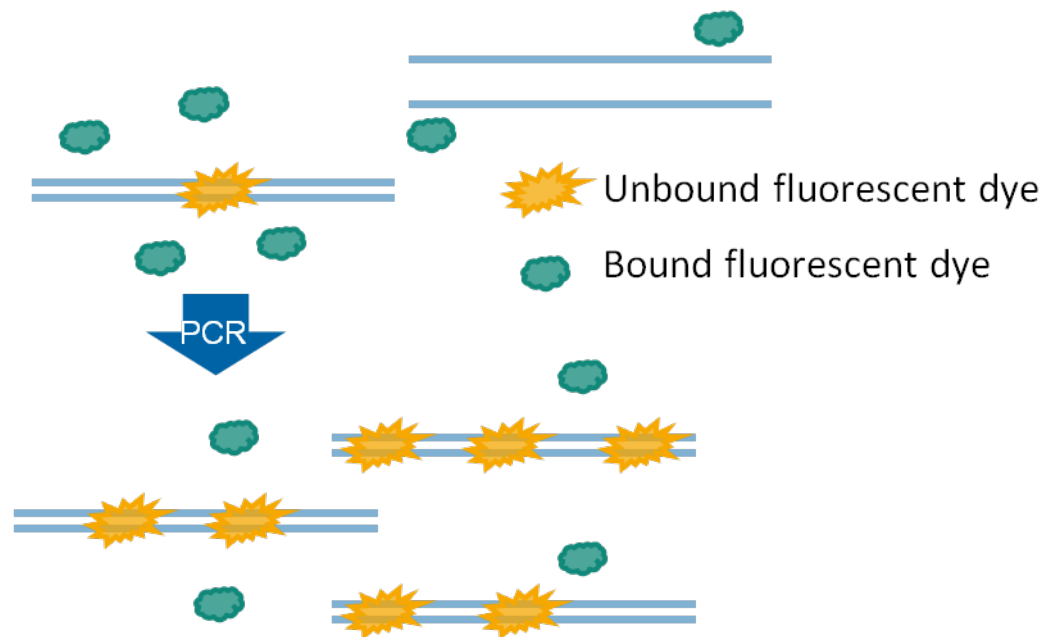


**Figure 3-6:** The mechanism of real-time PCR using fluorescent dye. The dye only binds onto dsDNA and then emits a fluorescent signal (yellow). The more dsDNA is formed during the PCR, the higher the overall fluorescent signal becomes.

As more and more DNA is amplified the signal increases. When looking at the accumulation of DNA during PCR it ideally looks like Figure 3-7.

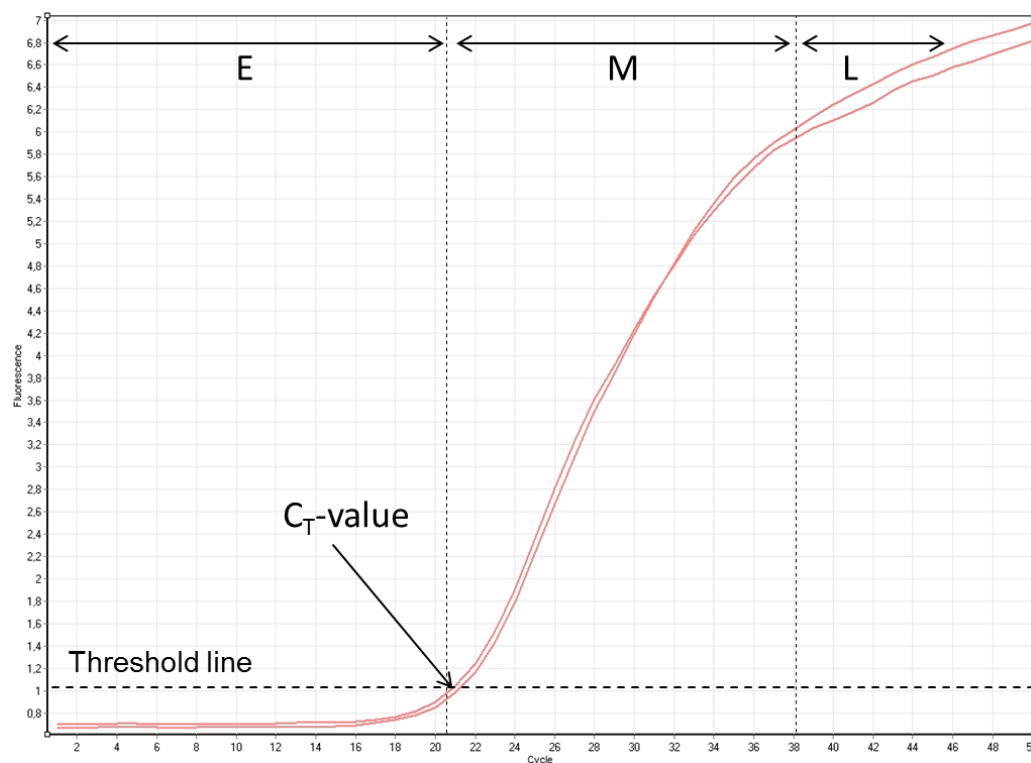


**Figure 3-7:** The kinetics of a PCR reaction. In the early cycles (E), as primers search the few template copies available, amplification is slow. During the mid cycles (M) there is almost exponential amplification until in the late cycles (L) when the reaction plateaus as primers become the limiting factor, modified from [116]

The amplification curve can be divided into three stages. In the early cycles (E), there is not yet much amplification happening. The primers are rather in search of the complementary sequence of their respective template, “effectively acting as a probe” [116] as there are few copies of the DNA template and an excess of both primers. During the mid cycles (M) the amplification phase is progressing. The primers find complementary binding sites much easier now as there are more of them as the reaction proceeds. However after a certain number of cycles the amplification slows down and eventually stops, reaching a so called plateau in the late cycles (L). This happens because at some point primers become the limiting factor, as each cycle consumes more and more primers, elongating them into full copies of the target region. Furthermore the activity of the DNA polymerase decreases over time, thus the reaction and the amplification comes to a halt [116].

When evaluating the amplification curve the threshold cycle ( $C_T$ ) value is used. This value is calculated “by determining the cycle number at which the fluorescence exceeds a threshold

limit” [133]. The  $C_T$ -value is indirectly proportional to the initial DNA template concentration. So the more template is present at the start of the reaction the lower the  $C_T$ -value will be thus indicating the performance of the amplification. To determine the  $C_T$ -value the software calculates the point of interception between the (manually input) threshold line and the amplification curve.

There are currently a number of real-time PCR dyes commercially available like SybrGreen, PicoGreen or EvaGreen. One can basically differ between two types of dyes. SybrGreen for example is a non-saturating dye which means that in course of binding there are still to some extent free binding sites left.<sup>5</sup> This fact becomes a problem when the DNA is melted as a redistribution of the dye molecules can occur which leads to a non-reliable signal (see Figure 3-8).

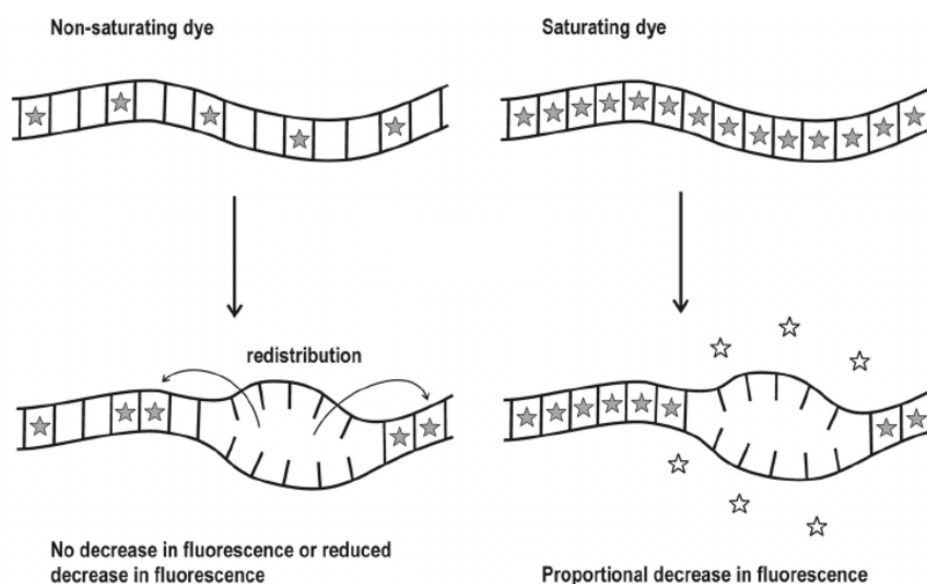


**Figure 3-8:** Differences between non-saturating and saturating PCR dyes during the melting process, modified from [135]

### 3.3.5 High resolution melting analysis

In terms of post-PCR analysis, high resolution melting (HRM) was used. This method of amplicon analysis or rather a prototype thereof was first described by Wittwer *et al.* in 1996 [136]. Not only is HRM applicable to genotyping and mutation analysis, it can be used to solve a variety of problems, because it distinguishes the amplicons by their length and sequence [137,138]. The working group around Carl Wittwer since published various papers dealing with the mechanism of the complex melting process [122,139–141]. The background

<sup>5</sup> When using a higher concentration of a non-saturating dye, the saturation level would rise. But these very high concentration would inhibit the polymerase during PCR [134].



of HRM is to make use of the DNA sequence when the double strand melts into two single strands [142].

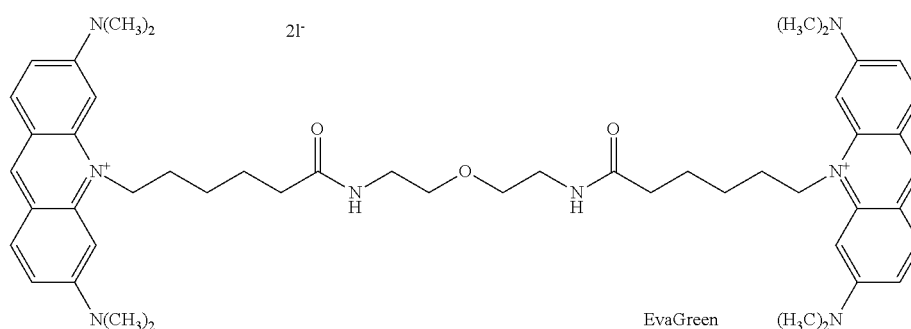


**Figure 3-9:** Structure of the EvaGreen dye. This dye is non-toxic, non-mutagenic, and uses a “release-on-demand” mechanism while binding thus complying not only to the needs of PCR but HRM, too [143].

For HRM saturating dyes like EvaGreen (see Figure 3-9) are used and the decrease in the fluorescent signal, as the double strand melts into two single strands, is monitored. This process is not unlike the denaturation step in PCR, but the melting occurs in smaller, more precise intervals (of 0.017°C/s to 0.3°C/s). This generates raw fluorescence data which is plotted against the temperature and thus transformed into melting curves [139]. Although the melting temperature can be used to characterize the melting curves, there are more precise methods used for analysis (see Figure 3-10).

- Normalized melting curves are obtained after the removal of the background and subsequent fluorescence normalization between 100% (dsDNA) and 0% (dsDNA), which equals 100% ssDNA. When doing so the information about the absolute fluorescence signal's intensity is lost but on the other hand it facilitates comparison between different melting curves [144–146]
- Melting plots are obtained by calculating the first negative derivative of fluorescence with respect to temperature ( $-dF/dT$ ). For symmetrically shaped curves the peak is approximately the melting temperature. The comparison of these melting plots can be used to assign an unknown sample to a reference [140]
- Difference plots are used when the differences between melting plots are small. These plots are obtained by subtracting the normalized reference curve from the sample curve [147]

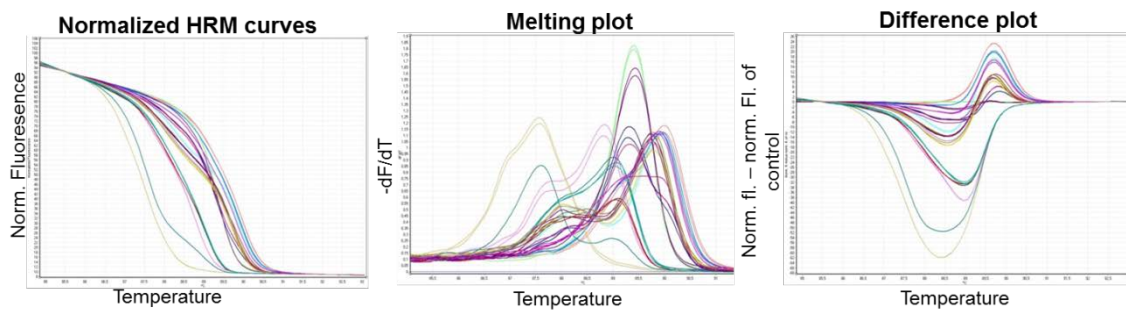


**Figure 3-10:** Overview over different representations of the results of an HRM experiment

The characteristic differences between melt curves derive from the length of the respective amplicon, and the GC content, but also the general sequence of the PCR product formed during the reaction.

### 3.4 Agarose gel electrophoresis

A very simple but effective method to investigate DNA fragments – so this applies to amplicons, too – is agarose gel electrophoresis. The underlying principle of this form of gel electrophoresis is the separation and analysis of macromolecules based on their size. This means that in the process of developing a gel, a current is passed through horizontally. The DNA fragments, because they are negatively charged, therefore migrate in the direction of the anode. The larger the size of the fragments, the slower is the migration and thus the shorter the distance the fragment migrates within a fixed time. So when the first (and smallest) fragments reach the end of the gel, larger ones have not travelled that far, allowing for a separation on the basis of size. By comparing the migration distance to the migration distance of standards containing DNA fragments of known size, the length of the unknown samples can be determined (see Figure 3-11).

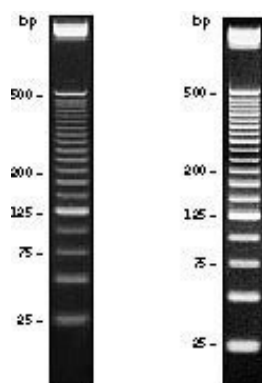


**Figure 3-11:** DNA ladder showing the impact in size on the velocity of migration and leads to the formation of bands [148]

Not only the gel itself needs an auxiliary but the samples have to be processed specifically as well. A so called “loading dye” or “loading buffer” is used to dilute and load the amplicon solution prior to subjecting it to gel electrophoresis.

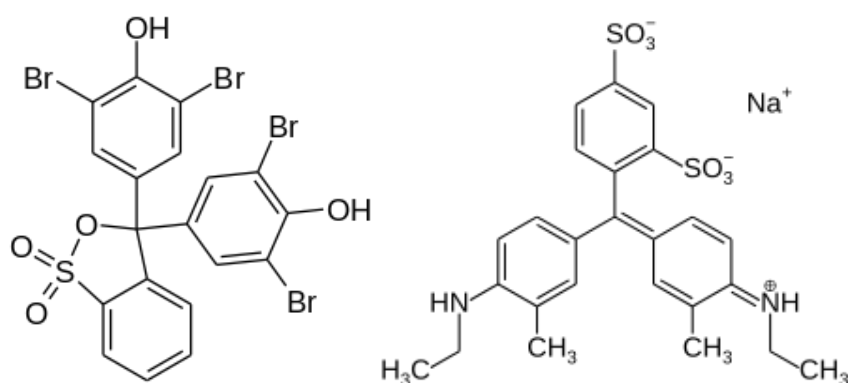


**Figure 3-12:** Bromophenol blue (left) and xylene cyanole FF (right), two dyes used as loading dye.

As the DNA sample migrates through the gel and is separated by size the loading buffer allows to monitor this migration. Both of the dyes seen in Figure 3-12, are used in low concentrations. They are negatively charged and therefore migrate in the same direction as the DNA. Bromophenol blue migrates with the velocity of small DNA fragments whereas xylene cyanole FF rather behaves like bigger DNA fragments due to its many methyl groups and thereof resulting reduced hydrophilic properties [149].

As the name suggests the compound used to obtain a gel is agarose (see Figure 3-13), a polysaccharide which is extracted from a certain type of red seaweed [150].

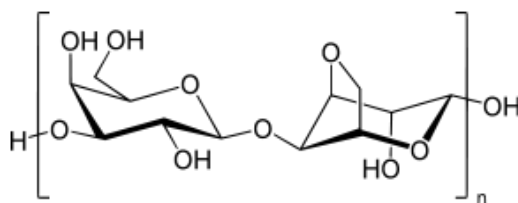


**Figure 3-13:** Structure of agarose, a disaccharide made up of D-galactose and 3,6-anhydro-L-galactopyranose [151].

Agarose as a powder is white and dissolves in hot water and therefore in hot aqueous solutions. Upon cooling a gel is formed. The density of this three dimensional matrix can be controlled via the percentage of agarose used. A buffer is used to dissolve the agarose. A commonly used buffer is TAE (Tris-Acetate-EDTA) [152]. To allow for subsequent analysis of the DNA in course of preparing the gel a staining reagent is added to the buffer-agarose mixture.

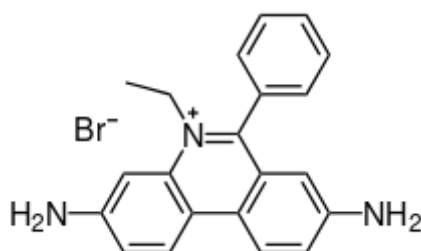


**Figure 3-14:** Structure of ethidium bromide, commonly used in nucleic acid staining. Due to health concerns other, less toxic fluorescent dyes are on the market.

One method of DNA staining is using ethidium bromide (see Figure 3-14). This agent can intercalate into the DNA and – upon excitation with UV light – emits a fluorescent signal thus making the DNA visible. The advantage of ethidium bromide, namely the selective intercalation into DNA, is its major disadvantage as this reagent does not discern between sample DNA and the DNA of the experimenter thus posing a high risk at exposure. Newer, safer dyes are commercially available, like GelRed, which basically consists of two ethidium subunits bridged by a spacer [153].

## 4 Experimental part

### 4.1 Working with DNA

When working with DNA, contamination control is crucial. PCR is a very sensitive method, thus even small amounts of unwanted DNA can have a huge effect on the outcome. So the DNA extraction was done exclusively in one laboratory while pipetting the Master Mix was performed in another one. Even adding the DNA extracts to the Master Mix was done spatially apart in a third laboratory. In the laboratory where the DNA extraction took place, all the surfaces, and mortar and pestle were cleaned with DNA-Exitus Plus™ IF to avoid cross contamination between samples. Separate PCR Workstations were used (VMR Peqlab) to pipette the Master Mix and add the DNA extracts, respectively.

### 4.2 Samples

Commercial samples were obtained at local supermarkets in Austria, Germany and the Czech Republic. For the positive controls plants (*V. macrocarpon*, *V. oxycoccos*, and *V. vitis-idaea*) were obtained at local gardeners and nurseries, some fresh berries and leaves were obtained from our cooperation partners of the Ss. Cyril and Methodius University Skopje, Macedonia. From the Herbarium of the University of Vienna dried and pressed sample specimen were obtained (see Table 4-1). The different commercial food groups were purchased ranging from jams and juices to cereal bars and teas (see Table 4-2). Matrix components for validation were purchased in local supermarkets and nurseries (see chapter 7.7.3).

**Table 4-1:** Herbarium samples and their origin

species	ID	herbarium number	origin	date
<i>V. vitis-idaea</i>	H1	61340	Styria, Austria	01.07.2007
	H2	4823	Styria, Austria	25.10.1997
	H3	4854 (ssp. Minus)	North-Siberian Lowland, Russia	27.07.2004
<i>V. oxycoccos</i>	H4	4883	Styria, Austria	05.07.1987
	H5	4237	Lichtenberg, Austria	04.06.1995
	H6	3114	Mitterbach, Austria	28.11.1921
	H7	5824	Latvia	17.08.2013
<i>V. macrocarpon</i>	H13	4680	Ontario, Canada	12.07.1966
	H14	319	New Jersey, USA	27.06.1948
	H15	249	Londonderry, UK	1977

The DNA of the herbarium samples was extracted during a previous study by Iva Nikolikj using the same protocol with the exception of PVP which was not added. As the amount of samples was limited, we decided to use the extracts even though the extraction protocol deviated slightly.

**Table 4-2:** Summary of the different commercial food groups used

<b>Food groups</b>	
Cereal bar	As for the food groups a variety of foodstuff was obtained with emphasis on variations within the respective group. The group “dried fruit” consists of dried berries mixed with either other berries or nuts.
Chocolate	
Dairy product	
Div	
Dried fruit	The group “Div” includes cranberry sauce, horseradish with lingonberries, mustard, a paste made of European cranberries and a vinegar variation.
Jam	
Juice	
Supplements	
Tea	

The samples ID 3 (*V. macrocarpon*), ID 4 (*V. oxycoccos*), and ID 16 (*V. vitis-idaea*) were used as main references samples throughout the study.

### 4.3 DNA extraction with QiAamp®DNA Mini and Blood Mini Kit

For each commercial sample, a 50 mL tube was taken as a retain sample. From this, a representative sample of about 5 mL was taken and further prepared.

All the liquid samples were considered as homogenous and therefore they were weighed in without further sample preparation. Solid samples were ground to a powder like consistency or a paste with mortar and pestle, depending on the dampness of the product. Inhomogeneous samples like cereal bars and chocolate were sorted in order to accumulate the berry content. E.g. pieces of chocolate containing no berry pieces were not used, as well as cereal bar pieces containing only grains.

Subsequently DNA from all samples was extracted using the QiAamp®DNA Mini and Blood Mini Kit. The manufacturer's protocol was adapted using polyvinylpyrrolidone (PVP), for better results [112]. The protocol used for all DNA extractions is described in chapter 4.3.1.

The main reference samples were extracted three times each (on different days) to provide enough DNA extract for all the experiments.

#### 4.3.1 DNA extraction protocol with polyvinylpyrrolidone (PVP)

At first, 3.6 mg PVP were mixed with 180 µL ATL Buffer and 20 µL proteinase K (600 mAU/mL) were added. This solution was added to 25 mg of the homogenized sample

material (see chapter 4.3) and pulse vortexed for 15 s. Afterwards the mixture was incubated in a thermal block (Thermal Mixer, ThermoFisher Scientific) for 2 h and 15 min at 56°C and 1400 rpm. To remove drops from the inside of the lid, thereafter the tubes were centrifuged and 20 µL ribonuclease A (RNase A; c=20-40 mg/mL) were added. The mixture was pulse vortexed for 15 s and incubated at room temperature for 2 min. After being briefly centrifuged, 200 µL AL Buffer were added and the mixture was incubated at 70°C for 10 min in a thermal mixer. Then, 200 µL absolute Ethanol was added and the mixture was vortexed and centrifuged again. The supernatant and possible precipitate were transferred onto the QIAamp® Mini spin column and centrifuged at 14000 rpm for 1 min.

To purify the DNA, four washing steps were carried out. 500 µL of the Buffer AW1 was loaded on the column and centrifuged 1 min at 14000 rpm. This step was done twice. Then 500 µL of the Buffer AW2 were loaded on the column and centrifuged at 14000 for 3 min. This step too, was done twice. In order to avoid carry over from the washing steps, another centrifugation step at 14000 rpm for 1 min was carried out. As the last step, the QIAamp® Mini spin column was placed on a 1.5 mL Eppendorf tube and 100 µL elution Buffer (AE Buffer) was added. After 5 min incubation at room temperature the DNA was eluted at 8000 rpm for 1 min.

The DNA extracts were then stored at -20°C.

#### **4.4 Determination of DNA concentration and purity**

All samples were subjected to spectrophotometric measurements to determine the purity of the extract and the DNA concentration. In the course of the work we also determined the DNA concentration via fluorometric measurements.

##### **4.4.1 Spectrophotometric measurements**

For all spectrophotometric measurements the NanoDrop™ instrument was used. Before starting the measurements one measurement was taken with the AE buffer from the QIAamp®DNA Mini Kit as a reference. Subsequently, the DNA extracts were vortexed and 1 µL per sample was loaded on the lower pedestal of the NanoDrop™.

##### **4.4.2 Fluorometric measurements**

For measurements the Qubit™ dsDNA HS Assay Kit and the Qubit™ 2 or Qubit™ 3 were used. The sample preparation was done according to the manufacturer's instructions: 199 µL Qubit™ dsDNA HS buffer and 1 µL Qubit™ dsDNA HS reagent per DNA extract were mixed together, thus forming the Qubit™ working solution. 10 µL of each of the two standards, S1 and S2, were mixed with 190 µL Qubit™ working solution. 2 – 20 µL of each sample was used and filled up to a total of 200µL with the Qubit™ working solution. After vortexing the

samples and standards were incubated for 2 min at RT in the dark and afterwards analysed with the Qubit™ 2 or 3.

#### 4.5 PCR/HRM

Up until the point where we switched to fluorometric measurements as the Qubit system became available for our working group, we diluted samples to a concentration of 5 ng/μL to perform PCR; samples below that concentration were used undiluted. All samples were re-measured using the Qubit system and subsequently a DNA concentration of 0.1 ng per reaction tube (e.g. 0.05 ng/μL) was used to perform all PCR experiments. These normalized DNA concentrations were investigated with respect to the amplification and the C<sub>T</sub>-value respectively.

**Table 4-3:** Primer sequences in different target regions used in this study

Primer	Sequence 5' → 3'	Target region	Amplicon length
CP12 fw	TTAAATCGATAGGATAAAATCTGAT	CP12	214 bp
CP12 rv	GATTCTATTTGAATATACCTCGAATG		
ITS 1.1 fw	AAACCCGCGAACTCGTCT	ITS1	135 bp
ITS 1.1 rv	GTTCTGTTGTTGACAAGCAGG		
ITS 2.1 fw	TTAAACGGCACTCCAGGGTC	ITS2	227 bp
ITS 2.1 rv	CCTGGGCGTCACGCATTG		
ITS fw	ATTGTCGAAAACCTGCCA	ITS	286 bp
ITS rv	GAGATATCCGTTGCCGAG		
ITS_BB fw	GCAGAAAACCCGCGAACTC	ITS	99 bp
ITS_BB rv	CGCATCTGCTCGCAAGGG		
MatK 1.2 fw	AGCGAAATTTTGTAACGTGTTAGG	MatK	140 bp
MatK 1.2 rv	TCATTTTTTTTAATGATCCGCTAT		
MatK 1.4 fw	TTTTTGGGGTACAATACAAAT	MatK	155 bp
MatK 1.4 rv	GGAAATATTGAATGAAGTGATC		
MatK 1.5 fw	GAACTAGATAGATCTCAGCAACAT	MatK	251 bp
MatK 1.5 rv	TTTGTATTGTACCCCAAAAATTTA		

For this work multiple primer sets were used. One of them was found by Jaakola *et al.* [55] originally to distinguish bilberries (*V. myrtillus*) from other berry species (ITS fw and ITS rv). Furthermore a modified improved primer set for the differentiation of bilberry and blueberry (*V. corymbosum*) was designed in our working group (Doris Feurle) (ITS\_BB fw, ITS\_BB rv). Also, specific primer sets for the differentiation of *V. macrocarpon*, *V. oxycoccos* and *V. vitis-idaea* were designed in the course of this work. A compilation of these primer sets is shown in Table 4-3.



Apart from using each primer set alone, various combinations thereof were also tested (see Table 4-4).

**Table 4-4:** Combinations of primer sets

<b>ID</b>	<b>Primer sets</b>
Duplex D1	MatK 1.4, ITS
Duplex D2	MatK 1.4, ITS_BB
Duplex D3	MatK 1.2, MatK 1.4
Multiplex M1	MatK 1.4, ITS, ITS_BB

#### **4.5.1 Primer Design**

As mentioned above new primers were designed in course of this work. To align the sequences found in the NCBI database the MEGA7 software was used (see Figure 4-1). Particular emphasis was placed on conserved regions identical in VM, VO and VV within the barcoding region and significant differences in the variable part. After discerning a reasonable locus for potential primers the PyroMark Assay Design software was used to actually design the primers (see Figure 4-2).

**M7: ClustalW Parameters**

**DNA**

Pairwise Alignment

Gap Opening Penalty: 15

Gap Extension Penalty: 6.66

Multiple Alignment

Gap Opening Penalty: 15

Gap Extension Penalty: 6.66

DNA Weight Matrix: IUB

Transition Weight: 0.5

Use Negative Matrix: OFF

Delay Divergent Cutoff (%): 30

☐ Keep Predefined Gaps

Specify Guide Tree:

? Help OK Cancel

**Figure 4-1:** Default settings used for the automatic alignments with the MEGA7 software.

PCR Primer	
Min Primer Length [nt]	18
Max Primer Length [nt]	24
Optimal Amplicon Length From [nt]	50
Optimal Amplicon Length To [nt]	250
Max Amplicon Length [nt]	600
Allow Primer Over SNP	<input type="checkbox"/>
Melting Temperature Algorithm	Nearest Neighbor
Primer Concentration [μM]	0.2
Min Melting Temperature [°C]	56.0
Max Melting Temperature [°C]	86.0
Max Allowed Tm Difference [°C]	10.0
Max GC Difference [%]	30

**Figure 4-2:** Default settings used for the automatic primer design with the PyroMark Assay Design software.

Before ordering the primers, the secondary structure was checked using webserver (oligocalc and RNA fold). All primer sets were synthesized by Sigma Aldrich, purified via reverse-phase cartridge and quality checked by mass spectrometry. Prior to using the primers they were diluted with RNase free water according to the manufacturer's instruction obtaining a primer stock solution with a concentration of 100  $\mu$ M. Also, 10  $\mu$ L aliquots were prepared and stored at -20 °C. Prior to use, these aliquots were filled up to 100  $\mu$ L with RNase free water, thus obtaining a primer concentration of 10  $\mu$ M.

#### **4.5.2 PCR and HRM**

PCR was done using the EpiTect® HRM PCR kit and the Rotor-Gene® thermal cycler. At a later point in the research the MeltDoctor™ HRM Master Mix was used with the QuantStudio 5 by Thermo Fisher. As described in chapter 4.1. the Master Mix was prepared in another room. The EpiTect® HRM PCR kit was used to perform the majority of PCR reactions and subsequent HRM analyses, as it uses a fluorescent dye (EvaGreen) appropriate for HRM. Unless specified otherwise the volumes shown in Table 4-5 were used to prepare the respective Master Mixes.

DNA was diluted to 5ng/ $\mu$ L (unless mentioned otherwise) and all samples were analysed in technical duplicates. For the no-template-control (NTC) RNase free water was used instead of the (diluted) DNA extract.

**Table 4-5:** Pipetting scheme for the EpiTect® HRM PCR Master Mix

<b>Component</b>	<b>Volume per reaction [<math>\mu</math>L]</b>
RNase free water	7
HRM Master Mix	10
Primer forward (10 $\mu$ M)	0.5
Primer reverse (10 $\mu$ M)	0.5
Master Mix	18
DNA (5ng/ $\mu$ L)	2
Total	20

The Master Mixes when using the MeltDoctor™ HRM Master Mix were prepared as shown in Table 4-6.

**Table 4-6:** Pipetting scheme for the MeltDoctor™ HRM Master Mix

Component	Volume per reaction [μL]
RNase free water	18.5
HRM Master Mix	25
Primer forward (10 μM)	1.25
Primer reverse (10 μM)	1.25
Master Mix	46
DNA (5ng/μL)	4
Total	50

Table 4-7 shows the PCR profile used for all experiments with the all different primer sets on the Rotor-Gene® thermal cycler.

**Table 4-7:** PCR parameters used on the Rotor-Gene® thermal cycler

	Temperature	Time
Initial Denaturation	95°C	5 min
Denaturation	95°C	10 s
50x Annealing	65.7°C	30 s
Extension	72°C	30 s
Final Elongation	72°C	10 min
Denaturation	95 °C	1 min
Hybridization	40 °C	1 min
HRM	65 - 95°C	0.1°C per 2s

#### 4.5.3 Optimization of PCR conditions

Optimization was done regarding annealing temperature, primer concentration and additional Magnesium.

There are numerous online tools and formulas to calculate the optimal annealing temperature for each primer set, yet we relied on empirical data to determine the ideal annealing temperature. In a first step each primer set was subjected to a gradient PCR, meaning that different annealing temperatures were investigated at the same time. The respective annealing temperatures used started 5°C below the melting temperature of the higher melting primer of each primer set (see Table 5-2, Table 5-7, and Table 5-9) with a

range of 10°C. To achieve this, the BioRad iCycler was used. This thermal cycler is capable of creating a temperature gradient allowing for PCR under the same conditions with up to 8 different annealing temperatures. But no HRM could be done with this tool. So subsequently the PCR products were transferred to striptubes suitable for the Rotor-Gene and a HRM analysis was performed.

Simultaneously, two different primer concentrations (250nM and 100nM) were tested for each annealing temperature. For the MatK 1.4 primer set, the influence of additional Magnesium was investigated with two different concentrations (1.25 µM and 2µM).

For the binary mixtures the DNA extracts of the reference samples (VM: ID 3, VO: ID 4, and VV: ID 16) were used. The reference samples were diluted and mixed to obtain 7 binary mixtures for each pairing (VM/VV, VM/VO, and VV/VO) with a berry DNA content of 1%, 10%, 33%, 50%, 67%, 90%, and 99%, respectively. When mixing the 1% DNA extract of one reference samples with the 99% DNA extract of one of the other reference samples, it added up to the 5ng/µL DNA that were used for the commercial samples.

#### 4.5.4 Analysis

Analysis of the data obtained by HRM was performed via Rotor-Gene® Q software.  $C_T$  values and amplification plots were analysed as well as normalized melting plots (see Figure 4-3) and melting plots. A threshold of 0.0085 was used for the  $C_T$  value evaluation. The amplification plots were used to evaluate the selectivity of the respective primer set for VM, VV and VO. When investigating commercial samples the melting plot was used to differentiate between the three berry species and subsequently to assign the tested foodstuff to one of the berry species.

The image shows a software window titled "Normalisation Regions". It contains three main sections:

- Leading Range:**
  - Start: 84
  - End: 85.5
- Trailing Range:**
  - Start: 91
  - End: 92.5
- Confidence Percentage:**
  - Threshold: 10 %

**Figure 4-3:** Normalisation Range and Confidence Threshold used for the analysis with the Rotor-Gene Q Series Software

## **4.6 Gel electrophoresis**

Gel electrophoresis was done to discern the optimal annealing temperature and to verify the identity of the DNA products.

### **4.6.1 Preparation**

After amplification, the amplicon samples were prepared prior to gel electrophoresis as follows: 5  $\mu$ L of each sample to be analysed were mixed with 1.25  $\mu$ L Nucleic Acid Sample Loading Dye (5x) from BioRad. For the gel 1x TAE buffer was prepared using 50x TAE buffer. Furthermore, a 2% agarose gel was prepared by mixing 2 g agarose in 100 mL 1x TAE buffer while heating it up on a magnetic stirrer with heater until the solution was clear. After the agarose was completely dissolved, 10  $\mu$ L Gel Red™ Nucleic Acid Stain were added, and the hot mixture poured into the gel caster. Air bubbles were removed with a pipette tip. Immediately after, a comb was set into place. The gel was left to cool and firm at room temperature for at least 30 minutes or the gel looked turbid. The gel casting equipment was placed into the buffer tank and filled up with 1x TAE buffer until completely submerged. At this point, the comb was removed and the gel loaded with the samples and a DNA Ladder for reference. The buffer tank was closed and connected to the power unit. The power supply was adjusted to 120 V, leaving the gel to develop for 1 h.

### **4.6.2 Gel analysis**

To visualize the bands upon electrophoresis, after completing the run the gel was carefully placed under UV light, irradiated with 312 nm (UV transilluminator UVT-20M, Herolab GmbH) and photographed. If needed the intensity of the band can be used to determine the concentration of the amplicons formed. During the study this method was not utilized. The placement of the band in respect to the y-axis is an indicator of the size of the respective amplicon.

## 5 Results and Discussion

### 5.1 DNA extraction

DNA was extracted from commercially available foodstuff and plants as described in Chapter 3.1. Each primer set (see Table 4-3) was tested with DNA samples of the three *Vaccinium* species (*Vaccinium macrocarpon* ID 3, *Vaccinium oxycoccos* ID 4, and *Vaccinium vitis-idaea* ID 16) prior to application to other DNA samples.

### 5.2 Spectrophotometric and fluorometric measurements

At the beginning of the research the DNA concentration was determined spectrophotometrically using the Thermo Scientific™ NanoDrop 2000c for not only gaining information about the DNA concentration of the extracts of all samples but about their purity as well. Results showed that for all DNA extracts (reference samples and foodstuff samples) the 230/260 ratio was out of the accepted range of 1.8 and 2.2 (see chapter 3.2).

Additionally, the concentration of all the DNA extracts was determined using the Qubit™ dsDNA HS Assay Kit and the Qubit™ 2 or Qubit™ 3 (see chapter 7.7). The concentration of some samples was below the LOD of the Qubit™ dsDNA HS Assay Kit. Nine of these 13 samples were juices, three were supplements and the last one a jam.

### 5.3 Differentiation of the berry species in the MatK Region

Different DNA barcoding regions were tested. First, the MatK region, a gene located in the plastid, was investigated. Primers in the MatK barcoding region were designed. The accession numbers of the sequences found in the NCBI data base and used to design the primers are shown in Table 5-1.

**Table 5-1:** Accession numbers and definitions of the MatK sequences used

accession number	definition
AF382819	<i>Vaccinium vitis-idaea</i> maturase K (matK) gene, complete cds; chloroplast gene for chloroplast product.
KX677788	<i>Vaccinium oxycoccos</i> voucher HERB0235 maturase K (matK) gene, partial cds; chloroplast.
U61316	<i>Vaccinium macrocarpon</i> ribosomal maturase (matK) gene, partial cds; chloroplast gene for chloroplast product.

The alignment (see Figure 5-1) of these three sequences showed conserved regions as well as variable ones. The goal was to design primer sets yielding amplicons of different length and covering different sections of the gene.



**Figure 5-1:** Alignment of the sequences of *V. macrocarpon* (above), *V. vitis-idaea* (middle), and *V. oxycoccos* (below) in the MatK barcoding region. Variable positions are labelled.

Primers were designed using the PyroMark Assay Design software. All the primer sets were designed to meet the criteria mentioned in chapter 3.3.3. Figure 5-2 shows where the respective primer sets MatK 1.2, MatK 1.4 and MatK 1.5 are located. As the primer sets were designed to bind to the conserved regions of the sequence and the conserved regions were the same in all three sequences, only the *Vaccinium macrocarpon* sequence is shown here.

For the MatK 1.2 and the MatK 1.5 primer set the same reverse primer was used resulting in a larger amplicon for the latter.



ATTCAAAAGATATTTA **GA**ACTAGATAGATCTCAGCAACAT GACTTCATATATCCACTTATTTTTCAGGAGTATAT  
 TTATGCACTTGCTCATGATCGTGGTTTAAATAGATCTATTGTTTTTCAAAATGCAGATTATGACAATAAATCTAG  
 CTTACTAATTAGGAAACGTTTAATCACTCATTTAATTACTCAAATGTATCAACAGAATCATTTTCTTTTTTATACT  
 AATGATTTTAATCCAAA **TAAA** **TTTTGGGGTACAATACAAA** **T**TTTGATTCTCAAATGATATTTGAAGGATTGCG  
 GTCGTTGTGGAAATTCATTTTATCTACAATTACTATCTTTTCTAGAAGGGAAAGAAAGAGTCAAATCTCATAAT  
 TTAC **GATCACTTCATTCAATATTTCC**GTTTTTAGAGGACAAATTTTCCATTTAAATTATGTGTTAGATATACTAA  
 TACCTTATCCCGTCCATATGGAAATCTTGGTTCAAACCTCTTCGCTACTGGGTAAAAAGATCCCTCTTCTTGCATTT  
 ATTACGATTTTTTCTCCACGAGTATCCTAATCGGAATAGTCTTATTACTCAAAGAAATATAGTTTTTCTTTTTCA  
 AAAAGAAATCAAAAATTCTTCTTGTTCTATATAATTTTCATGTATGTGAATACGAATCTATCTTCGTTTTTCTTC  
 GCAATCAATCTTCTCATTTATGCTCAATATCTTTGAAACCTTTCTAGAACGAATCTTGTTCTATAAAAAAATAGA  
 ACTAGAAGTCTTTGTTAAGGATTTTAAGGGCATTCTATGGGTTTTCAAAGACCCTTCTGCATTATGTTAGATA  
 TCGAGGAAAAATCCATTTTAGCTTCAAATGGTTCGTCTCTTTGATGAATAAATGGAAATATTACCTTGTCAATTT  
 CTGGAATGTTATTTTTCCATATGGGCTCAACCAAGAAGGATCCATATAAACCAATTATCCAATAATTCCTTCGA  
 CTTTCTGGGCTATCTTTCAAGCGTACGATTAACCTTCAATGGTACGGAATCAAATGATAGAAAATTCATTTCT  
 AATAGAGAATGCTATTAAGAAGTTCGATACTCTAGTGCCAATTACTCCAATGATTGCATCATTGTCTAA **AGCGA**  
**AATTTTGTAACGTGTTAGG**ACATCCCATGAGTAAGCCGGTCTGGAGCGGTTTATCAGATTCTGATATTATTGAA  
 CGATTGGGGCTATATATAGAAATCTTCTCATTATTATAGCGGATCATTAAAAAAATGAGTTTGTATCGAAT  
 AAAGTATATACTTCGACTTTCTTGTGCTAGAACTTTGGCACGTAAACACAAAAGTACGGTACGTTCTTTTTTGAA  
 AAGATTAGGAGTGGGATTATTAGAAGAATTTTTACGGAGGAAGAGCAGGTTTTTTATTTGACCTTTCAAAA  
 GCTTCTTCGACTTCAAGGAAGTTATATCAAAGGCGTATTTGGTATTTGGATATTTTTTGTGTTAATGATACGGCA  
 AATCATGAATGA

**Figure 5-2:** Primer binding sites for the MatK region of *V. macrocarpon* (Accession number U61316),  
 light blue: MatK 1.2 forward, dark blue: MatK 1.2. reverse, dark pink: MatK 1.4 forward, light pink:  
 MatK 1.4 reverse, green: MatK 1.5 forward, dark blue MatK 1.5 reverse



After designing and ordering the primer sets all of them were diluted according to the manufacturer's data sheet. The data sheet did come with a calculation of the melting temperature of each primer. When performing a gradient PCR (see chapter 4.5.3) to determine the optimal annealing temperature these data were considered and the highest annealing temperature was set to be 5°C below the lower melting temperature of the two primers forming a set. For each temperature, a NTC (no template control) was tested as well as DNA extracts of VM, VV and VO separately. After performing PCR (see Table 4-8) in the BioRad iCycler iQ5, where a gradient PCR was possible, all the samples were transferred to strip tubes and subjected to HRM using the Rotor-Gene® thermal cycler. The resulting melting plots were investigated regarding the melting profile of the different berry species and possible formation of primer dimers in the NTC samples (see chapter 4.5.3).

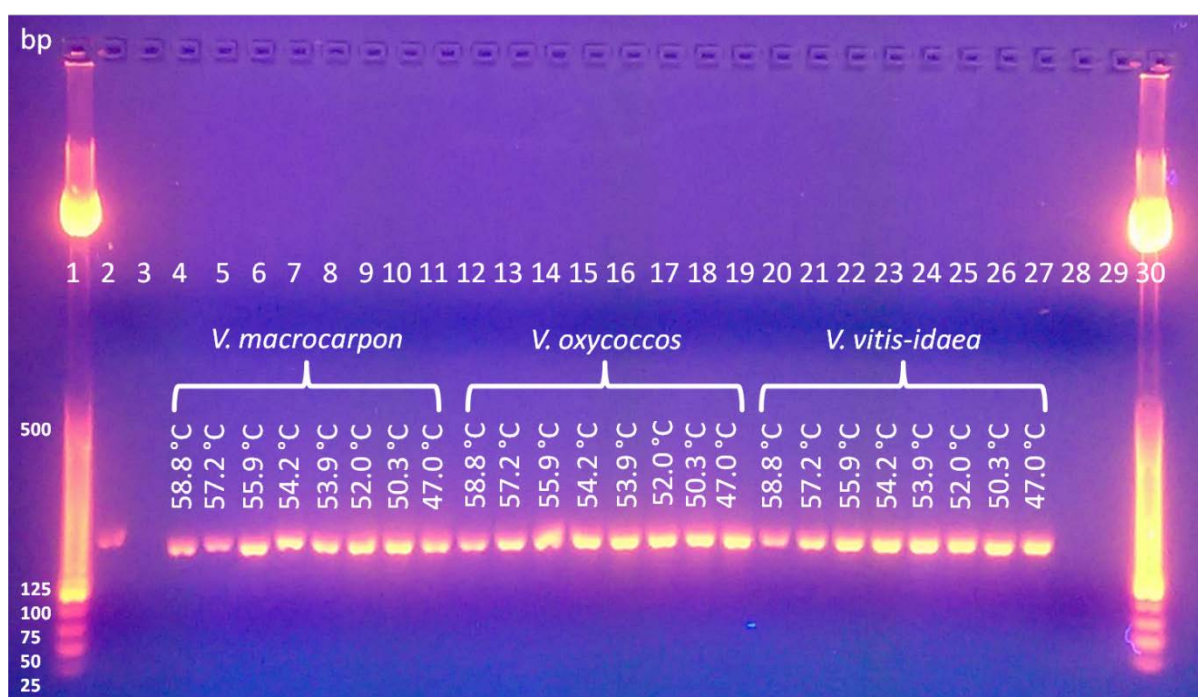


**Figure 5-3:** Agarose gel of different samples after PCR using the MatK 1.4 primer set at different annealing temperatures. Lanes 2,3, 28, 29: NTC, lanes 4-11: VM = ID 3, lanes 12-19: VO = ID 4, lanes 20-27: VV = ID 16 (see 7.7.1 for ID information)

Figure 5-3 shows a gel displaying amplicons formed with the MatK 1.4 primer set of VM, VV and VO at various annealing temperatures. For all species and all annealing temperatures, amplicons of the expected size (155 bp, see Table 4-3) were obtained. The brightness of the band was used to decide which annealing temperature yielded highest concentration of

amplicons. At 55.9 °C the band was the brightest so this temperature was used in subsequent PCR/HRM analysis. As for the melting plot Figure 5-4 shows how the different annealing temperatures influence the shape (and height) of the curve; the melting curves for amplicons yielded by *V. oxycoccos* and *V. vitis-idaea* showed the same melting behaviour. As all the melting curves looked very much alike the optimal annealing temperature was solely decided by the results of gel electrophoresis.

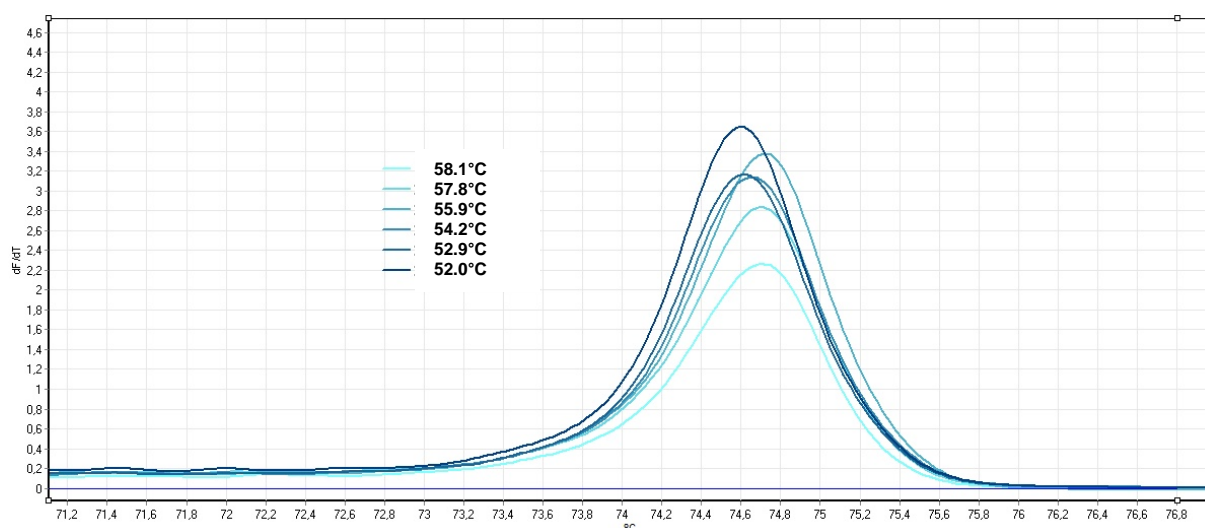


**Figure 5-4:** The influence of the annealing temperature on the melting curve of the amplicons of VM (ID 3, see chapter 7.7.1) obtained by PCR with the MatK 1.4 primer set; the lighter the colour, the higher the annealing temperature ranging from 58.1 to 52.0 °C. Typical results are shown.

Furthermore – as the EpiTect® HRM PCR kit does not specify how much magnesium it contains – additional magnesium was added to investigate effects of the addition of magnesium on the amplification and melting plot. All three reference samples were tested, all of them with similar results (see Figure 5-5).

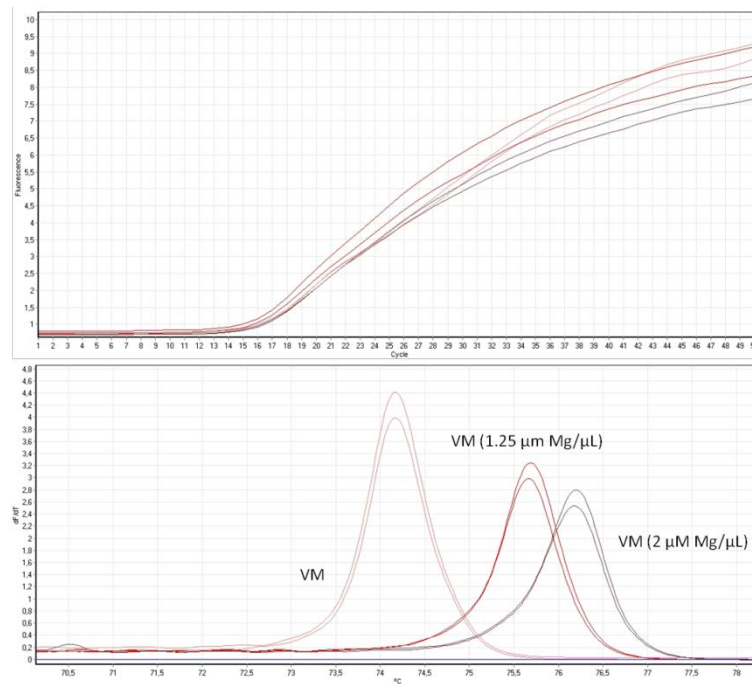


**Figure 5-5:** The influence of  $Mg^{2+}$  concentration on the amplification and melting plot. Typical results are shown. VM (ID 3), MatK 1.4 primer set, annealing temperature: 52°C (similar results for VO (ID 4) and VV (ID 16)).

Regarding the amplification there was no improvement, as the additional magnesium did not change the  $C_T$  value. The additional Magnesium shifted the maximum of the melting plots to higher temperatures. The general shape of the melting curve and the peak maximum did not change except being broader. So no further experiments were done investigating the influence of Magnesium with other primer sets.

For all three primer sets targeting the MatK region melting curves of the PCR products of the positive controls (VV, VM and VO) were very similar to one another with regards to the peak shape and peak maximum. The primer set MatK 1.5 (see Figure 5-7) even yielded three overlapping curves. The other primer sets were able to distinguish between VO and the other two berry species (MatK 1.2, see Figure 5-6) and VM and the other two berry species (MatK 1.4, see Figure 5-8) respectively. The latter primer set was used to investigate a few randomly chosen DNA extracts of commercial food samples.

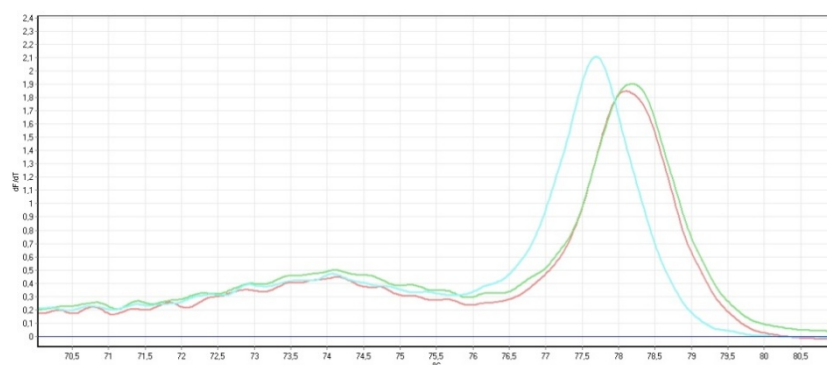


**Figure 5-6:** Resulting melting plots for the PCR products obtained with the primer set MatK 1.2. Reference samples: red=VM (ID 3), green=VO (ID 4), blue=VV (ID 16).

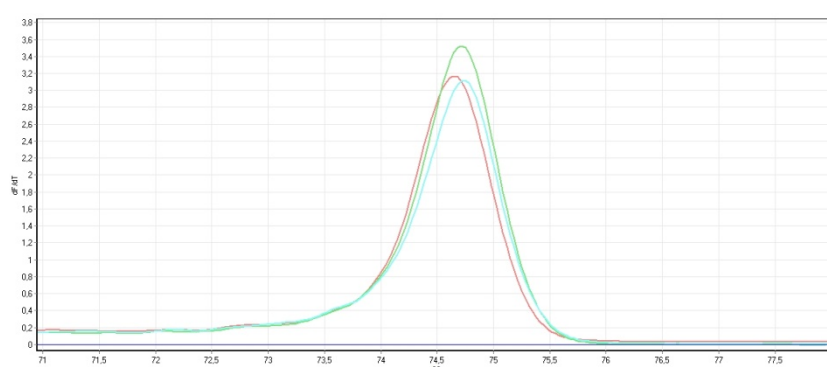


**Figure 5-7:** Resulting melting plots for the PCR products obtained with the primer set MatK 1.5. Reference samples: red=VM (ID 3), green=VO (ID 4), blue=VV (ID 16).

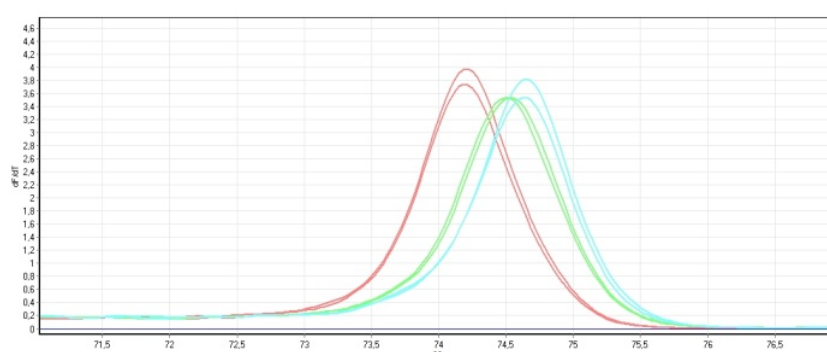


**Figure 5-8:** Resulting melting plots for the PCR products obtained with the primer set MatK 1.4. Reference samples: red=VM (ID 3), green=VO (ID 4), blue=VV (ID 16).

The analysis of these processed food samples (see Figure 5-9) showed how difficult differentiating between the berries species was when more complex matrices and a larger variety of samples are involved. These results led to the conclusion that the MatK region,



although frequently used as barcoding region for plants, was not able to differentiate between VV, VM and VO in a manner applicable to processed food.

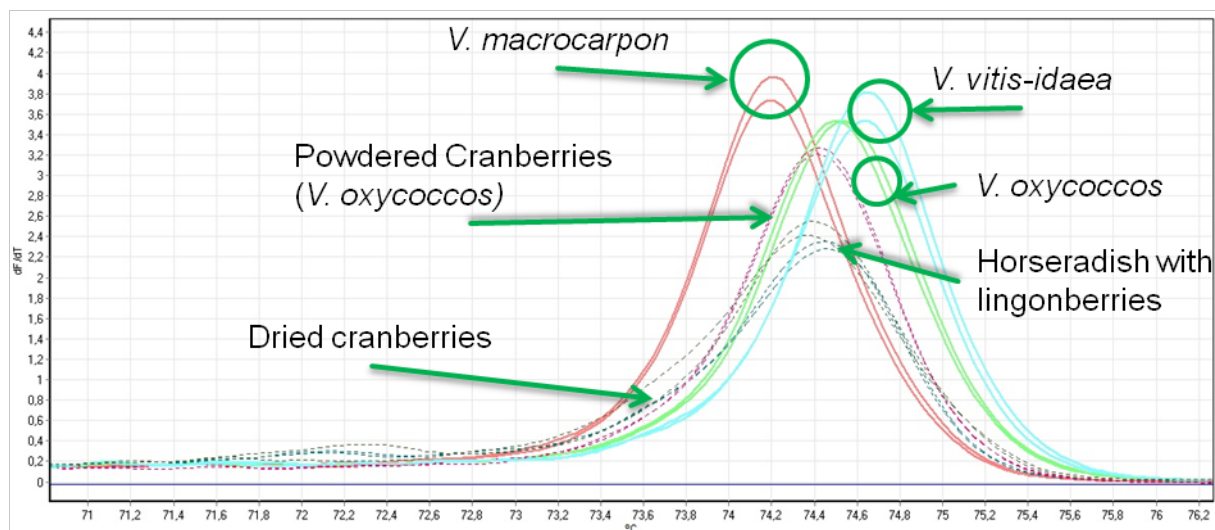


**Figure 5-9:** Melting plots for the PCR products obtained with the MatK 1.4 primer set. Reference samples: red=VM (ID 3), green=VO (ID 4), blue=VV (ID 16). Dotted teal=dried cranberries (ID 7), dotted pink=powdered cranberry (labelled *V. oxycoccus*, ID 11), dotted olive=horseradish with lingonberries (ID 33). It can be seen, that no differentiation is possible.

#### 5.4 Multiplexing approaches and the CP12 barcoding region

In course of this research a variety of combinations of primer sets (see Table 4-4) were tested as well as another barcoding region (CP12).

In an attempt to improve the (poor) results obtained by using the MatK 1.4 primer set, this set was used simultaneously with the ITS primer set initially used by Jaakola *et al.* [55]. The target region of this particular primer set lies in the ITS1 region. The goal was to obtain two amplicons per each DNA sample (one for each barcoding region) and thus melting curves that lead to a more distinct differentiation. For this experiment two more *Vaccinium* species were investigated, because Jaakola *et. al* had tested their ITS primer on different other *Vaccinium* species, also. Figure 5-10 shows that use of this combination (D1) did not lead to an improvement concerning the differentiation of the three *Vaccinium* species *V. macrocarpon*, *V. oxycoccus*, and *V. vitis-idaea*. Although it is observable, that a distinction between *Vaccinium myrtillus* (bilberry) and *Vaccinium corymbosum* (blueberry) is possible. (This – in detail – was investigated within the scope of another master's thesis.)

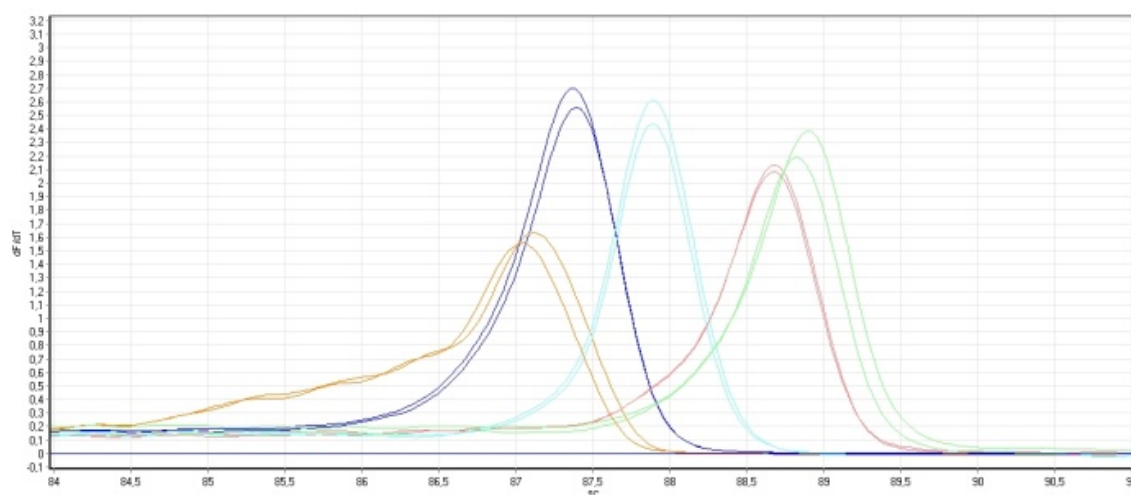


**Figure 5-10:** Melting plot for the PCR products obtained with the primer set D1. Red= VM (ID 3), green= VO (ID 4), light blue= VV (ID16), dark blue= bilberry (1A), ochre= blueberry (2B).

Another approach was the combination (D2) of the above mentioned primer set MatK 1.4 with the primer set ITS\_BB (see Table 4-7). The latter was especially designed for the distinction between *Vaccinium corymbosum* and *Vaccinium myrtillus* in our working group by Doris Feurle<sup>6</sup>. When testing only the reference samples, all five *Vaccinium* species could be distinguished. But when this combination was used to investigate the herbarium samples (see Table 4-1), it was unreliable concerning the distinction between different *Vaccinium* species, as can be seen in Figure 5-11.

**Table 5-3:** Mean  $C_T$  values (n=2) of the DNA extracts of the herbarium samples obtained with the D2 primer set.

ID	mean $C_T$ value
3	18.39
4	14.69
16	13.54
H1	14.49
H2	16.00
H3	16.25
H4	16.36
H5	19.74
H6	18.79
H7	17.45
H13	27.04
H14	27.46
H15	26.48

The DNA extracts of all samples did amplify and yielded a PCR product. The mean  $C_T$  values of the DNA extracts of the herbarium samples were similar to the  $C_T$  values of the DNA extracts of the reference samples (see Table 5-3). Only the herbarium samples H13, H14, and H15 (all VM samples, see Table 4-1) had higher  $C_T$  values.

The three herbarium samples labelled as VV (H1-H3) all showed a melting curve very similar to the VV reference sample. Of the four herbarium samples labelled as VO (H4-H7), only the melting curve of H4 matched the reference sample, the melting curves of the other samples differed in shape and number of peaks. For the

<sup>6</sup> As the primer set ITS\_BB was designed for the differentiation between bilberry and blueberry, these berries too, were investigated additionally.



herbarium samples labelled as VM (H13-H15), only the melting curve of H15 showed a similarity to a references sample, albeit the VV samples. The melting curves of the other samples did no share similarities to any of the reference samples. Whether this is because the herbarium samples were mislabelled in the first place or the DNA was degraded too much due to the samples being preserved by drying, could not be established.

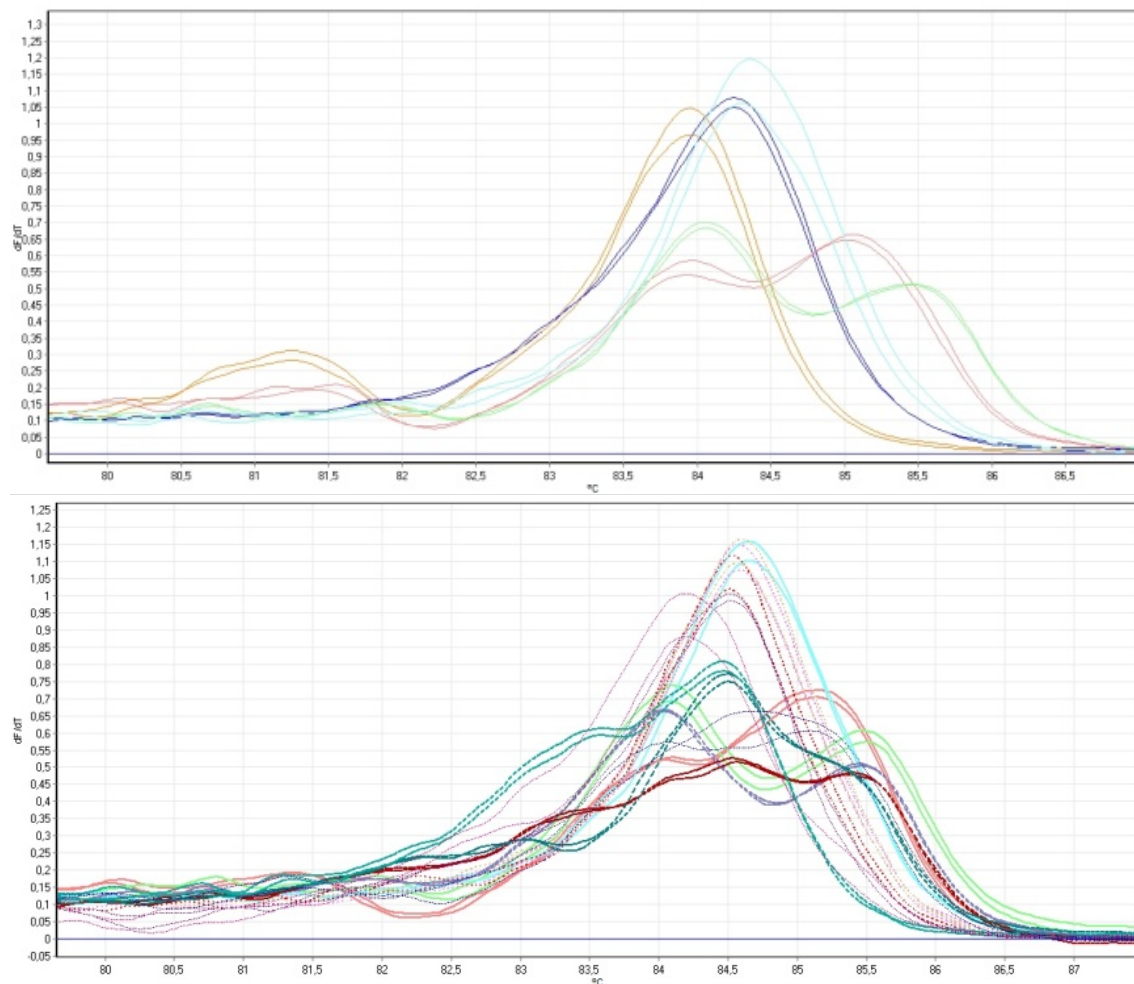


**Figure 5-11:** Melting plot for the PCR products obtained with the D2 primer set. Above: reference samples: red= VM (ID 3), green= VO (ID 4), light blue= VV (ID 16), dark blue= bilberry (1A), ochre= blueberry (2B). Below: reference samples: red= VM (ID 3), green= VO (ID 4), light blue= VV (ID 16), herbarium samples VV (H1-H3): dotted lines, VO (H4-H7): dashed lines, and VM (H13-H15): small dotted lines.

Furthermore a combination the three primer sets mentioned above, namely MatK 1.4, ITS and ITS\_BB, was investigated. This combination (M1) yielded promising results as can be seen in Figure 5-12. The three *Vaccinium* species *V. macrocarpon*, *V. oxycoccos*, and *V. vitis-idaea* showed different melting curves (VM and VV vs. VO) as well as a difference in the temperature at the peak maxima (VM and VV).

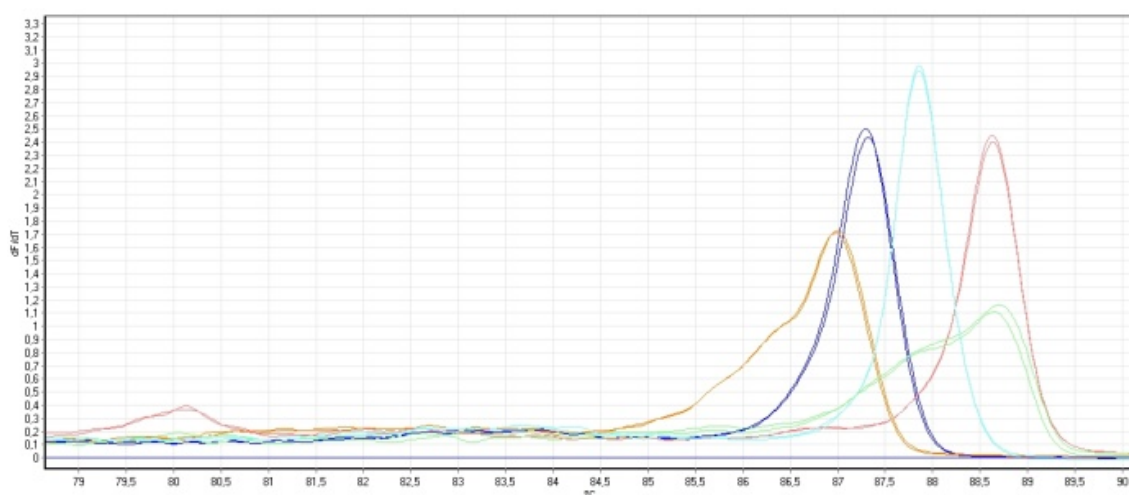


**Figure 5-12:** Melting plot for the PCR products obtained with the primer set M1. Red= VM (ID 3), green= VO (ID 4), light blue= VV (ID 16), dark blue= bilberry (1A) , ochre= blueberry (2B)

So in a next step the primer set combination M1 was used to analyse the above mentioned herbarium samples as is shown in Figure 5-13. The results were somewhat inconclusive as the herbarium samples were difficult to assign to a distinct *Vaccinium* species although they were obtained from reliable sources such as nurseries. Some of these samples were nearly a hundred years old (see Table 4-1) and have been preserved by drying prior to extraction. The respective DNA extracts had been in storage at -20 °C for almost a year.

**Table 5-4:** Mean  $C_T$  values (n=2) of the DNA extracts of the herbarium samples obtained with the M1 primer set.

ID	mean $C_T$ value
3	11.42
4	12.45
16	12.69
H1	14.07
H2	15.53
H3	15.51
H4	16.16
H5	19.25
6H	18.75
7H	15.63
13H	26.76
14H	26.76
15H	26.18

As can be seen in Table 5-4 the mean  $C_T$  values of the DNA extracts of the reference samples are lower than the ones of the herbarium samples. Only the herbarium samples H13, H14, and H15, that were all labelled as VM had higher  $C_T$  values. The DNA extracts of the herbarium samples labelled as VV (H1-H3) yielded a melting curve very similar to the respective VV reference samples, thus they were easy to assign. For the DNA extracts of the herbarium samples labelled as VO the varying shapes of the melting curves made it difficult to assign them to a berry species. Two of the DNA extracts of the herbarium samples labelled as VM (H13 and H14) yielded melting curves that did not match any reference sample, a third one (H15), had a melting curve very

similar to that of the VV reference sample.

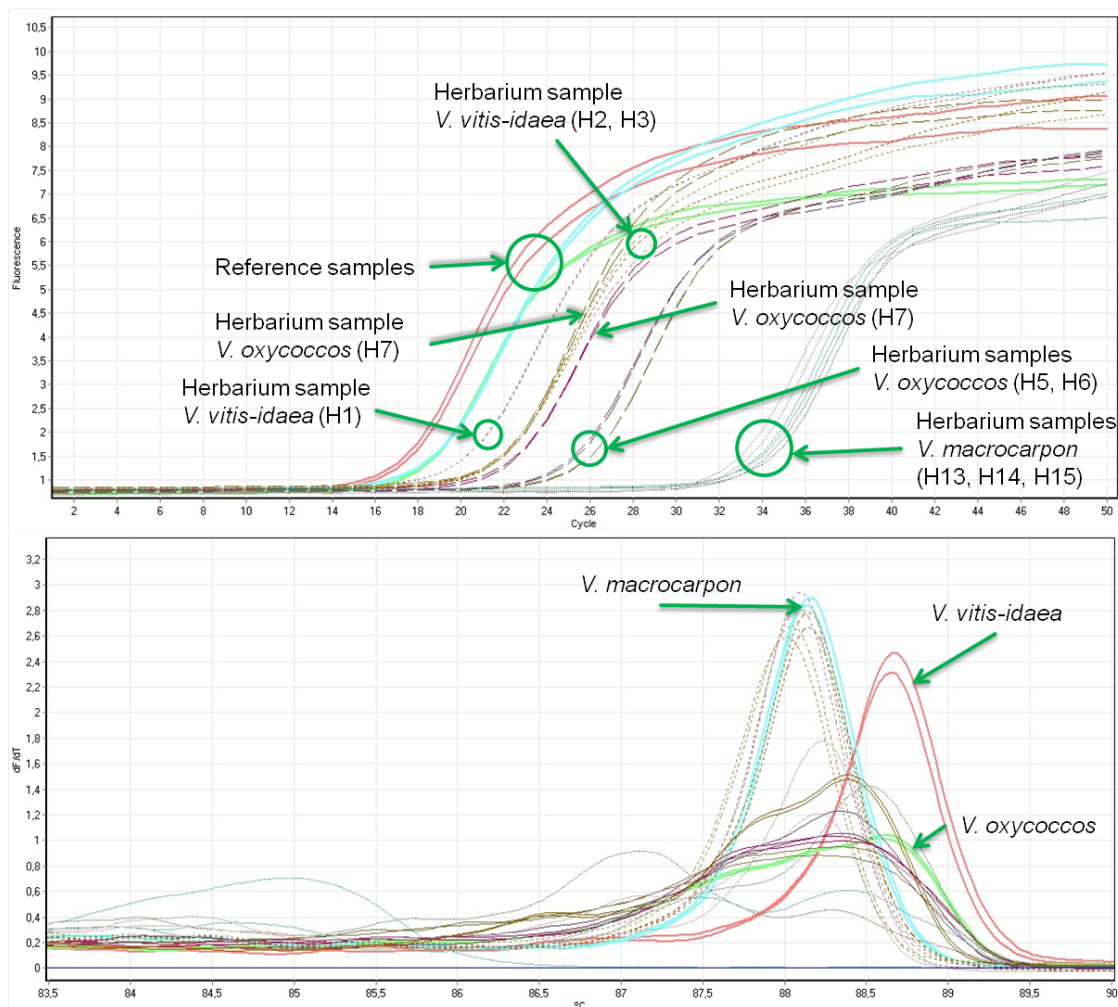


**Figure 5-13:** Amplification plot (above) and melting plot (below) for the PCR products obtained with the primer set M1. Reference samples: red= VM (ID 3), green= VO (ID 4), light blue= VV (ID 16), herbarium samples VV (H1-H3): dotted lines, VO (H4-H7): dashed lines, and VM (H13-H15): small dotted lines.

Likewise, a combination using two primer sets designed for the MatK region were tested (see Figure 5-2 and Table 4-7). In preceding experiments the primer set MatK 1.2 showed potential to differentiate VV from the other two berry species (see Figure 5-6) whereas the primer set MatK 1.4 could be used to distinct VM from VV and VO (see Figure 5-8). Our approach was that a combination of these two primer sets (D3) may lead to an increased differentiation.

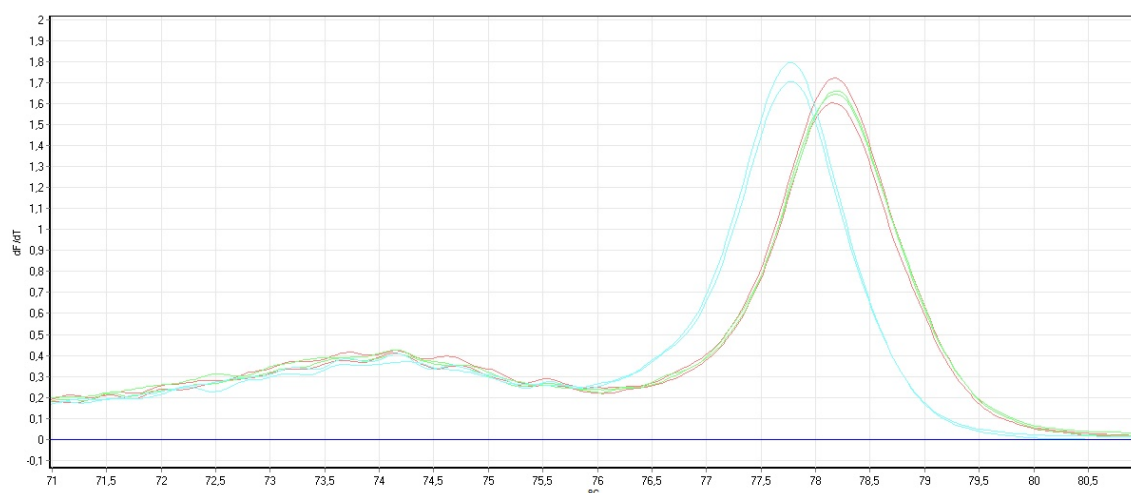


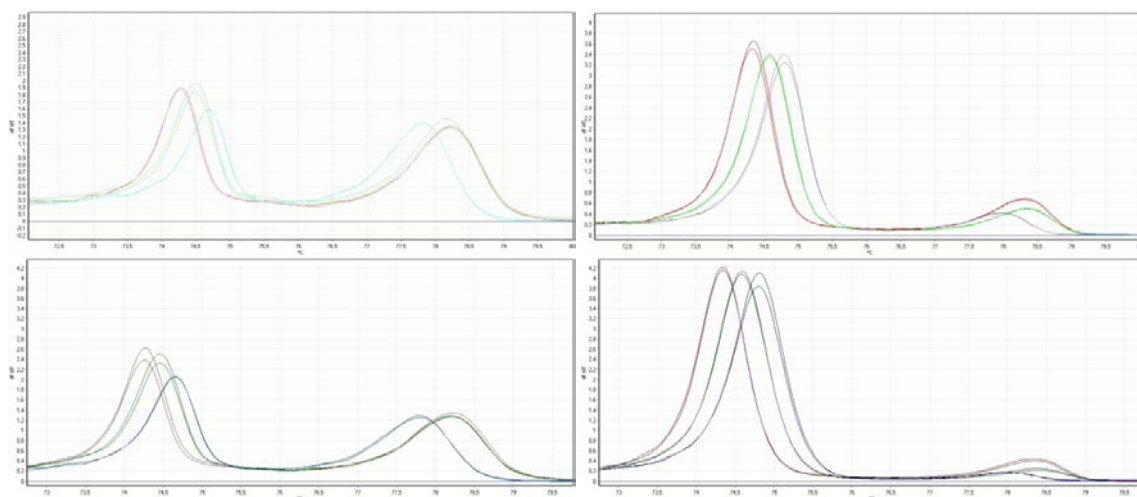
**Figure 5-14:** Melting plot for the PCR products obtained with the primer set D3. Reference samples: red=VM (ID 3), green=VO (ID 4), blue=VV (ID 16).

As can be seen in Figure 5-14 the PCR products for the MatK 1.2 primer set yielded very distinct peaks around 78 °C (see Figure 5-6). The peaks obtained for the PCR products of the MatK 1.4 primer set however at around 74 °C (see Figure 5-8) were rather unpronounced in comparison to the other peaks. So for the next step the different primer concentrations were adapted. The primer concentrations previously used before adaption were 100nM and 250nM (see chapter 4.5.3).

**Table 5-5:** Primer set combinations D4-D7

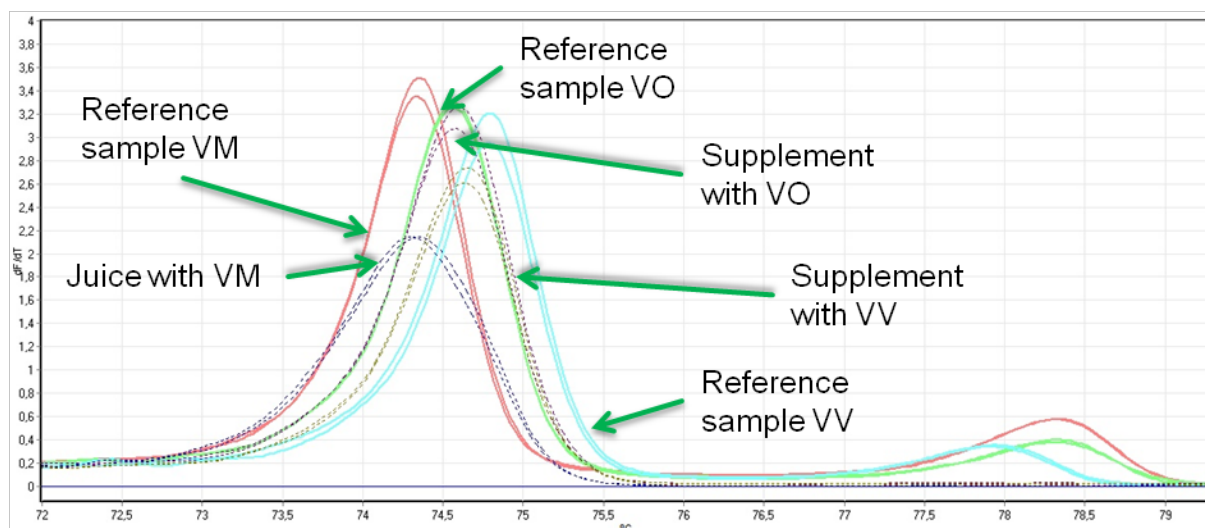
ID	MatK 1.2 [nM]	MatK 1.4 [nM]
D4	100	250
D5	50	375
D6	100	250
D7	50	375

Table 5-5 shows the combinations of primer concentrations used. The goal of these experiments was the increase the amplicon yield and therefore the peak height obtained for the amplicons with the MatK 1.4 primer set.



**Figure 5-15:** Melting plots for PCR products obtained with different primer sets. Reference samples: red=VM (ID 3), green=VO (ID 4), blue=VV (ID 16). Above: left: primer set D4. right: primer set D5. Below: left: primer set D6, right: primer set D7 (see Table 5-3)

This approach was successful insofar as the resulting melting plots showed two peaks of approximately the same height (see Figure 5-15, primer set D4). Unforeseen interaction between the two primer sets lead to a more differentiated melting profile as far as the MatK 1.4 primer set is concerned. This resulted in three melting peaks for the three berry species that were better distinguishable than the melting peaks that resulted from using only the MatK 1.4 primer set. So although the combinations D4 and D6 lead to peaks of even height we aimed for maximum differentiation. Therefore the combination D5 that had shown the most distinguishable melting peaks was used to carry out further experiments. This combination D5 was used to investigate processed food samples.



**Figure 5-16:** Melting plot for the PCR products obtained with the primer set D5. Reference samples: red=VM (ID 3), green=VO (ID 4), blue=VV (ID 16). Food samples: blue dotted=pure cranberry juice (ID 6), purple dotted=powdered cranberry (ID 11), olive dotted=powdered lingonberry (ID 12), (see 7.7.1 for more ID information).

A variety of samples was investigated using the D5 combination of primer sets at an annealing temperature of 55.9°C. Results showed (see Figure 5-16) that the peaks obtained with the MatK 1.4 primer set are hard to assign to a berry species as in this region there is no difference between the melting profile of VM and VO. The commercial samples did not show any peak expected for a PCR product obtained with the MatK 1.2 primer set (see Figure 5-6) around 78°C. In conclusion this primer set combination did not lead to a more distinct differentiation between the berry species.



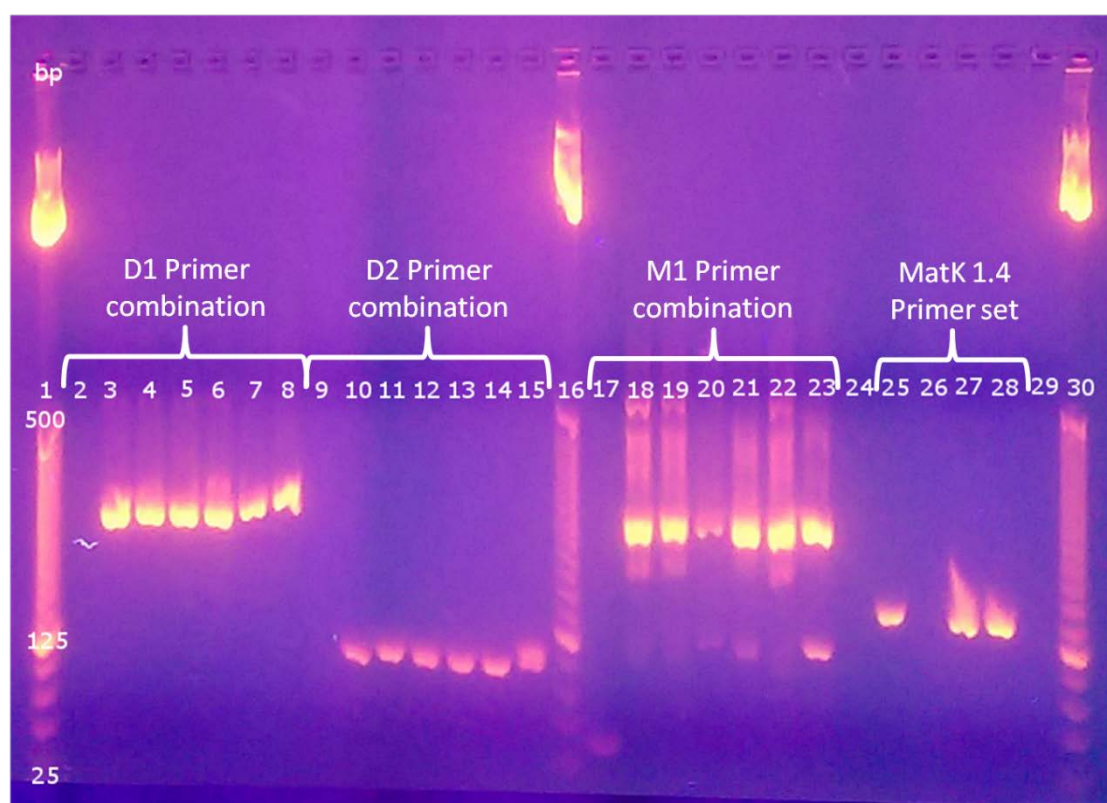


**Figure 5-17:** Developed agarose gel showing the size of the amplicons obtained with different primer sets. Lane 2-8: primer combination D1 (NTC, ID 1A, ID 2B, ID 3, ID 4, ID 16, ID 30). Lane 9-15: primer set D2 (NTC, ID 1A, ID 2B, ID 3, ID 4, ID 16, ID 30). Lane 17-23: primer set M1 (NTC, ID 1A, ID 2B, ID 3, ID 4, ID 16, ID 30). Lane 25-28: primer set MatK 1.4 for reference (ID 3, ID 4, ID 16, ID 30), see Table 5-3. Different ladder volumina<sup>7</sup> (1.88  $\mu$ L, 0.94  $\mu$ L und 1.24  $\mu$ L) were used (lane 1, 16, 30).

Agarose gel electrophoresis was used to verify the formation of different amplicons when using more than one primer set as shown in Figure 5-17. For the combination D1 the primer sets MatK 1.4, and ITS were used, that yielded amplicons with a size of 155bp and 286 bp, respectively (see Table 4-3). The developed agarose gel shows (lane 9-15), that the PCR products all match the size of amplicons obtained by the ITS primer set. The same is true for the combination D2, which used the MatK 1.4, and the ITS\_BB primer set (lane 18-23). In this case, too, the amplicon size matched the size of PCR products obtained with the ITS\_BB primer set. When using all three of the above mentioned primer sets (combination M1, see Table 5-5), the strongest signal derives from amplicons that match the size of PCR products obtained with the ITS primer set. Also, no amplicon of the size matching the PCR products obtained with the MatK 1.4 primer set could be detected. The results of these experiments point to a bias towards PCR amplification in the ITS region over the MatK region.

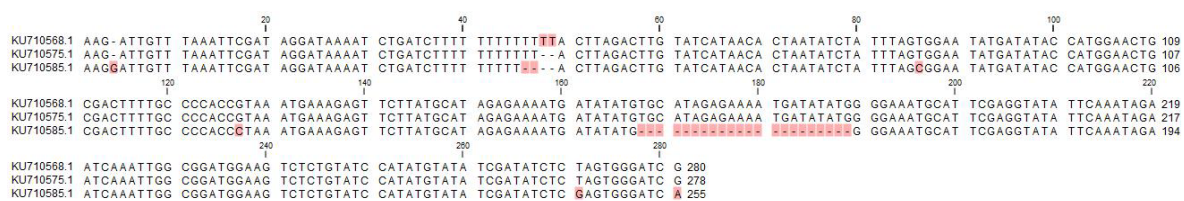
<sup>7</sup> A previous gel was developed using the recommended amount of ladder (2  $\mu$ L), but this lead to a smear of the bands. So the gel seen in (Figure 5-17) was also used to determine an optimal volume for the ladder.

Conclusively, the primer combinations did not enhance the differentiation between the three *Vaccinium* species.

Next to the barcoding regions discussed above one primer set was designed for the CP12 region (see chapter 1.3).

**Table 5-6:** Accession numbers and definitions of the CP12 sequences used

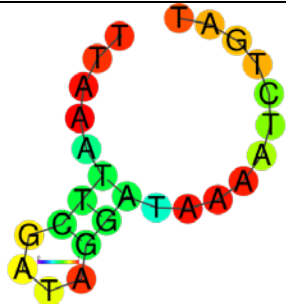
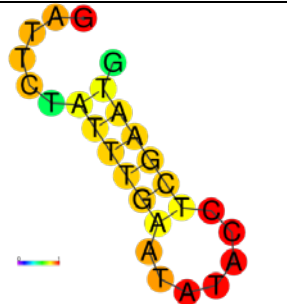
accession number	definition
KU710568.1	<i>Vaccinium macrocarpon</i> clone CP12_12-328 microsatellite CP12 sequence; chloroplast
KU710575.1	<i>Vaccinium oxycoccos</i> clone CP12_12-370 microsatellite CP12 sequence; chloroplast
KU710585.1	<i>Vaccinium vitis-idaea</i> clone CP12_12-382 microsatellite CP12 sequence; chloroplast



**Figure 5-18:** Alignment of the sequences of *V. macrocarpon* (above), *V. oxycoccos* (middle), and *V. vitis-idaea* (below) in the CP12 barcoding region. Variable positions are labelled.



**Table 5-7:** Predicted melting temperatures and secondary structures of the CP12 primer set

ID	CP12 fw	CP12 rv
Basepairs	26	26
Amplicon length	214 bp	
Tm° (Thermofisher)	59.0	59.7
Tm° (PyroMark Software)	64.7	65.4
RNA fold		

AAGATTGT **TTAAATTCGATAGGATAAAATCTGAT** CTTTTTTTTTTTTTACTTAGACTTGTATCATAAC  
 ACTAATATCTATTTAGTGGAATATGATATACCATGGAAGTGGACTTTTGCCCCACCGTAAATGAAAG  
 AGTTCTTATGCATAGAGAAAATGATATATGTGCATAGAGAAAATGATATATGGGGAAATG **CATTCGAG**  
**GTATATTCAAATAGAATCAAATTGGCGGATGGAAGTCTCTGTATCCATATGTATATCGATATCTCTAG**  
 TGGGATCG

**Figure 5-19:** Primer binding sites for the CP12 region of *V. macrocarpon* (Accession number KU710568), dark orange: CP12 forward, light orange: CP12 reverse

A gradient PCR was performed (54.0-59.0°C) using two different primer concentrations (see 4.5.3). The annealing temperature did not have much influence on the shape and size of the melting curve. The lesser primer concentration yielded smaller peaks that were even more undistinguishable as can be seen in Figure 5-20.

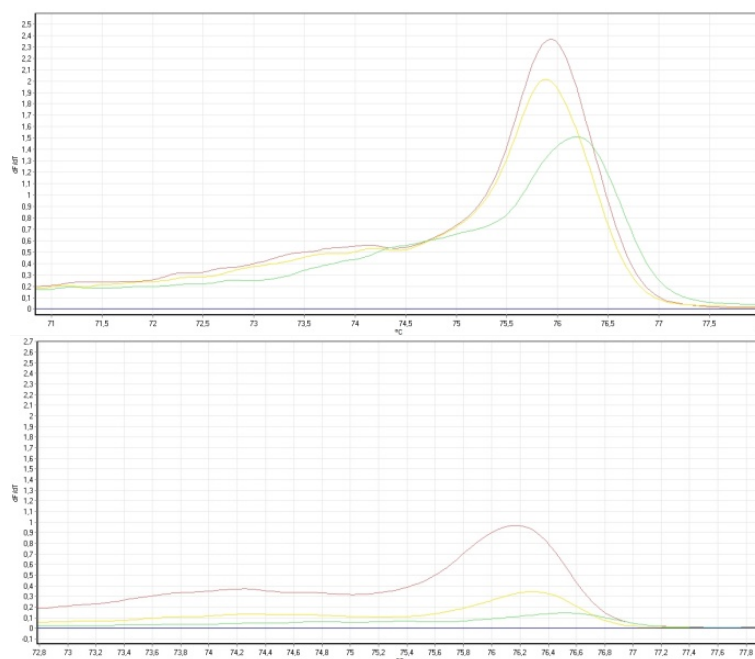


**Figure 5-20:** Melting plots for the PCR products obtained with the primer set CP12. Reference samples: red=VM (ID 3), yellow=VO (ID 4), green=VV (ID 16). Above: higher primer concentration (250nM), below: lower primer concentration (100nM).

Due to these results no further attempt of using this primer set were undertaken in course of this research.

## 5.5 Differentiation of the *Vaccinium* species in the ITS regions

In an attempt to improve the results obtained by using MatK as barcoding region and the primer set combination M1 both ITS regions – ITS1 and ITS2 – were investigated. For preliminary testing only the three references (VM, VV, VO) were used (see Table 5-8, Figure 5-21, Table 5-9, and Figure 5-22). A gradient PCR was performed ranging from 60.1 to 65.7°C<sup>8</sup> for both of the ITS regions. It was found that for both primer sets ITS1.1 and ITS2.1 the highest annealing temperature lead to the most distinct and distinguishable melting curves. Figure 5-23 shows the melting plot using the ITS 1.1 primer set as well as the ITS 2.1 primer set, each with an annealing temperature of 65.7°C.

<sup>8</sup> The annealing temperatures investigated were 65.7°C, 64.9°C, 63.7°C, 62.1°C, 60.9°C, and 60.1°C.

**Table 5-8:** Accession numbers and definitions of the ITS sequences used

accession number	definition
AF382730	Vaccinium macrocarpon internal transcribed spacer 1 5.8S ribosomal RNA gene and internal transcribed spacer 2 complete sequence
GU361898	Vaccinium vitis-idaea internal transcribed spacer 1 partial sequence 5.8S ribosomal RNA gene complete sequence and internal transcribed spacer 2 partial sequence
KX167293	Vaccinium oxycoccos voucher NMW3586 5.8S ribosomal RNA gene partial sequence internal transcribed spacer 2 complete sequence and 28S ribosomal RNA gene partial sequence

```

      20      40      60      80      100
GU361898.1 TTGCGCCTGA AGCCATTAGG CTGAAGGCAC GTCTGCCTGG GCGTCACGCA TTGCGTCACC CACCTCCCCC GCGCCCCAAG CGGGCACGTC GGTGCGTGCG CGGATATTGG 110
AF382730.1 TTGCGCCTGA AGCCATTAGG CTGAAGGCAC GTCTGCCTGG GCGTCACGCA TTGCGTCACC CACCTCCCCC GCGCCCCAAG CGGGCACGTC GGTGCGTGCG CGGATATTGG 110
KX167293.1 TTGCGCCTGA AGCCATTAGG TCTGAAGGCAC GTCTGCCTGG GCGTCACGCA TTGCGTCACC CACTCCCCC GCGCCCCAAG CGGGCGCGTC GGTGCGTGCG CGGATATTGG 110

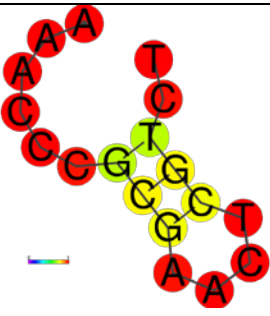
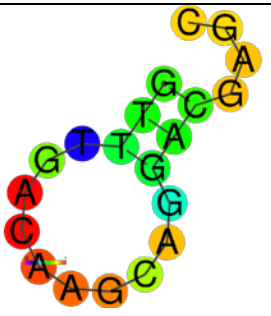
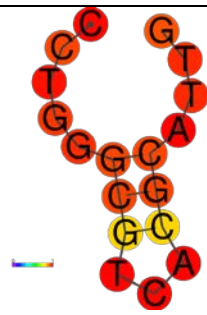
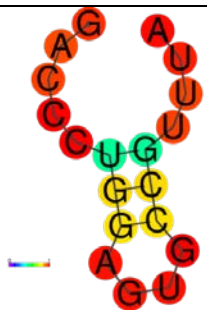
      120      140      160      180      200      220
GU361898.1 CCCCCCGTTC GCATCCGCGC GCGGTCGGCC TAAAAAACGG GTCCCCAATG ACGGACATCA CGACGAGTGG TGGTTGCTAA A-CCGTGCGG TCACGTCGTG CATGCCATCG 219
AF382730.1 CCCCCCGTTC GCATCCGCGC GCGGTCGGCC TAAAAAACGG GTCCCCAATG ACGGACATCA CGACGAGTGG TGGTTGCTAA A-CCGTGCGG TCACGTCGTG CGTGCCATCG 219
KX167293.1 CCCCCCGTTC GCATCCGTGC TCGGTCGGCC TAAAAAACGG GTCCCCAAGG ACGGACATCA CGACAAGTGG TGGTTGCTAA AKCCGTGCGG TCCGTCGTG CGTGCCATCG 220

      240      260      280
GU361898.1 TTTGTTGCGG GTTGCCCAT TTGACCTGG AGTGCCGTTT AAGTGGGCG CCTCAACT 277
AF382730.1 TTTGTTGCGG GTTGCCCAT TTGACCTGG AGTGCCGTTT AAGTGGGCG CCTCAACT 277
KX167293.1 TGTGTTGCGG GTTGCCCAT TGGACCTGG AGTGCCGTTT AAGGGGCGG CCTCAACT 278

```

**Figure 5-21:** Alignment of the sequences of *V. vitis-idaea* (above), *V. macrocarpon* (middle), and *V. oxycoccos* (below) in the ITS barcoding region. Variable positions are labelled.

**Table 5-9:** Predicted melting temperatures and secondary structures of the ITS1.1 and ITS2.1 primer sets (see Table 4-4)

ID	ITS1.1 fw	ITS1.1 rv
Basepairs	18	21
Amplicon length	135 bp	
Tm° (ThermoFisher)	64.48	64.5
Tm° (PyroMark Software)	69.8	69.9
RNA fold		
ID	ITS2.1 fw	ITS2.1 rv
Basepairs	18	20
Amplicon length	227 bp	
Tm° (ThermoFisher)	71.4	66.1
Tm° (PyroMark Software)	76.2	71.2
RNA fold		

TCGAAAACCTGCCAAGCAGAAAACCCGCGAACTCGTCTATACTCTCGGGGAACGATGTGGGGTTCGTG  
 GCCAGTTGCCTCGCTCCCGTCTTCCCTTGCAGAGCAGATGCGCACGGAACCTCCGGGCGACGTGCT  
 CGTCCTGCTTGTCAAACAACGAACCCCGGCGCAAAACGCGCCAAGGAAAATCGAACAAAGAGCGCGCG  
 TCCCTGCCCGTTCTCGGGCGGTGTTGGCGTCTGCAATCTTTCTTGTAACCTGAACGACTCTCGGCAACG  
 GATATCTCGGCTCTTGCATCGATGAAGAACGTAGCGAAATGCGATACTTGGTGTGAATTGCAGAATCC  
 CGTGAACCATCGAGTCTTTGAACGCAAGTTGCGCCTGAAGCCATTAGGCTGAAGGCACGTCTGCCCTGG  
 GCGTCACGCATTGCGTCACCCACCTCCCCCGCGCCCCAAGCGGGCACGTGCGTGGGCGGATATT  
 GGCCCCCGTTTCGCATCCGCGCGCGTTCGGCCTAAAAAACGGGTCCCCAATGACGGACATCACGACGA  
 GTGGTGGTTGCTAAACCGTCGCGTCACGTGCGTGCATCGTTTGTTCGGGTTGGGCCATTTGAC  
 CCTGGAGTGCGGTTTAAAGTGCGGCGCCTCAACT

**Figure 5-22:** Primer binding sites for the ITS regions of *V. macrocarpon* (Accession number AF382730), light green: ITS1.1 forward, dark green: ITS1.1 reverse, dark purple: ITS2.1 forward, light purple: ITS2.1 reverse

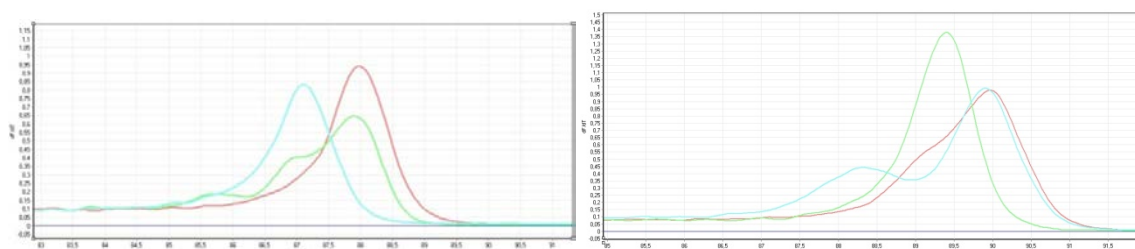


**Figure 5-23:** Melting plots of PCR products obtained with the ITS1.1 primer set (left) and the ITS 2.1 primer set (right), annealing temperature 67.5 °C. Reference samples: red=VM (ID 3), green=VO (ID 4), blue=VV (ID 16).

Regarding these results we decided to use the ITS 2.1 primer set for all subsequent research as the difference between the melting curves of the individual berries were most distinct. Although the maxima of the peaks of the VM and VV melting curve differ in 1°C when using the ITS 1.1 primer set, we opted for more reliable differentiation as the ITS 2.1 primer set led to 3 different shapes of melting curves.

## 5.6 Optimization and Validation

Optimization was done for each of the primer sets separately. For each primer set, the optimal annealing temperature was determined as well as the optimal primer concentration (see chapter 4.5.3). Subsequently for the MatK 1.4 primer set the influence of an increased Magnesium concentration was investigated (see Figure 5-5 and chapter 4.5.3). But as this led to no improvement concerning the differentiation of the melting plots we did not undertake more research in this direction. The same is true for different primer concentrations that were investigated. Furthermore, a variety of primer set combinations were tested (see chapter 5.4), equally yielding no improvement in the differentiation.

The ITS 2.1 primer set was optimized only with regards to the annealing temperature because previous research showed very little influence of Magnesium and primer concentrations (see chapter 4.5.3. and Figure 5-5).

One aspect we investigated in the context of validation was the reliability of the reference samples we used by comparing them to herbarium samples. Another thermal cycler, the QuantStudio® 5, was used, too, to determine whether the differentiation of VM, VV and VO was possible using other commercial available Master Mixes.

### 5.6.1 Matrices

A variety of matrix components were analysed. These components were chosen with particular attention to the ingredients of the various food groups also analysed. Matrices were investigated that were part of the processed food samples used in this study. Along with different berries that do not share a close evolutionary relation with the *Vaccinium* genus a variety of nuts was analysed. Furthermore DNA was extracted from different apple cultivars and selected other matrices (see Table 5-10 and chapter 7.7.2).

**Table 5-10:** Matrix components used throughout this study

ID	Name
A1	almond
B1	cashew
C1	walnut
D1	poppy seed
E1	raisin
F1	grape
G1	strawberry
H1	goji
I1	raspberry
J1	blackberry
K2	red currant
L1	apple
M1	pomegranate
N1	sour cherry
O	apple Evelina
P	apple Gala
Q	apple Granny Smith
R	apple Golden delicious
S	white currant leaves
T	red currant leaves
U	black currant leaves
V	black currant leaves

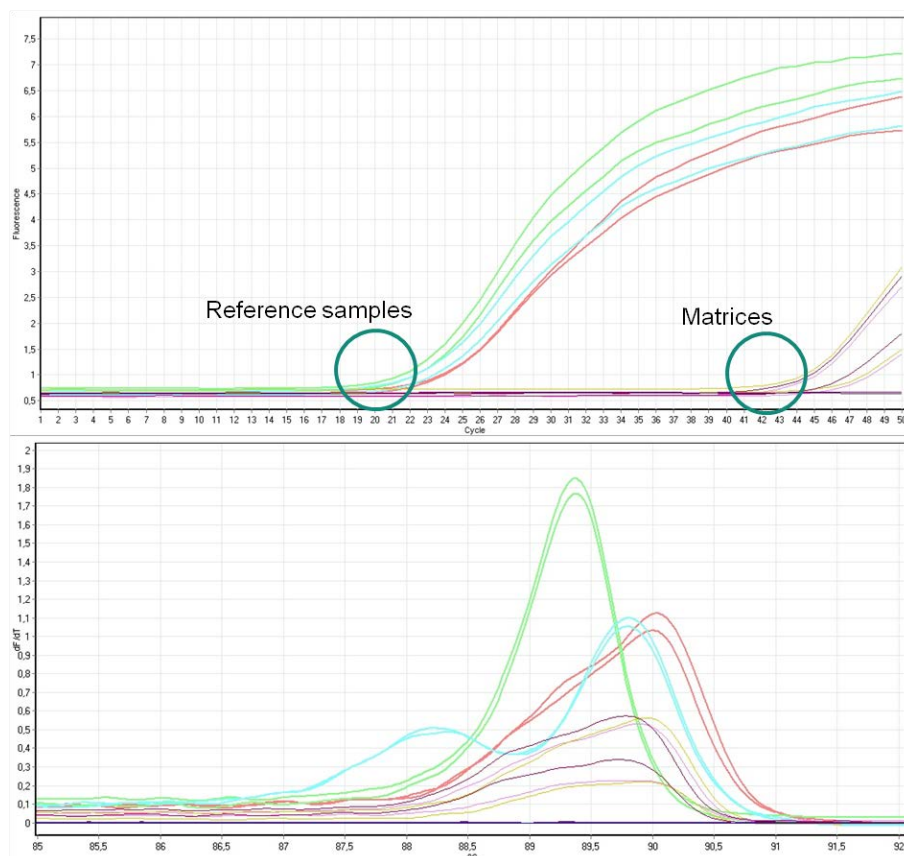


**Figure 5-24:** Amplification plot (above) and melting plot (below) of PCR products obtained with the ITS2.1 primer set. Reference samples: red=VM (ID 3), green=VO (ID 4), blue=VV (ID 16). Violet=cashew (ID B1), yellow= pomegranate (ID M1), magenta= sour cherry (ID N1), dark purple=apple “Gala” (ID P). The latter did not amplify.

Of all the matrix components investigated, the DNA extracts of walnut (ID C1), raisin (ID E1), grape (ID F1), raspberry (ID I1), all currant varieties (ID K2, S, T, U, and V) as well as three apple varieties (ID O, Q, and R) did not amplify at all (see Figure 5-24). The DNA extracts of the matrix components, that showed amplification, had  $C_T$  values that cluster around 40 (see Table 5-11) whereas the mean  $C_T$  values of the DNA extracts of the positive controls are between 16 and 17. The  $\Delta C_T$  values thus ranged from 14-24. This is a strong indicator for overall low and possible unspecific amplification (potentially cross reactivity of the primer set) of these particular DNA extracts.

**Table 5-11:** Mean  $C_T$  values (n=2) of the DNA extracts of the matrix components

ID	mean $C_T$ value	ID	mean $C_T$ value
A1	35.73	L1	39.22
B1	40.60	M1	40.79
C1	-	N1	40.16
D1	36.41	O	-
E1	-	P	41.86
F1	-	Q	-
G1	40.40	R	-
H1	38.23	S	-
I1	-	T	-
J1	41.57	U	-
K2	-	V	-
- ... no amplification			

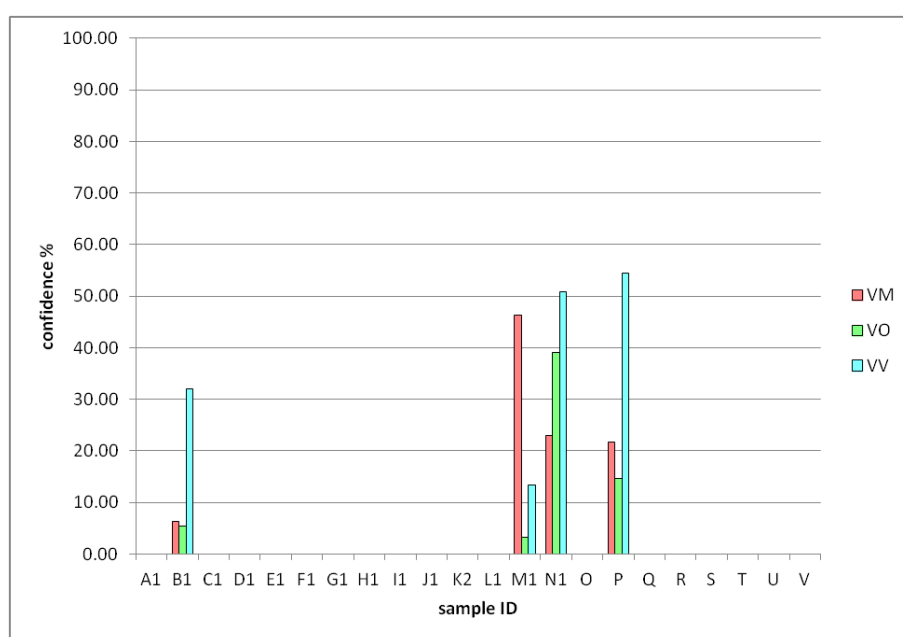


**Figure 5-25:** Confidence levels of the classification of the matrix component DNA obtained with the ITS2.1 primer set (see chapter 4.5.2). See chapter 7.7.3 for ID information.

In order to analyse the results the Rotor-Gene Q Series Software was used. High resolution melt analysis allows defining genotypes (the three different species) and – by calculating similarities and differences in the melting curves – assigns the samples to the set genotypes. In addition, an R value is given, indicating the percentage of confidence in the result. Subsequently, these values are shown and discussed for all the different sample groups.



Some of the DNA extracts of the samples (grapes, strawberries, some apple cultivars and some current varieties; see chapter 7.7.3) were not amplified by the method used. A number of matrix components showed amplification and certain level of confidence of classification (cashews, pomegranates, sour cherries and the apple variety “gala”, see Figure 5-25).

### **5.6.2 Spiking experiments**

In addition to the matrix components discussed above, a variety of other DNA extracts were tested in order to investigate if these matrices would interfere with the detection of the three berry species. These were prepared by Iva Nikolikj (ID A3B) and Doris Feurle (ID 1A, ID 2B, ID FHD, ID COC, ID APF, ID RET, ID BAL, ID KUE) during their respective research. The extracts were as follows: 1A – bilberry, 2B – blueberry, FHD – jam containing blueberries, A3B – aronia, COC – chocolate, APF – apple, RET – beetroot, BAL – cereal bar, and KUE – pumpkin. Solely the three samples containing other *Vaccinium* species (1A, 2B, FHD) showed overall lower  $C_T$  values than the other samples with  $\Delta C_T$  values between 7.8 and 10.7. The  $\Delta C_T$  values of the other sample extracts were between 18.00 and 28.00. None of the PCR products of these extracts showed a melting behaviour like the three *Vaccinium* species we were interested in (see Figure 5-26).

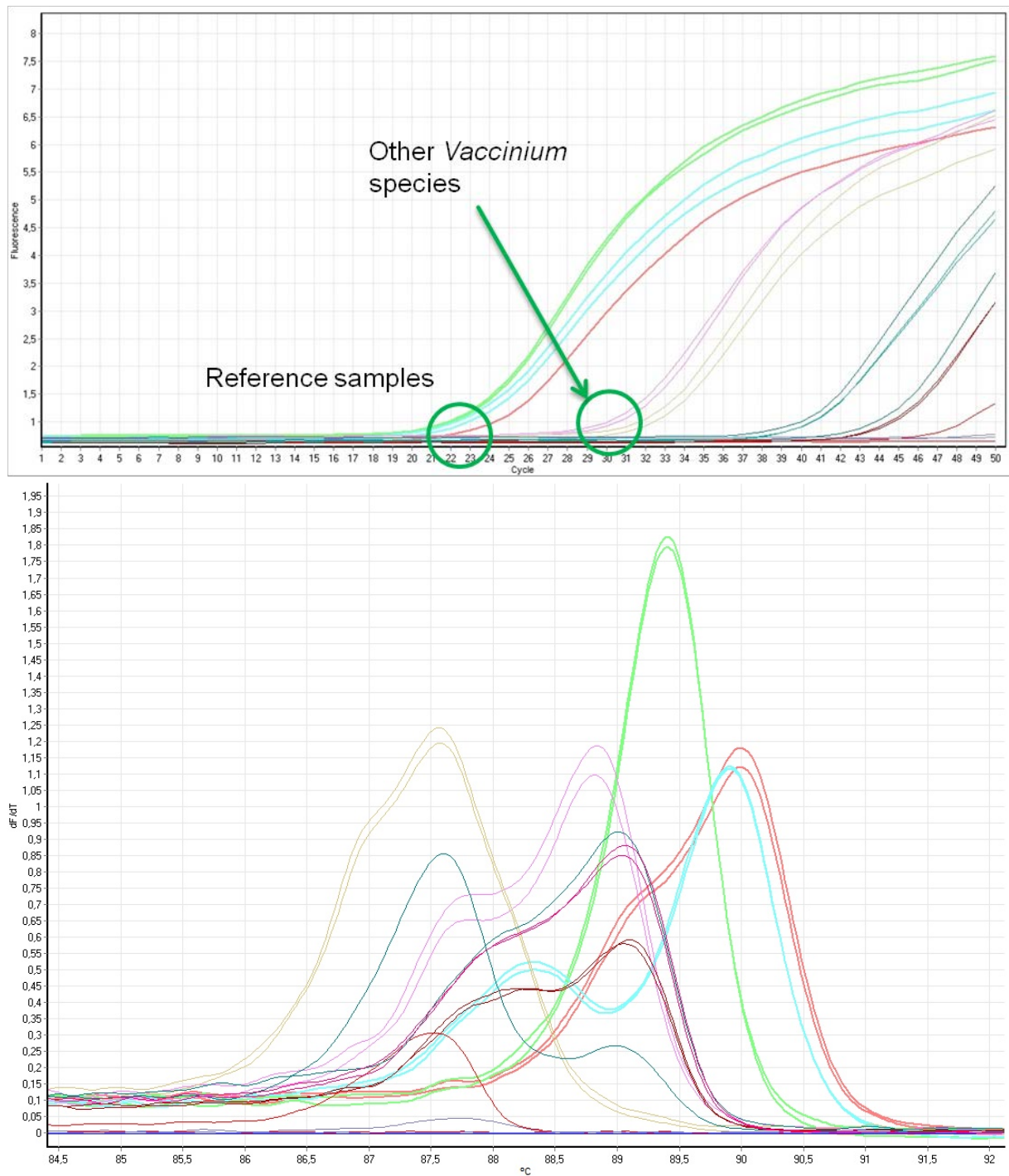


**Figure 5-26:** Melting plot (below) of PCR products obtained with the ITS2.1 primer set. Reference samples: red=VM (ID 3), green=VO (ID 4), blue=VV (ID 16), rosé=*V. myrtillus* (ID 1A), beige=*V. corymbosum* (ID 2B), crimson=aronia (ID 3AB), pale violet=chocolate (ID COC) no amplification, dark red=apple (ID APF), teal=beetroot (ID RET), magenta=pumpkin (ID KUE). NTC did not amplify.

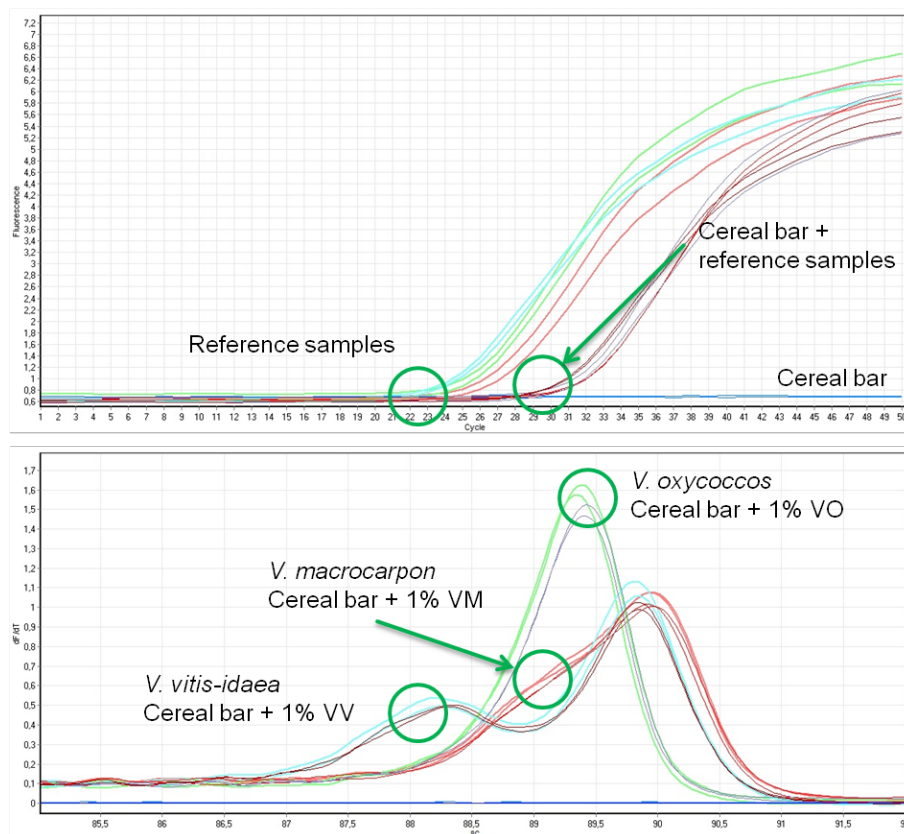
As can be seen in Table 5-12 none of these samples could be matched to either American or European cranberry or lingonberry.

**Table 5-12:** Mean  $C_T$  values (n=2) and level of confidence for other *Vaccinium* species and matrix components (see chapter 7.7.3)

ID	Confidence [%]			mean $C_T$ value
	VM	VO	VV	
1A	0	0	0	25.08
2B	0	0	0	26.61
FHD	0	0	0	27.92
A3B	0	0	0	42.61
COC	0	0	0	45.62
APF	0	0	0	38.77
RET	0	0	0	36.82
KUE	0	0	0	34.80

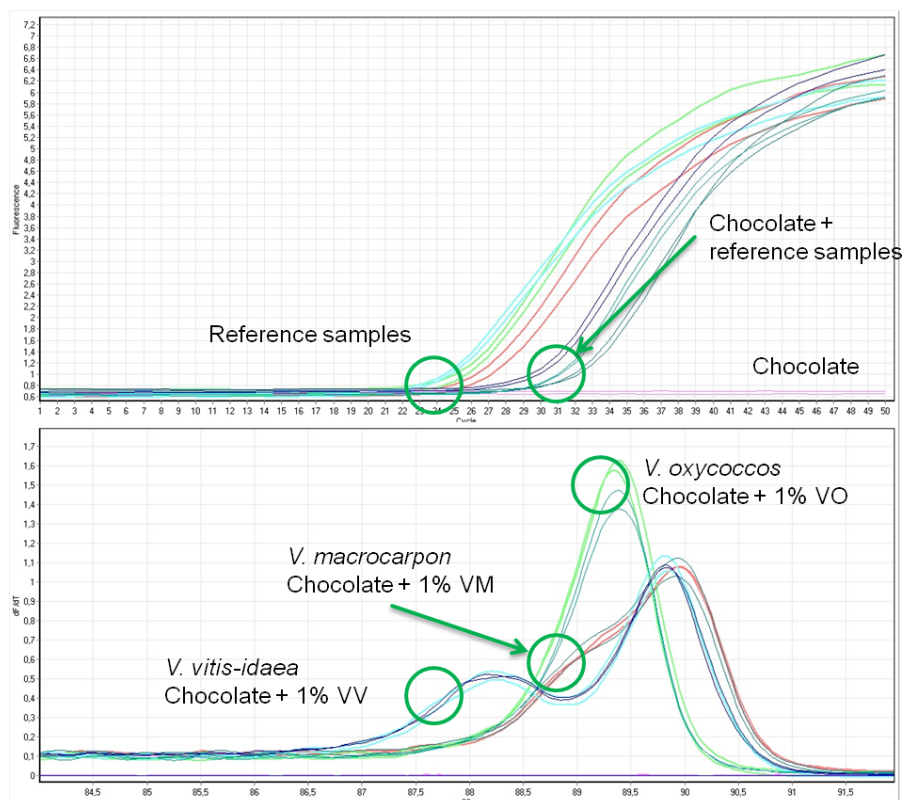
In a next step spiking experiments were performed to investigate the amplification and melting behaviour upon addition of a very low percentage of DNA extracts of *V. macrocarpon*, *V. oxycoccos*, and *V. vitis-idaea*. Goal was to investigate the selectivity of the primer set ITS2.1. In a first experiment, 1 vol% of each of the three *Vaccinium* species DNA was added to a blank cereal bar matrix (ID BAL), chocolate

(COC), and apple (L1).



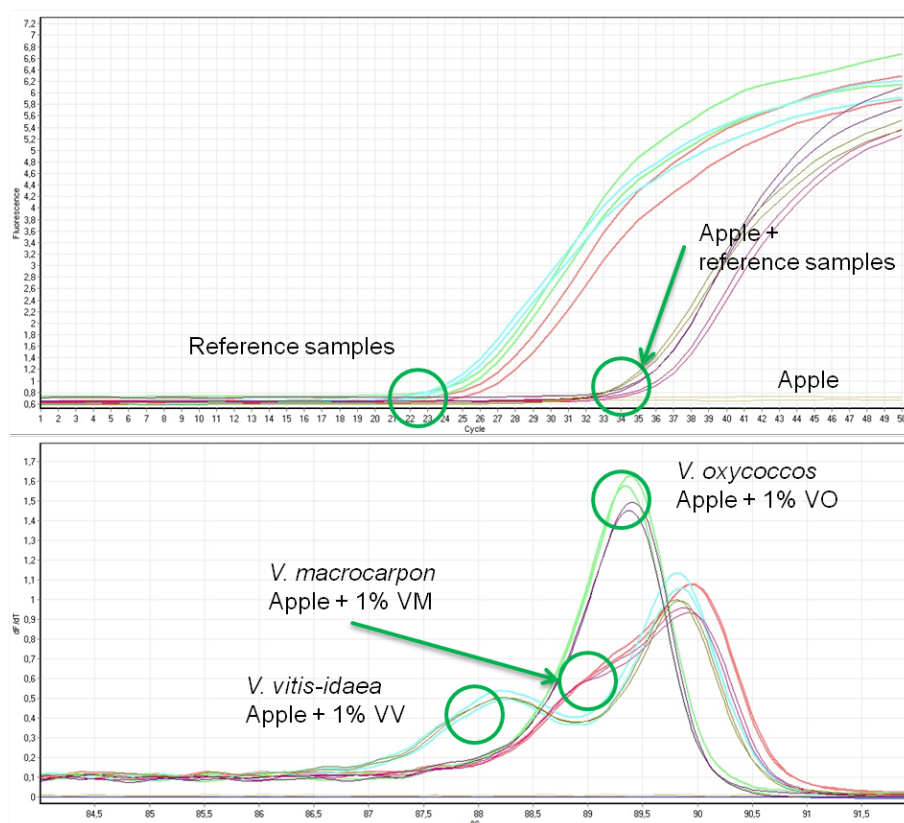
**Figure 5-27:** Amplification plot (above) and melting plot (below) of the PCR products obtained with the ITS2.1 primer set. Reference samples: red=VM (ID 3), green=VO (ID 4), blue=VV (ID 16). Sample used for spike experiments as matrix component=cereal bar (ID BAL).

The  $C_T$ -values of the reference extracts were lower than the values for the matrix DNA samples with an addition of 1% *Vaccinium* DNA. The DNA of the matrix sample cereal bar (ID BAL) did not amplify at all. When investigating the melting behaviour it can be seen (Figure 5-27) that the melting curves of the cereal bar DNA extract with the addition of 1% of *Vaccinium* DNA matched the melting curves of the respective reference sample.



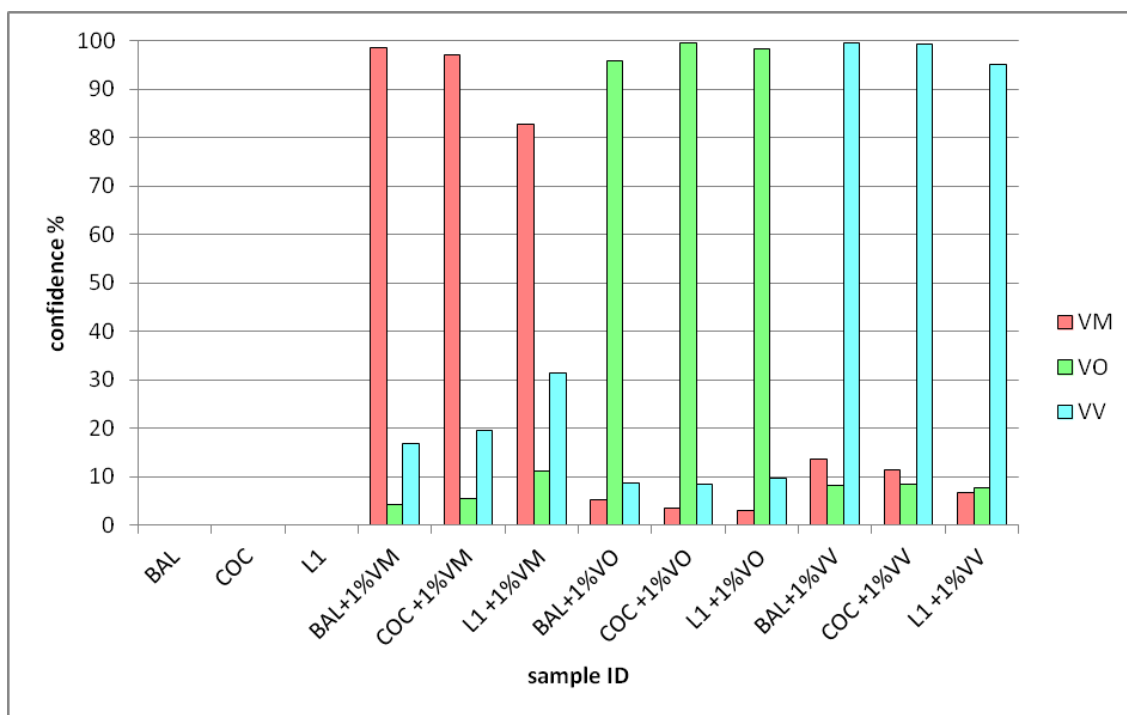
**Figure 5-28:** Amplification plot (above) and melting plot (below) of the PCR products obtained with the ITS2.1 primer set. Reference samples: red=VM (ID 3), green=VO (ID 4), blue=VV (ID 16). Sample used for spike experiments as matrix component=chocolate (ID COC).

The same results were acquired when instead of the cereal bar matrix DNA, chocolate (ID COC, see Figure 5-28) and apple (ID L1, see Figure 5-29) were used. In these cases too, matrix component DNA did not amplify, whereas the addition of 1% *Vaccinium* DNA lead to an amplification (although  $C_T$ -values were higher than the values of the reference samples).



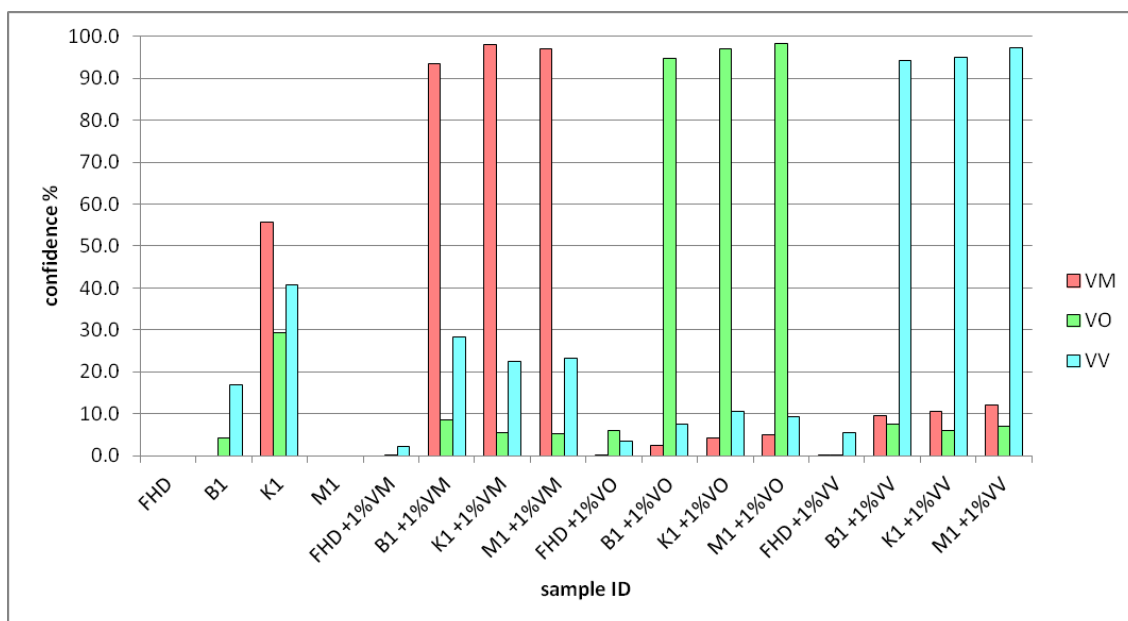
**Figure 5-29:** Amplification plot (above) and melting plot (below) of the PCR products obtained with the ITS2.1 primer set. Reference samples: red=VM (ID 3), green=VO (ID 4), blue=VV (ID 16). Sample used for spike experiments as matrix component=apple (ID L1).

The melting curves of the matrix component DNA samples with an additional 1% of *Vaccinium* DNA matched the melting curves of the respective reference samples. This lead to a high level of confidence of classification (see Figure 5-30).



**Figure 5-30:** Confidence level for the DNA extracts spiked with 1% *Vaccinium* DNA extract obtained with the ITS2.1 primer set with the matrix components BAL, CO, and L1. See chapters 7.7.2 and 7.7.3 for ID information.

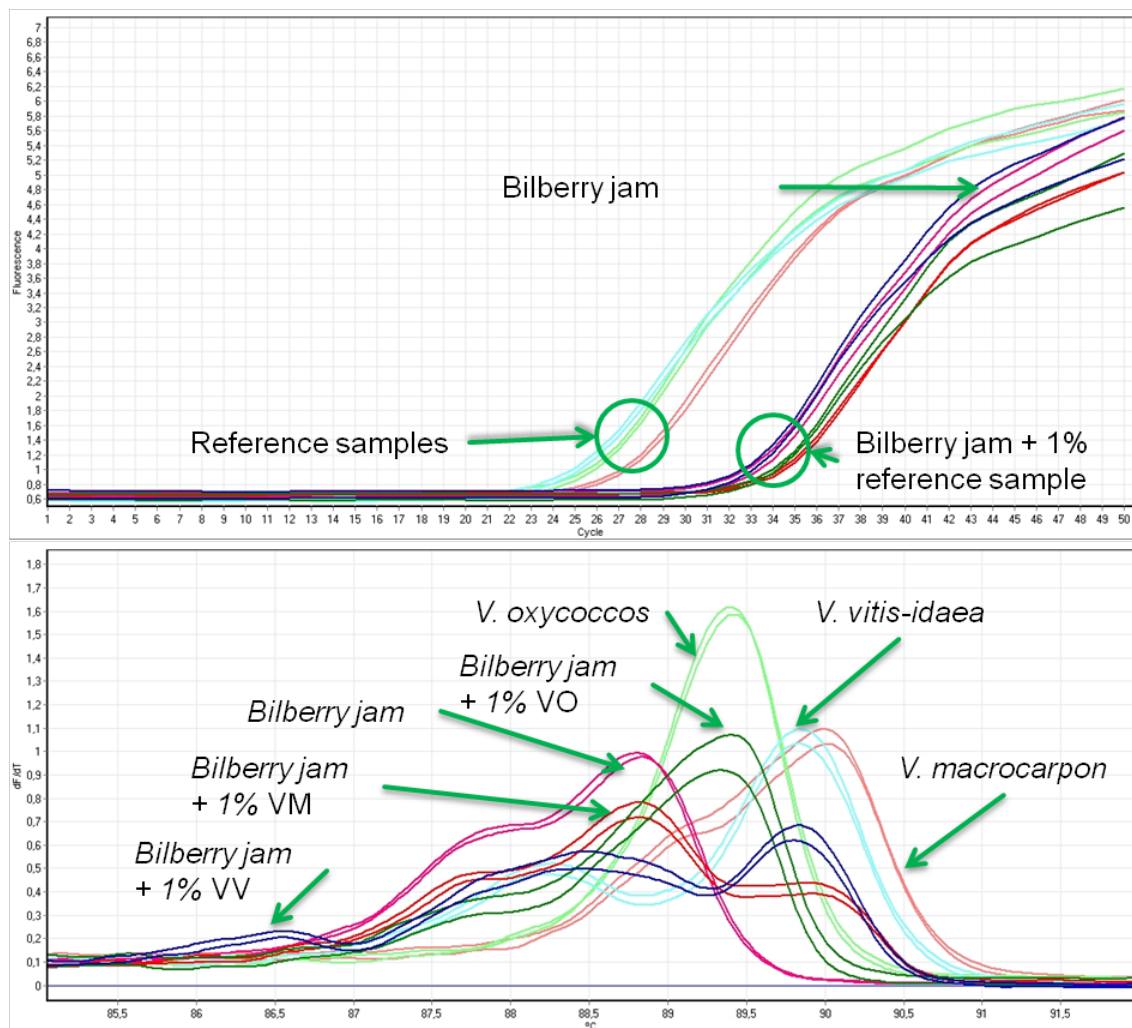
So, the results showed that an addition of as low as 1% of *Vaccinium* DNA extract to a matrix that did not contain any other *Vaccinium* DNA lead to a clear rise in confidence regarding the classification of the respective sample. This leads to the conclusion, that the matrix component does not affect the melting behaviour of the reference samples. In a subsequent experiment, other matrices were investigated under the same circumstances. Matrices were chosen that had previously lead to an amplification (see Table 5-11) (B1 – cashews, and K1 – red currant). Furthermore a matrix containing another *Vaccinium* species was used (FHD) as well as M1 – pomegranate.



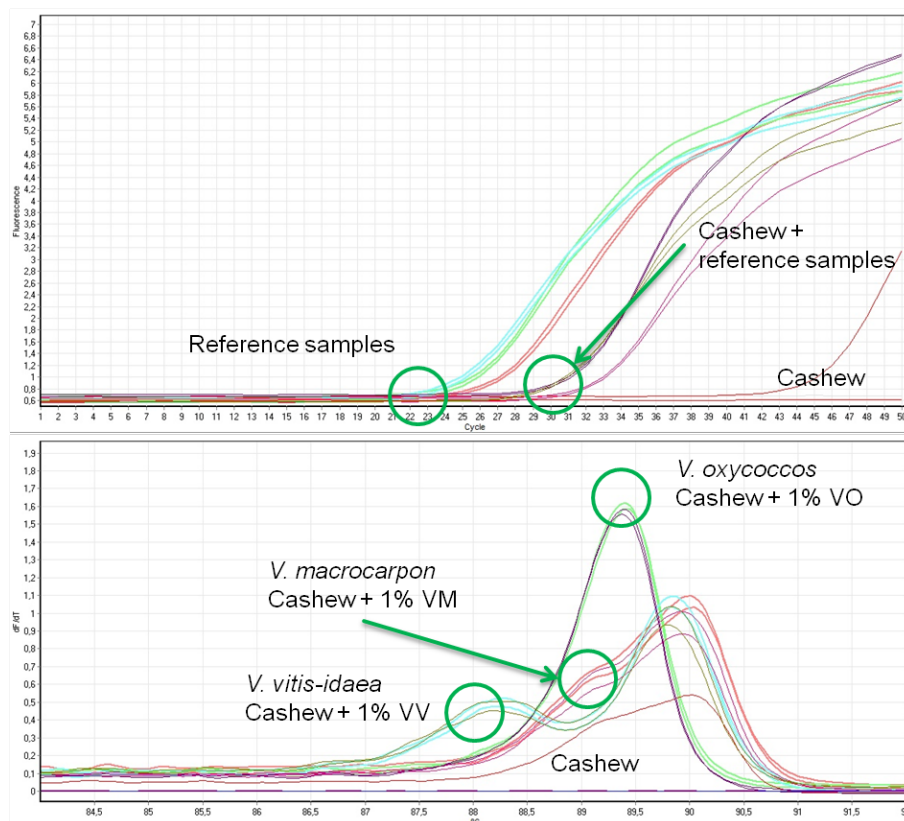
**Figure 5-31:** Confidence level for the DNA extracts spiked with 1% *Vaccinium* DNA extract obtained with the ITS2.1 primer set with the matrix components FHD, B1, K1 und M1. See chapters 7.7.2 and 7.7.3 for ID information.

As can be seen in Figure 5-31 the results for the matrices B1, K1, and M1 showed the expected increase of the confidence level (up to 98%) upon addition of 1% *Vaccinium* DNA. However, almost no change occurred when the FHD matrix was used. Although a slight increase of the confidence level occurred upon addition of 1% VO DNA and 1% VV DNA. For the addition of 1% VM DNA no classification could be obtained (see Figure 5-32).





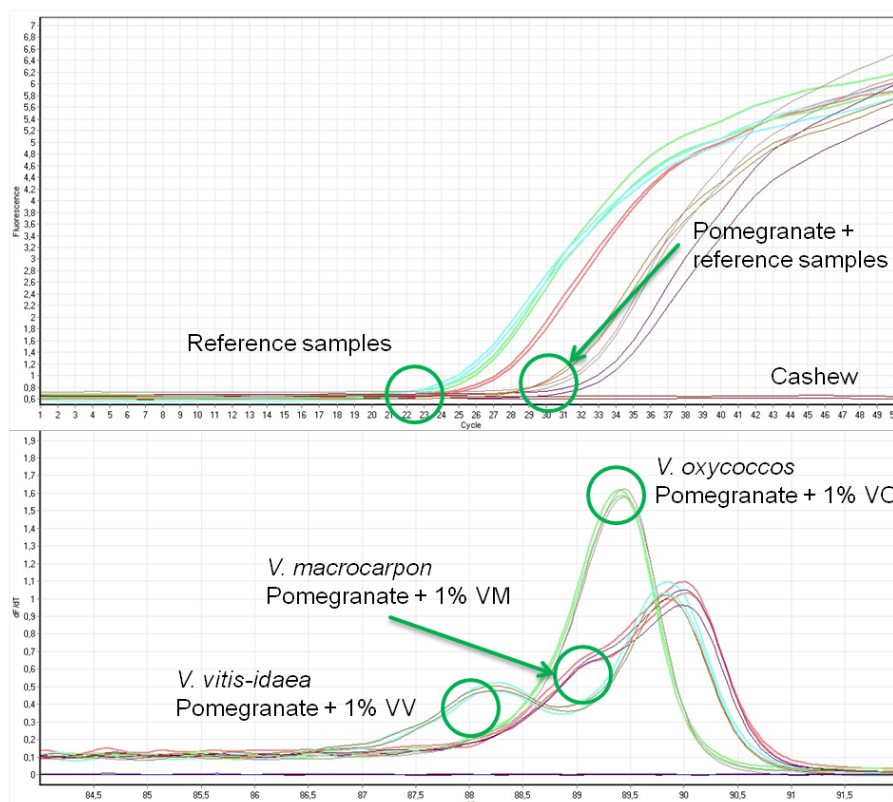
**Figure 5-32:** Amplification plot (above) and melting plot (below) of the PCR products obtained with the ITS2.1 primer set. Reference samples: red=VM (ID 3), green=VO (ID 4), blue=VV (ID 16). Sample used for spike experiments as matrix component=bilberry jam (ID FHD). See chapters 7.7.2 and 7.7.3 for ID information.



**Figure 5-33:** Amplification plot (above) and melting plot (below) of the PCR products obtained with the ITS2.1 primer set. Reference samples: red=VM (ID 3), green=VO (ID 4), blue=VV (ID 16). Sample used as matrix component=Cashew (ID B1). See chapters 7.7.2 and 7.7.3 for ID information.

Figure 5-32 shows that the  $C_T$ -values of the reference samples (VM: ID 3, VO: ID 4, VV: ID 16) are lower than the values of the matrix DNA sample with an additional 1% *Vaccinium* DNA. The matrix DNA sample cashew (ID B1) was analysed – like all the samples – as a technical duplicate (see chapter 4.5.2). One of the duplicates did not amplify, whereas the other showed a high  $C_T$ -value ( $>40$ ). When looking at the melting plot the melting curve of the duplicate sample of the cashew matrix (ID B1) that amplified, resembles the melting curve of a reference sample.

The matrix DNA sample with the 1% *Vaccinium* DNA matched the melting curves of the reference samples of the additional *Vaccinium* species well. The addition of 1% of *V. macrocarpon* DNA lead to an increase in the confidence level when classified as VM ( $>93\%$ ).



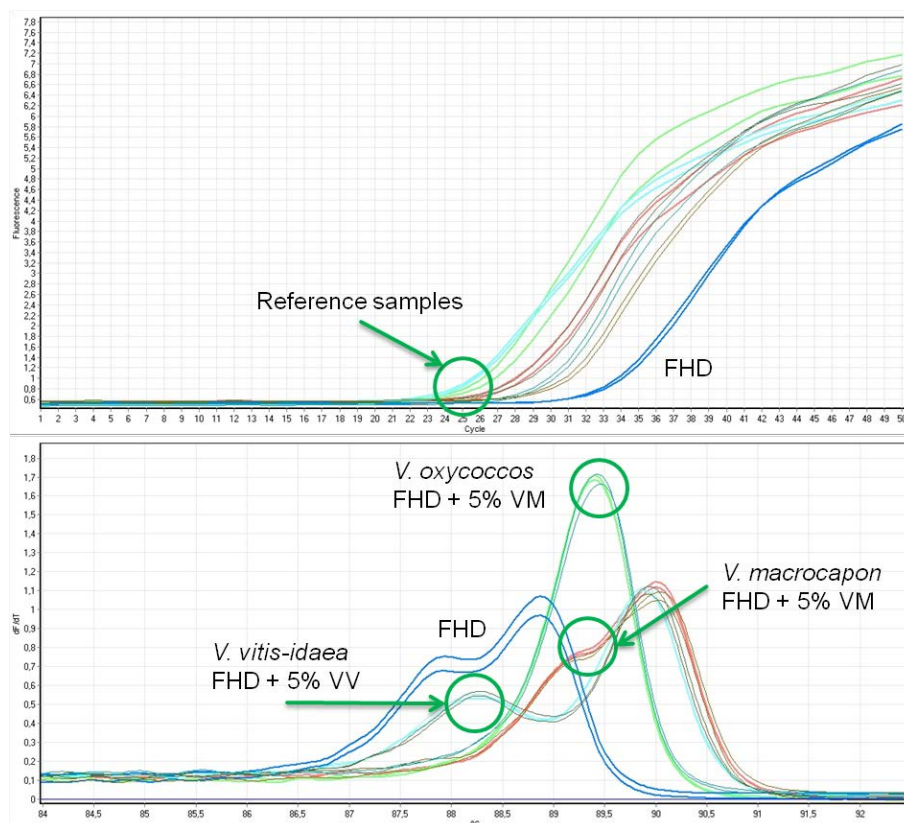
**Figure 5-34:** Amplification plot (above) and melting plot (below) of the PCR products obtained with the ITS2.1 primer set. Reference samples: red=VM (ID 3), green=VO (ID 4), blue=VV (ID 16). Sample used as matrix component=pomegranate (ID M1). See chapters 7.7.2 and 7.7.3 for ID information.

Figure 5-34 shows the results for the same experiment as Figure 5-33, but the matrix component DNA used was pomegranate (ID M1). Here too, the  $C_T$ -values of the reference samples were lower than the values obtained by the samples with an additional 1% of *Vaccinium* DNA were higher. The matrix DNA sample itself did not amplify.

When looking at the melting curves, it can be seen that the addition of 1% *Vaccinium* DNA resulted in a high similarity to the melting curves of the reference samples and thus lead to a high level of confidence in the classification (>96%).

Subsequently, it was investigated, if the addition of a higher percentage of reference DNA (5% and 10%) would lead to a different result when using a fourth *Vaccinium* species, (ID FHD<sup>9</sup>) as a matrix (as prior experiments with an addition of 1% did not shown any change in the melting curves; see above). Furthermore, a DNA mixture containing equal parts of each of the three *Vaccinium* berries DNA was also tested.

<sup>9</sup> The sample ID FHD consisted of a jam made solely out of *Vaccinium myrtillus* (see chapter 7.7.3).



**Figure 5-35:** Amplification plot (above) and melting plot (below) of the PCR products obtained with the ITS2.1 primer set. Reference samples: red=VM (ID 3), green=VO (ID 4), blue=VV (ID 16). Sample used as matrix component=bilberry jam (ID FHD). See chapters 7.7.2 and 7.7.3 for ID information.

The reference samples had a lower  $C_T$ -value than the samples containing only 1% of reference sample DNA, as can be seen in Figure 5-35. The matrix component DNA extract did amplify, which was expected, as previous results showed that the primer set ITS2.1 did lead to an amplification for other *Vaccinium* species, such as *V. myrtillus* (bilberry) and *V. corymbosum* (blueberry), as Figure 5-26 shows.

The melting curve of the matrix sample containing *V. myrtillus* (ID FHD) is clearly distinguishable from the melting curves of the three other *Vaccinium* species. However, when more than 1% DNA (e.g. 5% and 10%) of the reference samples was added, all of the melting curves match the ones of the respective *Vaccinium* reference samples added. This leads to a high level of confidence in classification, namely >96%, when 5% DNA was added, and >93% when 10% DNA was added.

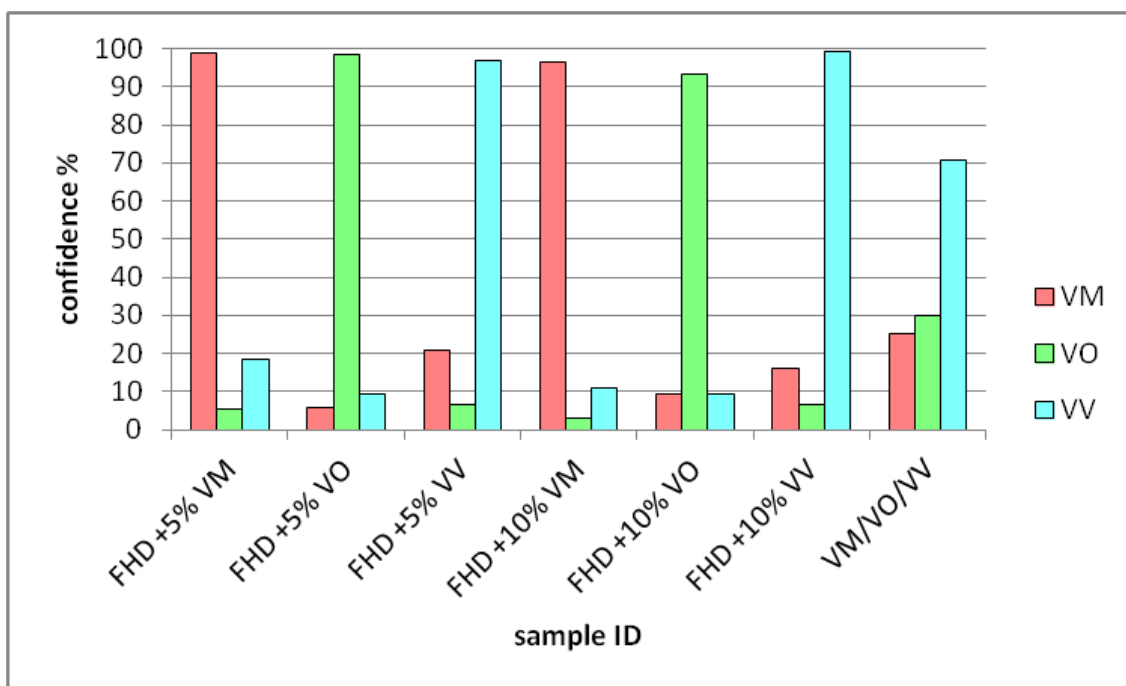


**Figure 5-36:** Confidence level for the DNA extracts spiked with 1% *Vaccinium* DNA extract obtained with the ITS2.1 primer set with the matrix components FHD with 5% and 10% addition of *Vaccinium* DNA, and a ternary mixture of three *Vaccinium* species VM (ID 3), VO (ID 4), and VV (ID 16), see chapters 7.7.2 and 7.7.3 for ID information.

When looking at the DNA mixture that contains DNA from all three *Vaccinium* species in equal amounts, the highest level of confidence was found for the classification as lingonberry (see Figure 5-36) with over 70% whereas the other two species were classified with a confidence level of 29.9% for VO, and 25.3% for VM (also see Figure 5-37). Whether this is a result of a bias of the ITS2.1 primer set towards the amplification of the *V. vitis-idaea* DNA in the presence of other *Vaccinium* species or if there is another reason, could not be determined conclusively.

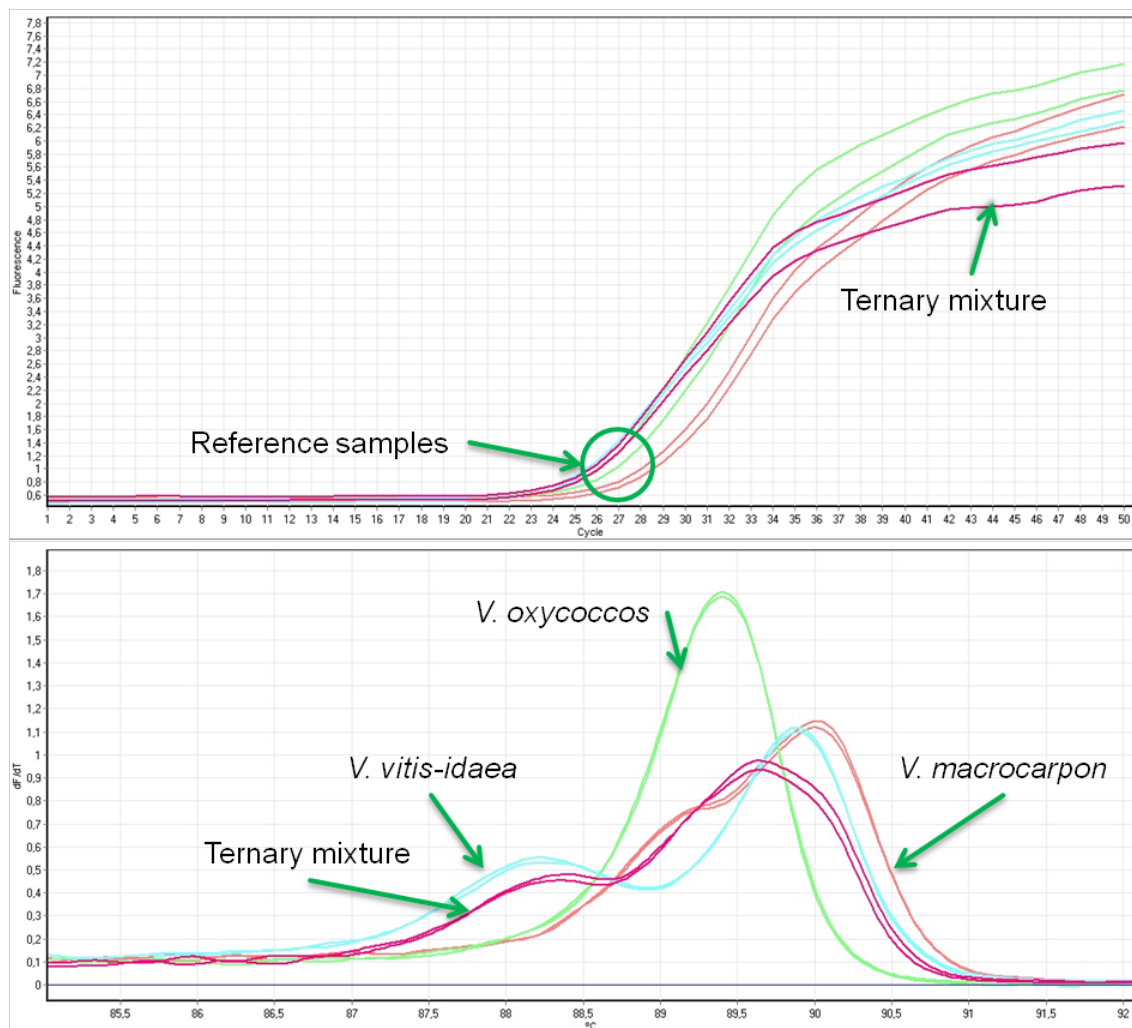


**Figure 5-37:** Amplification plot (above) and melting plot (below) of the PCR products obtained with the ITS2.1 primer set. Reference samples: red=VM (ID 3), green=VO (ID 4), blue=VV (ID 16) and the ternary mixture consisting of equal parts of DNA extracts of the three reference samples.

Furthermore, it was investigated if it was possible to distinguish mixtures between two of the berry species and if, at which concentrations.



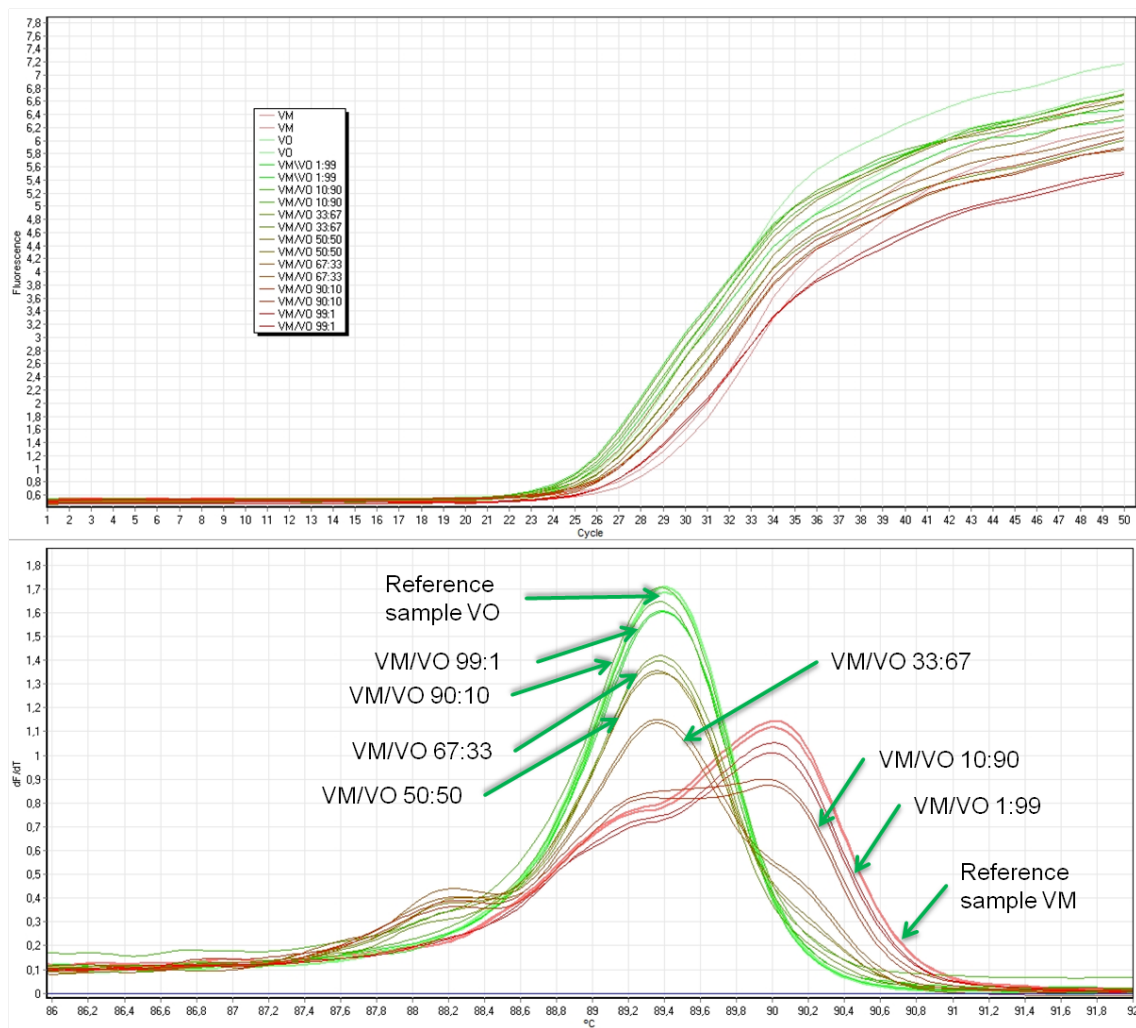


**Figure 5-38:** Amplification plot (above) and melting plot (below) of the PCR products for binary mixtures obtained with the ITS2.1 primer set. Reference samples: red=VM (ID 3), and green=VO (ID 4).

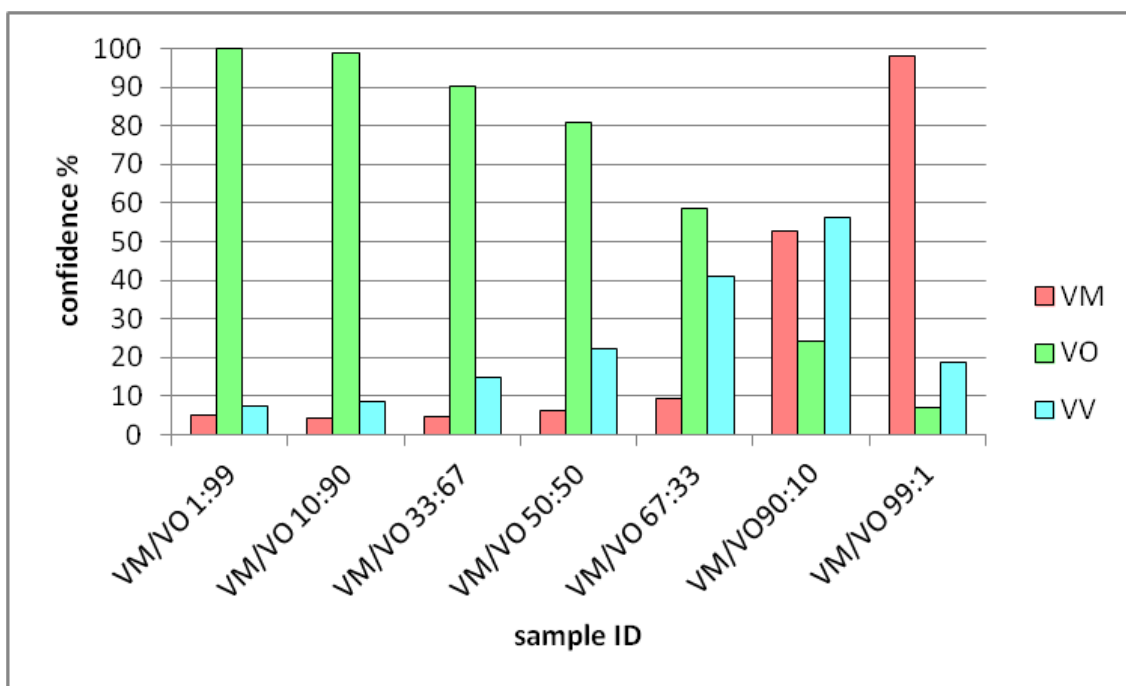


**Figure 5-39:** Confidence levels for the binary mixtures of VM and VO obtained with the ITS2.1 primer set, see chapters 7.7.2 and 7.7.3 for ID information.

As for the binary mixture of *V. macrocarpon* and *V. oxycoccos*, 0.1 ng of DNA was used for each PCR reaction, which equals 2  $\mu$ L DNA extract with a concentration of 0.05 ng/ $\mu$ L (see chapter 4.5.2). The respective concentration of the berry species DNA was ranging between 1% and 99% (see chapter 4.5.3). Clearly, the melting plot (see Figure 5-38), shows that the melting curves of the binary mixtures match the melting curves of the references samples according to the percentage of the respective *Vaccinium* DNA. As can be seen in Figure 5-39 the higher the percentage of one berry species the higher the confidence in their classification. The graph shows an increased level of confidence for the classification as lingonberry. Only when containing 90% or more of the *V. macrocarpon* DNA extract, the classification as American cranberry was predominant.



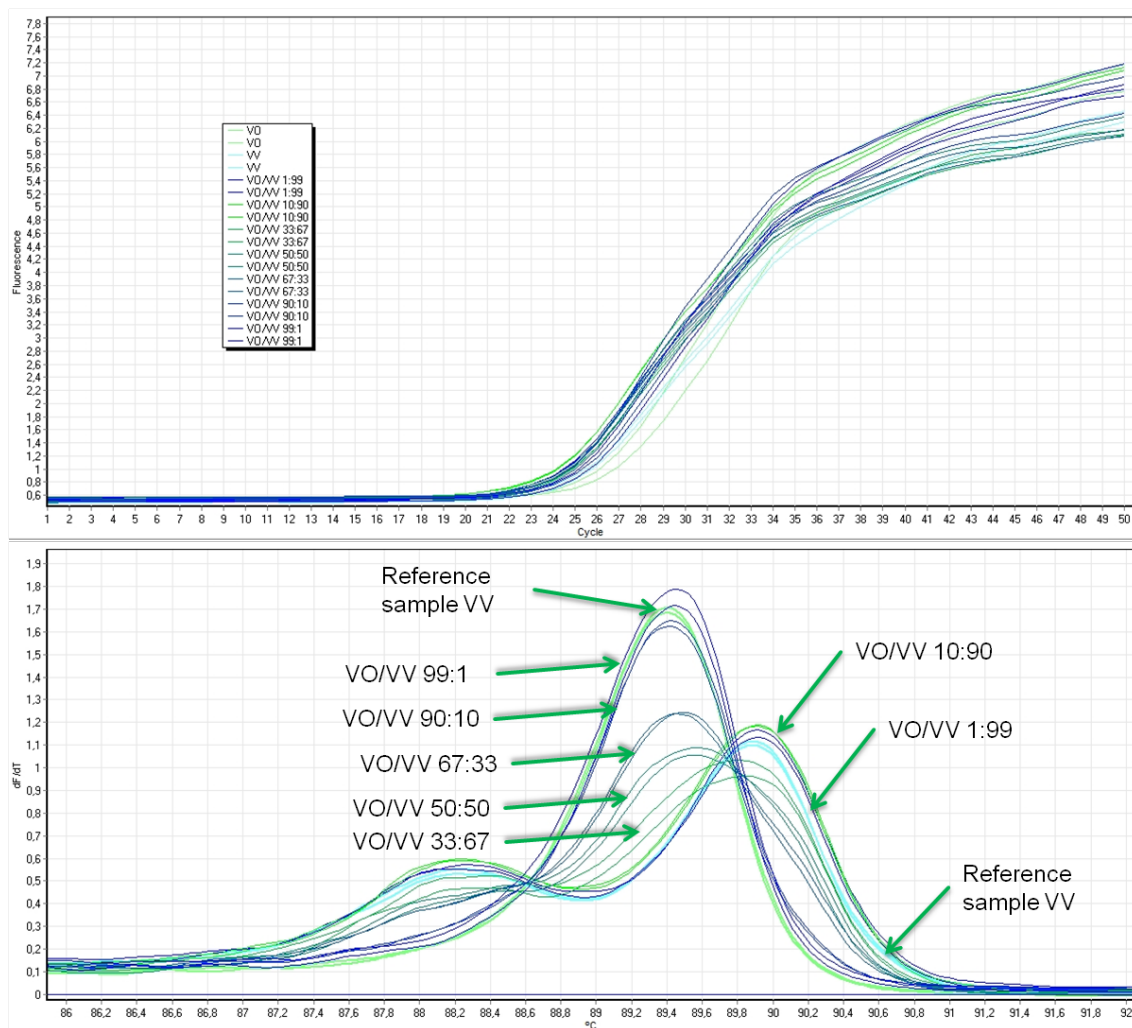


**Figure 5-40:** Amplification plot (above) and melting plot (below) of the PCR products for binary mixtures obtained with the ITS2.1 primer set. Reference samples: green=VO (ID 4), and blue=VV (ID 16).

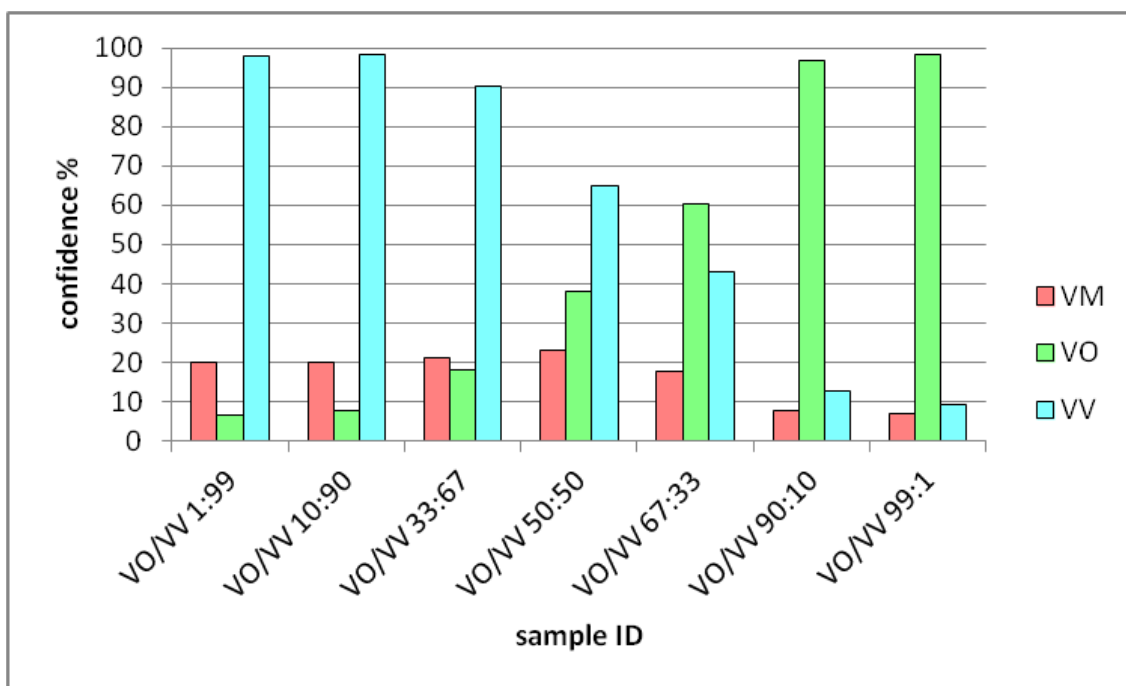


**Figure 5-41:** Confidence levels for the binary mixtures of VV and VO obtained with the ITS2.1 primer set, see chapters 7.7.2 and 7.7.3 for ID information.

When looking at the results for the binary mixtures of lingonberry and European cranberry DNA (Figure 5-40 and Figure 5-41) it is evident too, that the melting curves as well as the confidence level of the classification follows the increase or decrease of the respective DNA percentage.

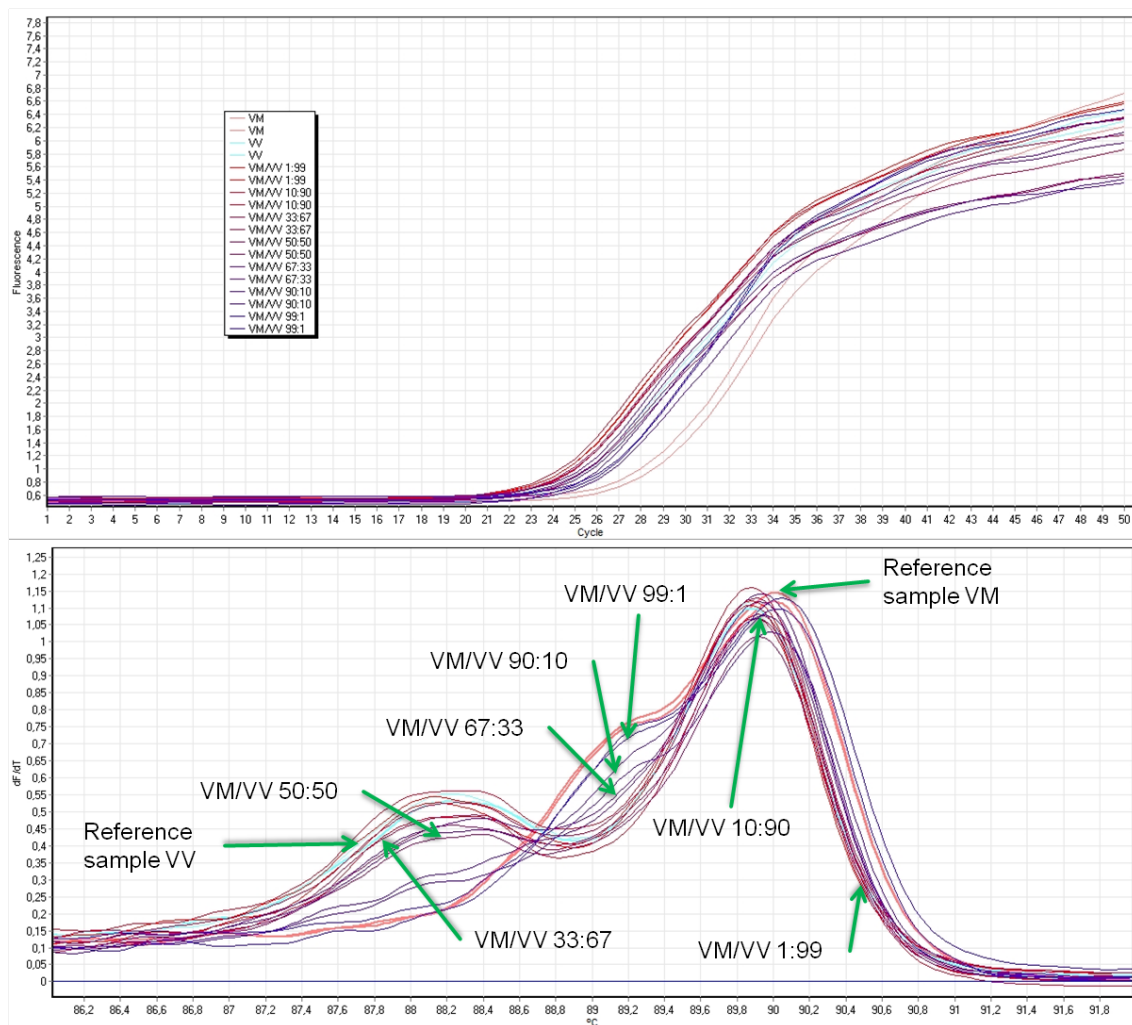


**Figure 5-42:** Amplification plot (above) and melting plot (below) of the PCR products for binary mixtures obtained with the ITS2.1 primer set. Reference samples: red=VM (ID 3), and blue=VV (ID 16).

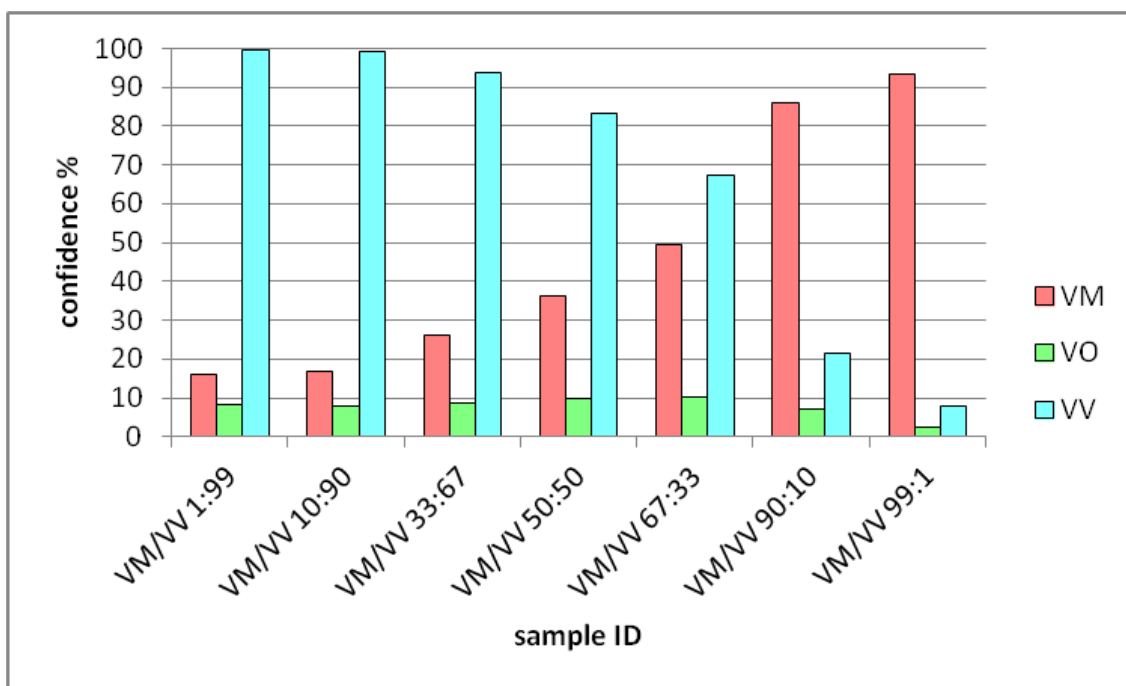


**Figure 5-43:** Confidence levels for the binary mixtures of VM and VV obtained with the ITS2.1 primer set, see chapters 7.7.2 and 7.7.3 for ID information.

The binary mixtures of *V. macrocarpon* and *V. vitis-idaea* DNA show a slightly different result (see Figure 5-42 and Figure 5-43). Again, the level of the DNA concentrations of the different berries matches the level of confidence of the classification. However, this was the only experiment conducted within this series that did not show a high confidence in assigning any of the mixtures tested to the third berry species that was no part of the original binary mixture. As a conclusion, it is expected that the presence of *V. macrocarpon* does hardly interfere with the analysis of *V. vitis-idaea* and vice versa. However, as for the presence of *V. oxycoccos* this is not true, neither for lingonberry nor for American cranberry.

### 5.6.3 Robustness – Testing QuantStudio 5 and MeltDoctor™ chemistry

To investigate the robustness of the method, a second thermal cycler, the QuantStudio 5, and a different chemistry, the MeltDoctor™ was used. The samples analysed were the reference samples VM (ID 3), VO (ID 4) and VV (ID 16). The MeltDoctor™ Master Mix required 50 µL of total reaction volume and is suitable for 20 ng of DNA per reaction tube. So we used 4 µL of the DNA extracts diluted to 5 ng/µl or undiluted when having a lower concentration – all of these concentrations were obtained by NanoDrop™ measurements. For the preparation of the Master Mix see chapter 4.5.2. So in total the DNA concentration was lower than when using the EpiTect® Master Mix. The amplification plot shows (see

Figure 5-44), that the  $C_T$  values were higher than the ones obtained with the other chemistry (EpiTect® Master Mix /Rotor Gene). This correlates well with slightly lower overall DNA concentration used.

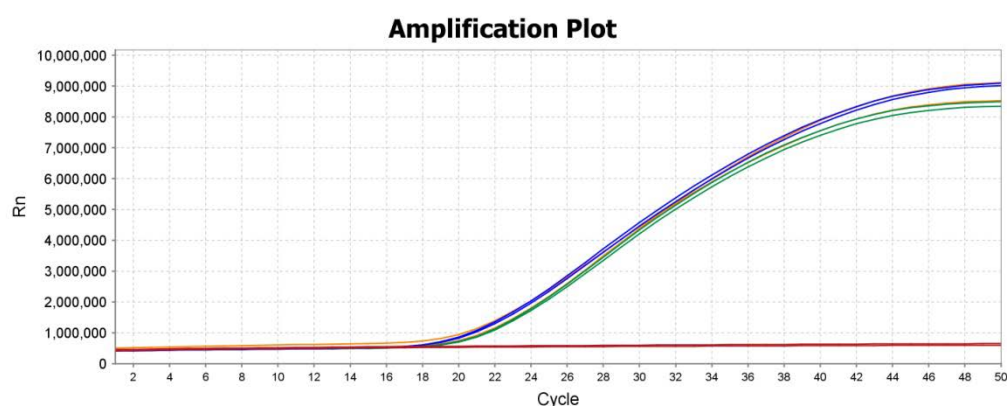


**Figure 5-44:** Amplification plot for the PCR products obtained with the ITS2.1 primer set using the MeltDoctor™ chemistry and the QuantStudio 5 cyclor. Blue= VM (ID 3), green= VO (ID 4), ochre= VV (ID 16).

The melting curves resemble the ones obtained with the EpiTect® Master Mix using the Rotor-Gene® with the melting curve of *V. oxycoccos* being very symmetrical whereas *V. vitis-idaea* yielded two peaks. The peak shape obtained by *V. macrocarpon* however was slightly different in both Master Mixes. The peak maxima of the melting plots did differ, too (see Table 5-13). Over all the peak maxima with the EpiTect® Master Mix occurred at slightly higher temperatures than with the MeltDoctor™.

**Table 5-13:** Comparison of the peak maxima of the melting plots of the reference samples with the EpiTect® and MeltDoctor™ Master Mixes.

	VM	VO	VV
MeltDoctor™	88.5°C	88.5°C	87.25/89.25°C
EpiTect®	90.0°C	89.4°C	88.2°C/89.9°C

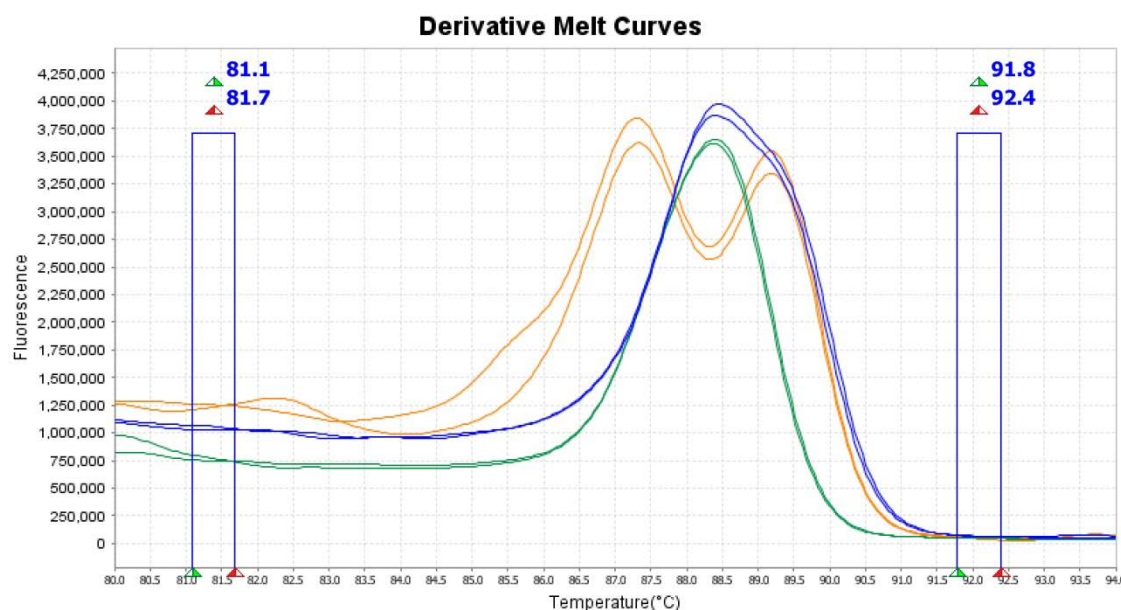


**Figure 5-45:** Melting plot for the PCR products obtained with the ITS 2.1 primer set. Blue= VM (ID 3), green= VO (ID 4), ochre= VV (ID 16), MeltDoctor™

However, all the berry species could be differentiated using the melting profile which leads to the conclusion, that the developed assay works with both thermal cyclers and both of the different Master Mixes (see Figure 5-45).

## 5.7 Detection of adulteration

As the ITS 2.1 primer set showed the best differentiation between the three berry species, all the commercial food samples (see chapter 7.7.1) were analysed using this particular primer set.

The main objective of these experiments was the classification of the food samples, and, in a second step the comparison of the assigned berry species with the labelled one. In order to analyse the results the Rotor-Gene Q Series Software was used (see chapter 5.6.1).

### 5.7.1 Herbarium samples and fresh plant samples

The herbarium samples – as discussed above – had been extracted with a slightly different method (without PVP) and kept in storage for an extended period of time prior to analysis (see chapter 4.2).

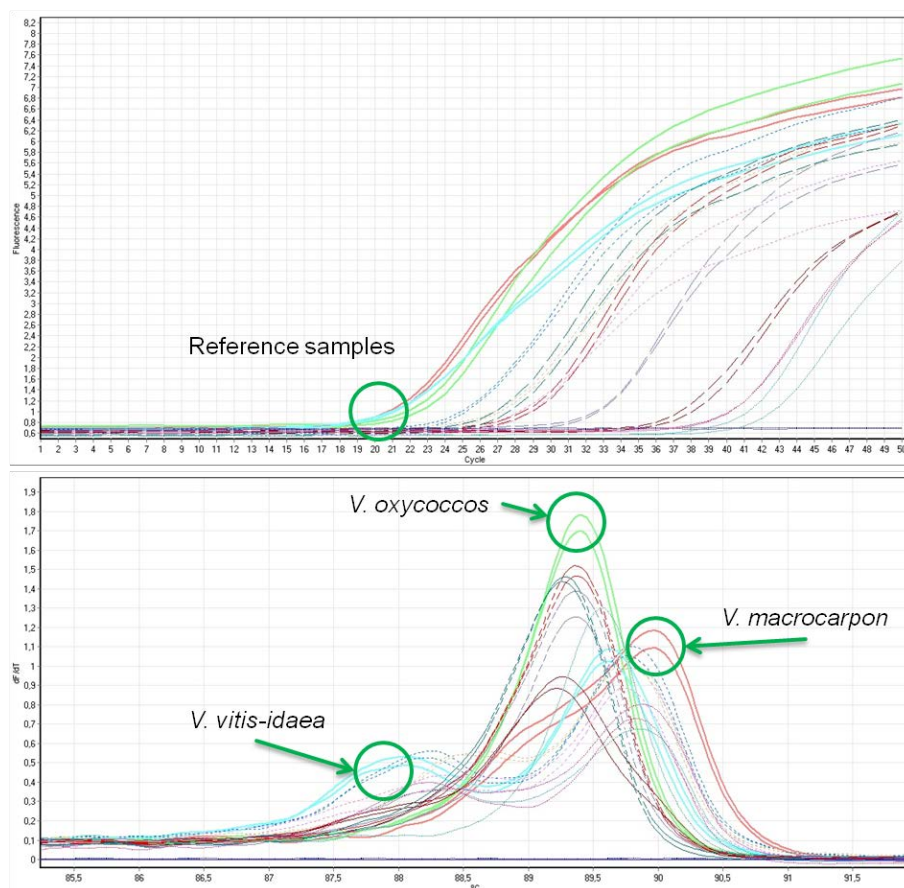


**Figure 5-46:** Amplification plot (above) and melting plot (below) of the PCR products obtained with the ITS2.1 primer set. Reference samples: red=VM (ID 3), green=VO (ID 4), blue=VV (ID 16). Dotted: VV species (H1, H2, and H3), dashed: VO species (H4 – H7), and small dots: VM species (H13, H14, and H15), see Table 4.2-1.

When looking at the amplification plot (see Figure 5-46) and the mean  $C_T$  values, it is obvious that they are higher than the mean  $C_T$  values of the respective references with  $\Delta C_T$  values<sup>10</sup> for the VV species (H1 – H3) ranging from 2.5 to 5.2. For the herbarium samples of the VO species (H4 – H7) the  $\Delta C_T$  values range from 4.4 to 14.9 and for the herbarium samples of the VM species (H13-H15) the  $\Delta C_T$  values range from 17.1 to 18.7 (see Table 5-14); one sample (H14) did not amplify. This is an indicator of possible degradation of the DNA extracts (see chapter 7.7.2).

<sup>10</sup> The  $\Delta C_T$  value is obtained by subtracting the mean  $C_T$  value of all the reference samples from the mean  $\Delta C_T$  value of the respective sample.

**Table 5-14:** Mean  $C_T$  values (n=2) and  $\Delta C_T$  values for the herbarium sample DNA extracts and the reference DNA samples

ID	mean $C_T$ value	$\Delta C_T$ value
3 (VM)	17.7	
4 (VO)	17.3	
16 (VV)	16.6	
H1	19.7	2.5
H2	22.4	5.2
H3	21.7	4.5
H4	23.4	6.2
H5	27.4	10.2
H6	32.1	14.9
H7	21.6	4.4
H13	35.9	18.7
H14	-	
H15	34.3	17.1
- ... no amplification		

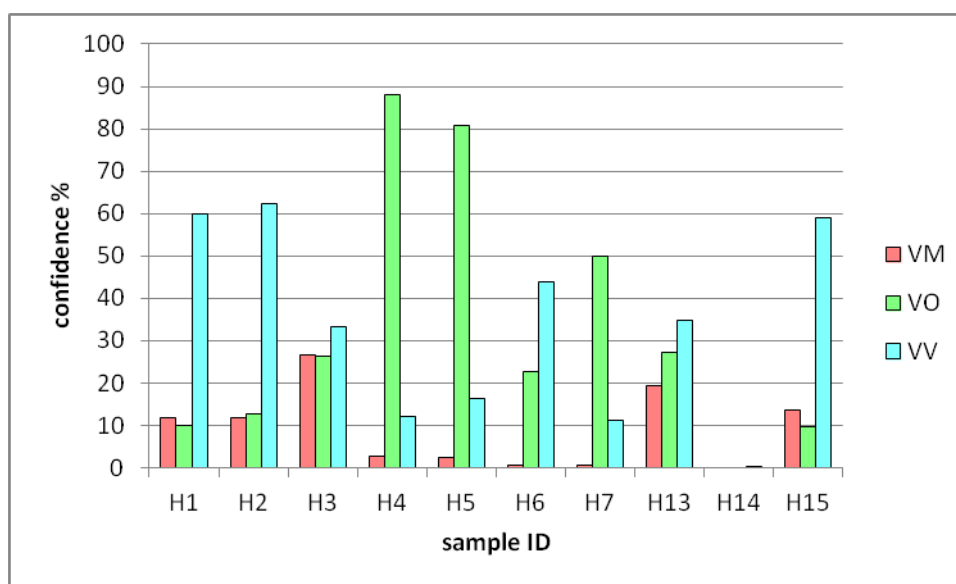


**Figure 5-47:** Confidence levels of the classification of herbarium sample DNA obtained with the ITS2.1 primer set. H1, H2, and H3 were VV species, H4 – H7 were VO species, and H13, H14, and H15 were VM species. (see Table 4-1).

The samples H1, H2, and H3 were labelled as *V. vitis-idaea* (see Table 4-1). All three of them showed the highest accordance with the VV genotype as can be seen in Figure 5-47. The samples H4 – H7 are all labelled *V. oxycoccos*, but H6 – one of the oldest herbarium



samples, collected in 1921 – has a higher resemblance to VV than to VO. As for the last herbarium sample group H13, H14, and H15, all labelled as *V. macrocarpon*, the results showed no or little accordance with the expected VM genotype. The reason for this outcome may be the fact, that the specimen had been dried and stored that way for an extended period of time prior to extraction.

**Table 5-15:** Mean  $C_T$  values (n=2) and  $\Delta C_T$  values for the sample DNA extracts labelled as *V. macrocarpon* obtained by other plant parts.

ID	mean $C_T$ value	$\Delta C_T$ value
3	17.7	
27	18.9	1.69
60	22.9	5.67
61	17.5	0.25
62	17.9	0.67
65	20.1	2.91
68	17.4	0.21
73	21.6	4.41
74	16.9	-0.22
75	20.4	3.17
76	17.2	-0.01

Alongside herbarium samples (leaves), other plant parts were subjected to our method. Seeds (ID 68, 76), leaves (ID 61, 62), and fresh fruit were tested (ID 27, 60, 65, 73, 74, 75), which all were labelled as *Vaccinium macrocarpon*. The  $C_T$  values were similar to the  $C_T$  value of the reference sample (ID 3), with leaves and seeds yielding the lowest values  $\Delta C_T$  values (see Table 5-15).

All of the samples showed a high (>85%) level of confidence when classified as *Vaccinium macrocarpon* (see Figure 5-48). This leads to the conclusion, that for our method tested it is irrelevant of which plant part DNA is extracted of.

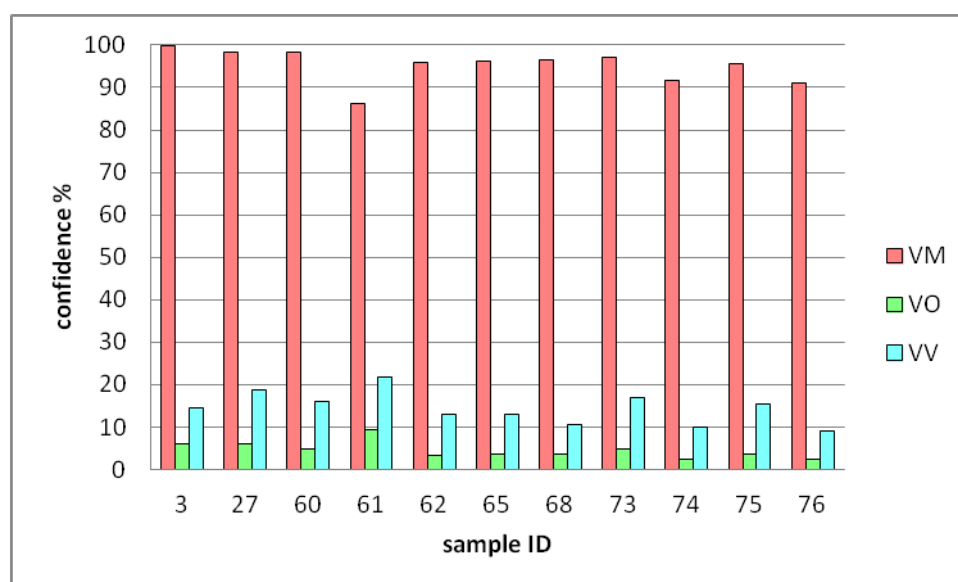


**Figure 5-48:** Confidence levels of the classification of seeds (ID 68, 76), leaves (ID 61, 62), and fresh fruit (ID 27, 60, 65, 73, 74, 75) obtained with the ITS2.1 primer set.

### 5.7.2 Products labelled as containing lingonberry

A variety of products that was declared containing lingonberry was analysed with regard to verifying this claim. We obtained juices (ID 19, ID 48, ID 52), jams (ID 44, ID 45, ID 53, ID 56), supplements (ID 12, and ID 43), a mustard (ID 51), a horseradish (ID 33), and a cereal bar (ID 77) from various sources. Furthermore, three plant samples – apart from the reference sample (ID 16), were investigated (ID 31, ID 34, and ID 46).

**Table 5-16:** Mean  $C_T$  values (n=2) and  $\Delta C_T$  values for samples labelled as containing *V. vitis-idaea*

ID	mean $C_T$ value	$\Delta C_T$ value
12	23.5	6.3
16	15.0	
19	33.0	15.8
31	18.2	1
33	33.3	16.1
34	17.3	0.1
43	32.9	15.7
44	26.9	9.7
45	35.4	18.2
46	17.3	0.1
48	36.8	19.6
51	40.0	22.8
52	37.6	20.4
53	22.8	5.6
54	25.5	8.3
55	29.3	12.1
56	34.7	17.5
77	30.9	13.7

When comparing the  $\Delta C_T$  values obtained for the DNA extracts of the samples with the ones obtained by the reference samples (VM ID 3, VO ID 4, VV ID 16; see Table 5-16), the values were higher. This correlates with the fact that the positive control samples were taken from unprocessed plants resulting in relatively pure and unfragmented DNA. When extracting DNA from processed foods however the level of degradation caused by processing is unbeknownst to the experimenter. Therefore, the  $C_T$  values obtained are a result of the fact that the DNA might have been degraded before the extraction on the one hand. On the other hand, none of the products investigated

contained 100% berries. This means, that only a fraction of the extracted DNA originated from the (lingon)berries in the product.

14 of the 17 samples show a high level of confidence when classified as *V. vitis-idaea* thus correlating with their respective label (see Figure 5-49). Sample ID 33 – a horseradish with lingonberries – shows almost the same confidence level for both, *V. vitis-idaea* and *V. macrocarpon*. Two samples, a concentrated juice (ID 52), and a cereal bar labelled as containing only lingonberry concentrate (ID 77), were clearly identified as containing cranberry instead of lingonberry.

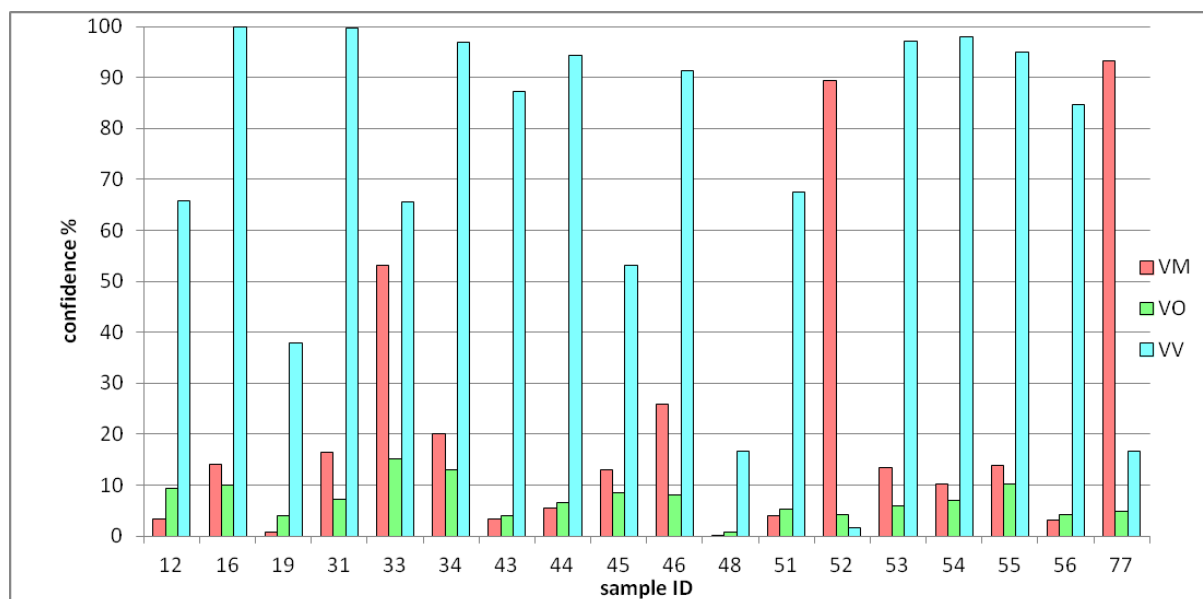


**Figure 5-49:** Confidence levels for samples declared as containing lingonberry obtained with the ITS2.1 primer set. Reference sample: ID 16. Samples: juices (ID 19, ID 48, ID 52), jams (ID 44, ID 45, ID 53, ID 56), supplements (ID 12, ID 43), mustard (ID 51), horseradish (ID 33), cereal bar (ID 77), plant samples – (ID 31, ID 34, and ID 46).

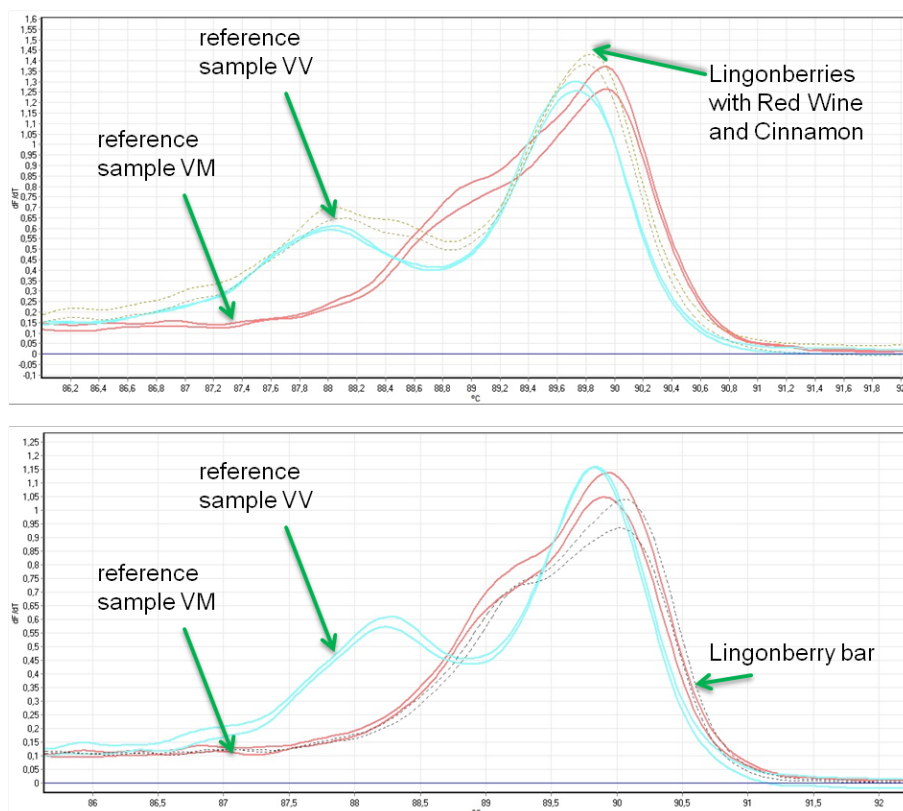


**Figure 5-50:** Melting plot of the PCR products obtained with the ITS2.1 primer set. Reference samples: red=VM (ID 3), blue=VV (ID16). Above: lingonberries with red wine and cinnamon (ID 53), below: lingonberry bar (ID 77).

As can be seen in Figure 5-50, the melting curve belonging to ID 53 matches the melting curve of the reference sample of VV (ID 4), resulting in a high level of confidence (>97%), whereas the melting curve belonging to ID 77 resembles the melting curve of the reference sample of VM (ID 3). This results in a low confidence level when assigned to VV (<20%), but a high level when assigned to VM (>93%).

### 5.7.3 Products labelled as containing European Cranberry

Of the three berry species investigated in course of this research products containing *V. oxycoccos* were most difficult to obtain. Apart from one reference specimen, another plant sold as “*V. oxycoccos*” turned out to classify as cranberry (ID 30).

**Table 5-17:** Mean  $C_T$  values (n=2) and  $\Delta C_T$  for samples labelled as containing *V. oxycoccus*

ID	mean $C_T$ value	$\Delta C_T$ value
4	17.3	
11	25.4	8.2
30	19.8	2.6
66	43.8	26.6
67	33.2	16

The DNA extract of the other plant specimen (ID 30) showed a similar  $C_T$ -value as the reference sample (ID 4). The DNA extracts of the supplement (ID 11) and the juice (ID 67) had higher  $C_T$ -values than the reference, most likely due to fragmented DNA in course

of the processing. The DNA extract of the paste (ID 66) had the highest  $C_T$ -value, indicating the highest grade of processing of the commercial samples labelled as containing European cranberry (see Table 5-17 for  $\Delta C_T$  values).

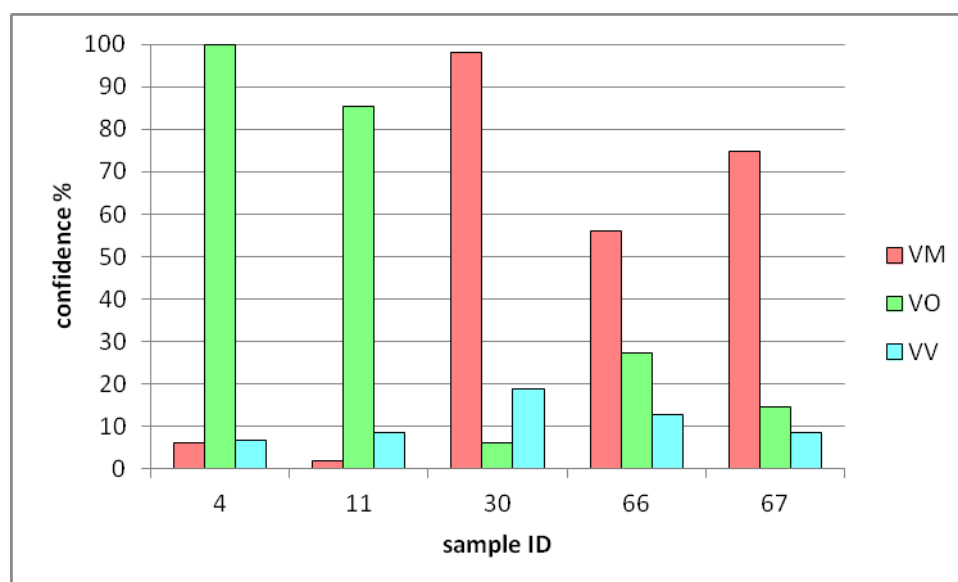


**Figure 5-51:** Confidence levels for samples declared as containing European cranberry obtained with the ITS2.1 primer set. Reference sample: ID 4. Samples: other plant specimen (ID 30), supplement (ID 11), juice (ID 67), paste (ID 66).

Two products, a paste (ID 66) and a juice (ID 67), were advertised to specifically contain *V. oxycoccus* (German: Moosbeere). By using our method this could not be verified (see Figure 5-51). Our result rather point to these products containing cranberry instead.

ID 11, a supplement named “Cranberrypulver” (powdered cranberries) and labelled “*V. oxycoccus*, Moosbeere”, was classified as *V. oxycoccus* (see Figure 5-52). This example shows the need for the method developed as the labelling is unclear and leads to confusion.

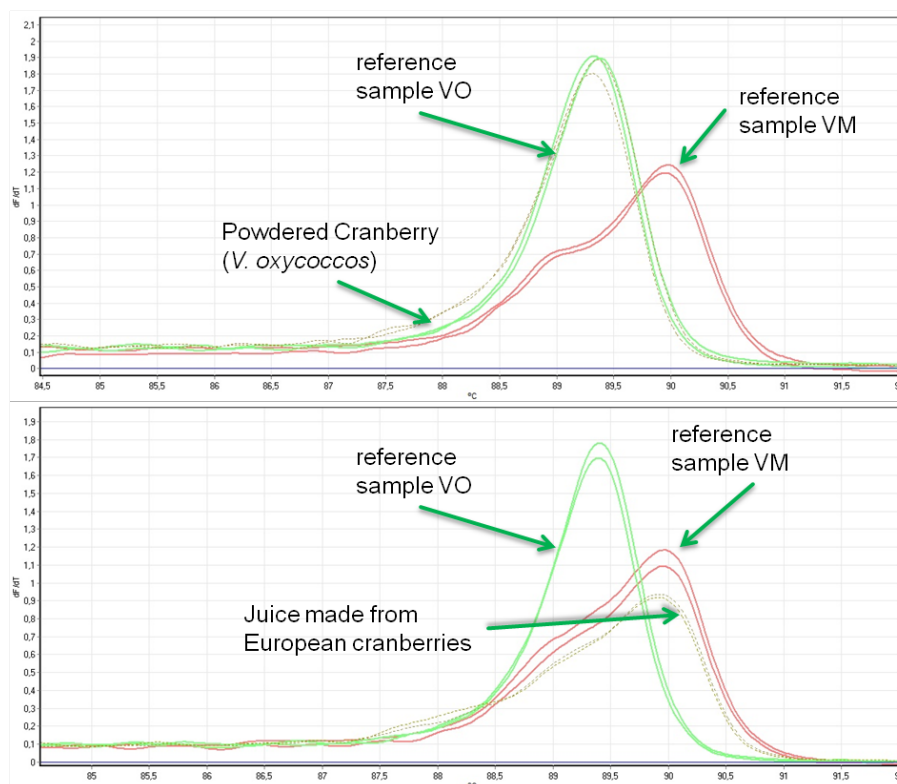


**Figure 5-52:** Melting plots of the PCR products obtained with the ITS2.1 primer set. Reference sample: red=VM (ID 3), green=VO (ID4). Above: powdered cranberry (ID 11). Below: juice made from European cranberries (ID 67).

#### 5.7.4 Products labelled as containing (American) Cranberry

The majority of commercial samples analysed were labelled containing cranberry. The biggest portion of these samples were juices (see chapter 7.7.1), six of them containing only cranberry (ID 5, 6, 47, 72, 82, and 83) and eight mixed ones (ID 18, 20, 22, 23, 29, 64, 81, and 84). Furthermore, different jams were analysed (ID 17, 59, 86, 87, and 88), as well as dried cranberry fruits accompanied by different sorts of nuts (“Fruit”, ID 2, 7, 8, 9, 24, 26, 63, 70, and 80). Other products tested were supplements (ID 10, 13, 14, and 15) and dairy (ID 1, and ID 91), and a variety of cereal bars (ID 21, 35, 36, 50, 78, and 79). Also, seven different chocolates (dark, milk, and white) were analysed (ID 32, 37, 57, 58, 71, 89, and 90) as well as teas (ID 38, ID 39, ID 40, and ID 41). The category “Diverse” consisted of “one of a kind” products, a jellied cranberry sauce (ID 28), cookies with cranberry (ID 42), a BBC sauce with cranberries (ID 49), and vinegar with cranberry concentrate (ID 85).

#### 5.7.4.1 Juices

14 different juices were investigated. Nine of these samples were pure juices meaning that no other relevant ingredients (apart from water and sugar) were present. Five juices were mixed, either with other juices, aloe vera (ID 29), or kombucha (ID 23).

**Table 5-18:** Mean  $C_T$  values (n=2) and  $\Delta C_T$  values for samples labelled as containing (*American*) *cranberry* (juices)

ID	mean $C_T$ value	$\Delta C_T$ value
5	27.7	10.5
6	30.2	13.0
18	33.2	16.0
20	38.2	21.0
22	-	
23	36.2	19.0
29	-	
47	34.5	17.3
64	36.1	18.9
72	33.9	16.7
81	29.0	11.8
82	32.7	15.5
83	34.9	17.7
84	31.8	14.6
- ... no amplification		

The mean  $C_T$  values of the DNA extracts were higher than the one of the reference samples (VM ID 3, VO ID 4, VV ID 16, see Table 5-18) resulting in high  $\Delta C_T$  values, most probably due to the reasons explained above: DNA degradation due to processing and lower amount of berry DNA in the extracts due to other ingredients.

Two of the samples, a pure juice (ID 22), and a mixed juice with aloe vera (ID 29) did not show any amplification during PCR, thus a classification was not possible.

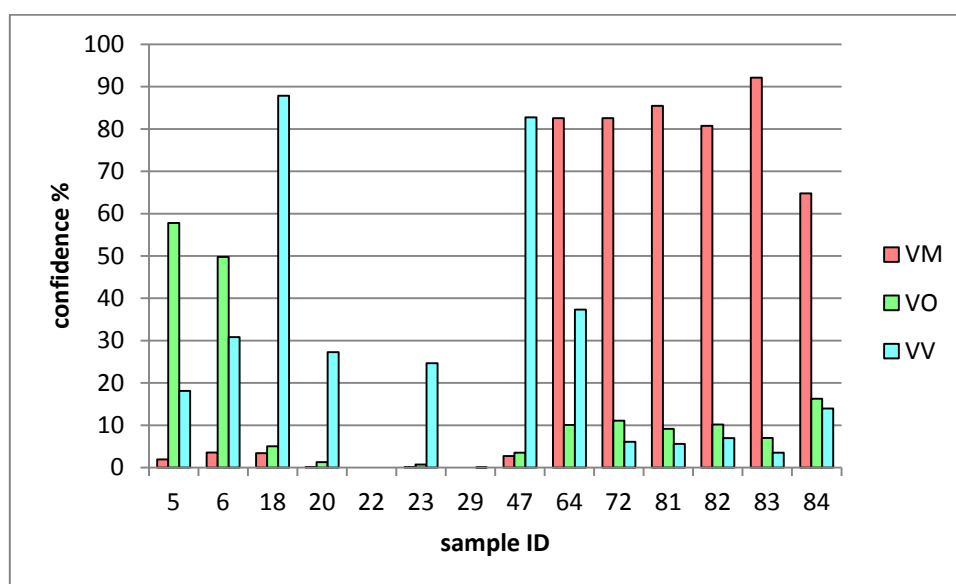


**Figure 5-53:** Confidence levels for juice samples declared as containing (*American*) *cranberry* obtained with the ITS2.1 primer set.

Four of the juices, three mixed ones (ID 18 “red fruits”, ID 20 “cranberry aronia”, and ID 23 “kombucha”), and one pure juice (ID 47), were classified as containing lingonberry rather than cranberry, as the label suggested. Interestingly, two of the juices (ID 5 and ID 6) were classified by the method as containing *V. oxycoccus*. For six of the juices the labelling matched our findings (see Figure 5-53 and Figure 5-54).

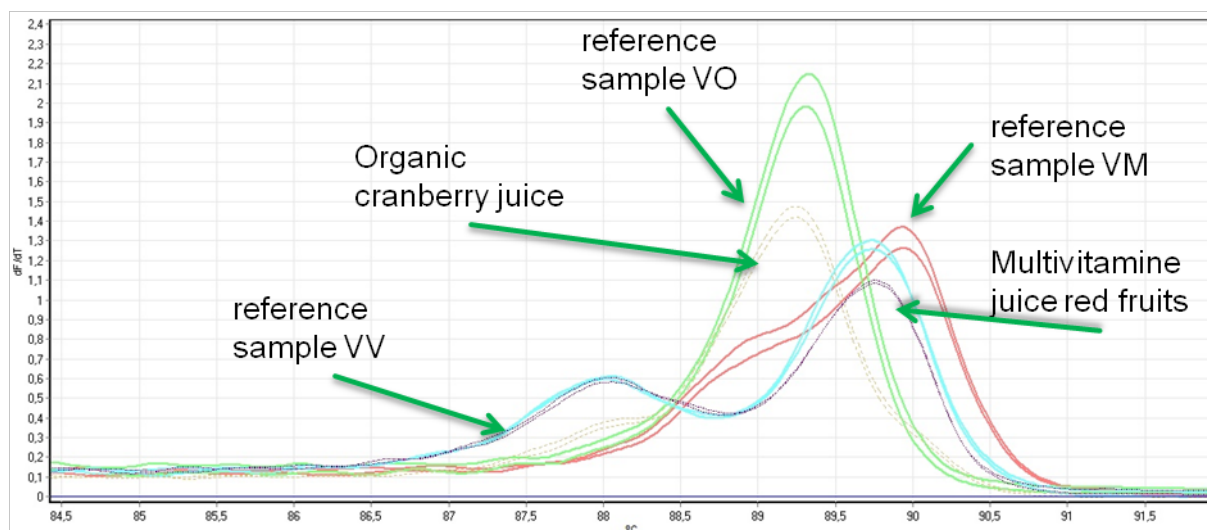


**Figure 5-54:** Melting plot of the PCR products obtained with the ITS2.1 primer set. Reference samples: red=VM (ID 3), green=VO (ID 4), blue=VV (ID 16). Grey dotted=organic cranberry juice (ID 5), purple dotted=multivitamin juice red fruits (ID 18).

#### 5.7.4.2 Diverse, Fruit, Jam:

We found that dried cranberry fruits accompanied by different sorts of nuts or without any addition were relatively common. We tested nine of these products (“Fruit”, ID 2, 7, 8, 9, 24, 26, 63, 70, and 80). Furthermore, 5 different jams were analysed (ID 17, 59, 86, 87, and 88). The last category “Diverse” consisted of “one of a kind” products, namely a jellied cranberry sauce (ID 28), cookies with cranberry (ID 42), a BBQ sauce with cranberries (ID 49), and vinegar with cranberry concentrate (ID 85).



**Table 5-19:** Mean  $C_T$  values (n=2) and  $\Delta C_T$  values for samples labelled as containing (American) cranberry (diverse, fruit, jam)

ID	mean $C_T$ value	$\Delta C_T$ value
28	30.94	13.7
42	36.27	19.1
49	34.27	17.1
85	35.10	17.9
2	33.29	16.1
7	30.56	13.4
8	26.70	9.5
9	28.15	10.9
24	22.68	5.5
25	24.08	6.9
26	35.85	18.7
63	28.61	11.4
70	31.91	14.7
80	28.15	10.9
17	28.94	11.7
59	36.51	19.3
86	31.83	14.6
87	32.56	15.7
88	29.33	12.1

The  $C_T$ -values for the DNA extracts of all these products were higher than the values of the reference samples (VM ID 3, VO ID 4, VV ID 16), this results in high  $\Delta C_T$  values (see Table 5-19). But all of the DNA extracts of the samples did amplify and yielded a PCR product and thus a melting curve.

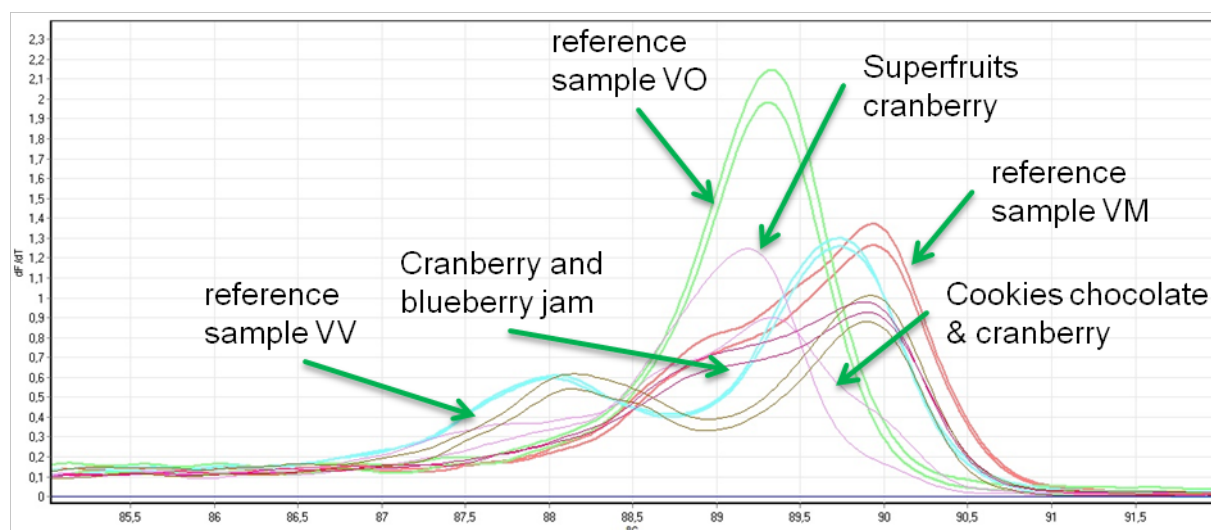


**Figure 5-55:** Melting plot of the PCR products obtained with the ITS2.1 primer set. Reference samples: red=VM (ID 3), green=VO (ID 4), blue=VV (ID 16). rosé=cranberry superfruits (ID 2), pink=cranberry and blueberry jam (ID 17), brown= cookies chocolate and cranberries (ID 42).

Only two samples of the product category “Diverse” could positively been identified as containing cranberry, namely the BBQ sauce (ID 49), and the cranberry vinegar (ID 85). For the cookie, the results showed a classification as *V. oxycoccos*, the results for the cranberry sauce, too, showed the highest match in the level of confidence with *V. oxycoccos*.

Apart from ID 9, a nut-cranberry mix, and ID 25, dried cranberries, which were both classified as *V. oxycoccos* by our method, the majority (ID 8, 24, 63, 70, and 80) were identified as cranberry. ID 2, dried cranberries that were formerly mixed with a variety of other fruits such as mulberries, pomegranate and bilberries, as well as ID 7, another variety of dried cranberries, were classified as lingonberry. ID 26 was classified as *V. vitis-idaea*, too, which is notable insofar as this sample was labelled “craisins dried cranberries”, but the term craisins was no further clarified.

As for the jams tested ID 17, ID 87, and ID 88 were identified as positively containing cranberries (although curiously enough the latter stated on its label “Cranberry” (Moosbeere) with Moosbeere being the German word for *V. oxycoccos*). The two other jams could not be assigned to the cranberry category as the assay identified them as containing lingonberry (see Figure 5-55 and Figure 5-56).

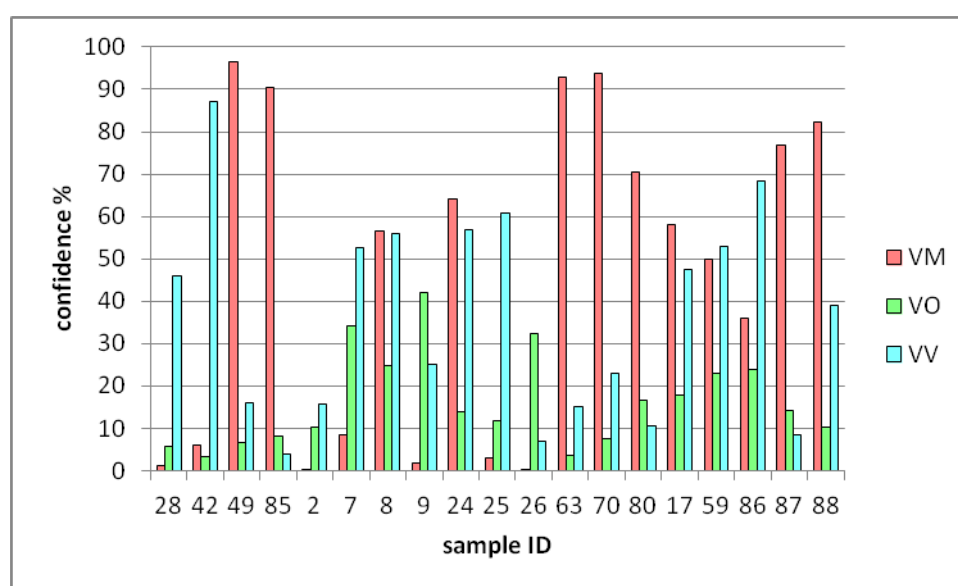


**Figure 5-56:** Confidence levels for diverse (ID 28, ID 42, ID 49, ID 85), fruit (ID 2, 7, 8, 9, 24, 26, 63, 70, and 80), and jam (ID 17, 59, 86, 87, and 88) samples declared as containing (American) cranberry obtained with the ITS2.1 primer set.

#### 5.7.4.3 Dairy, and Supplements

Supplements containing cranberries were also tested (ID 10, 13, 14, and 15). Furthermore, dairy products were analysed (ID 1, yoghurt, and ID 91, skyr).

**Table 5-20:** Mean  $C_T$  values (n=2) and  $\Delta C_T$  values for samples labelled as containing (*American*) cranberry (dairy, and supplements)

ID	mean $C_T$ value	$\Delta C_T$ value
1	34.5	17.3
91	33.6	16.4
10	39.0	21.8
13	36.0	18.8
14	35.3	18.1
15	28.6	11.4

All samples did amplify and yielded a PCR product. The  $C_T$ -values of all these products were higher than the ones of the reference samples (VM ID 3, VO ID 4, VV ID 16) thus leading to a high  $\Delta C_T$  value (see Table 5-20). This finding can be explained by a higher grade of processing and thus, degraded DNA.

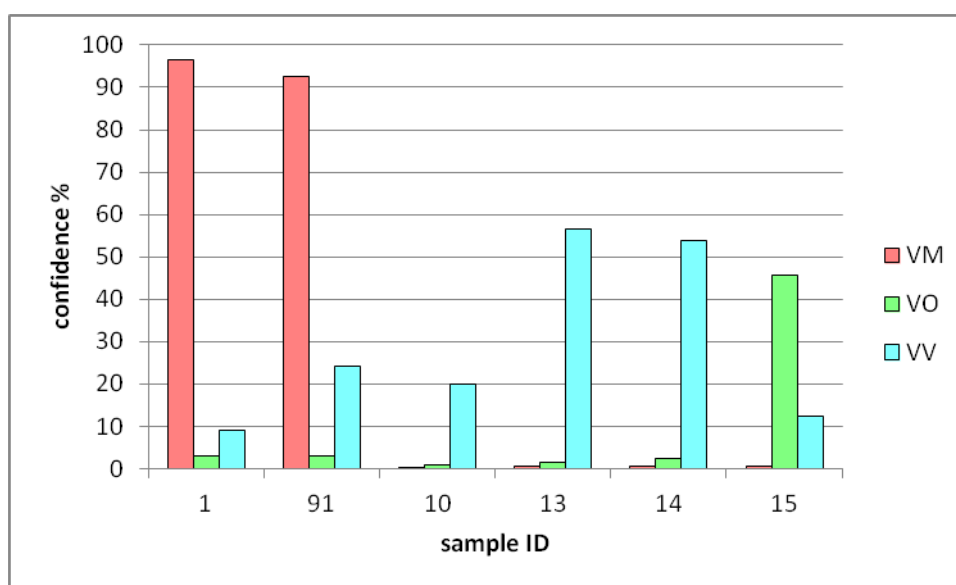


**Figure 5-57:** Confidence levels for dairy (ID 1, ID 91), and supplement samples (ID 10, 13, 14, and 15) declared as containing (*American*) cranberry obtained with the ITS2.1 primer set.

Both of the dairy products (ID 1, and ID 91) showed a high level of confidence concerning their classification as cranberry (>92%), as can be seen in Figure 5-57.

None of the supplement samples could be classified as containing *V. macrocarpon* with our method. Three of these samples were classified as containing *V. vitis-idaea*, and one (ID 15) was classified as containing *V. oxycoccos*. This is an interesting finding, as it was hard to

obtain commercial products labelled as containing *V. oxycoccus*. Of these products, for the majority this labelling could not be verified (see Figure 5-58).

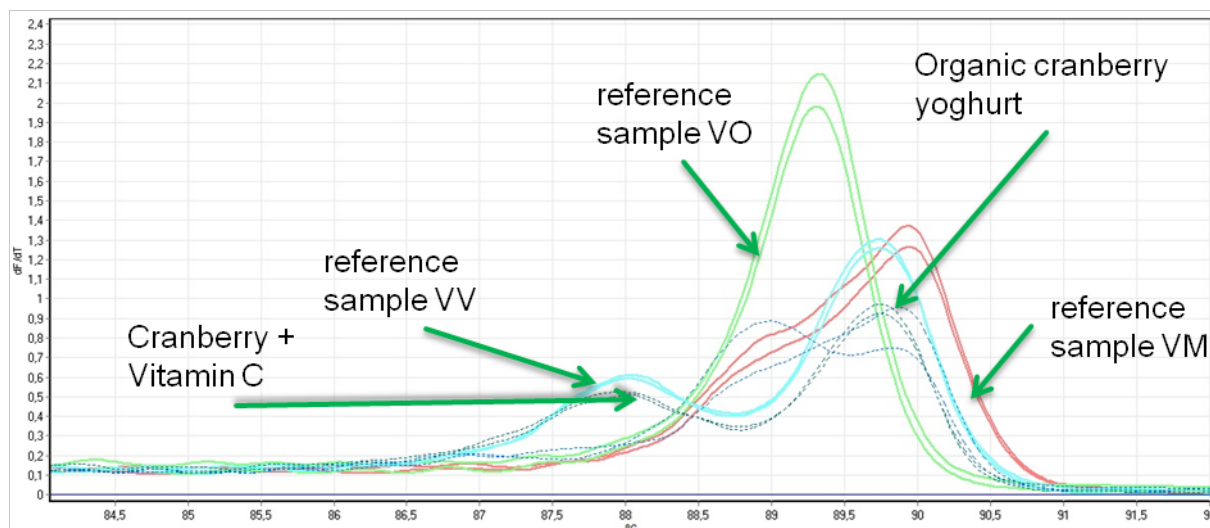


**Figure 5-58:** Melting plot of the PCR products obtained with the ITS2.1 primer set. Reference samples: red=VM (ID 3), green=VO (ID 4), blue=VV (ID 16). Blue dotted=organic cranberry yoghurt (ID 1), teal dotted=cranberry+Vitamin C (ID 13).

#### 5.7.4.4 Cereal bars, chocolates and tea:

Next to simple dried cranberries, a variety of cereal bars containing cranberries are commercially available; we investigated six different ones (ID 21, 35, 36, 50, 78, and 79). Seven different chocolates (dark, milk, and white) were analysed (ID 32, 37, 57, 58, 71, 89, and 90). The last group tested were teas. One pure cranberry tea (ID 40) was investigated, and three types of tea were labelled as mixed with other ingredients such as blueberry or raspberry (ID 38, 39, and 41).

**Table 5-21:** Mean  $C_T$  values (n=2) and  $\Delta C_T$  values for samples labelled as containing (*American*) *cranberry* (cereal bars, chocolates, tea)

ID	mean $C_T$ value	$\Delta C_T$ value
21	33.15	15.9
35	30.02	12.8
36	32.52	15.3
50	27.33	10.1
78	30.52	13.3
79	28.61	11.4
32	34.22	17.0
37	25.79	8.6
57	41.83	24.6
58	36.51	19.3
71	22.42	5.2
89	32.21	15.0
90	26.07	8.9
38	36.38	19.2
39	33.87	16.7
40	25.31	8.1
41	35.39	18.2

All samples of these three product groups did amplify and yielded PCR products. All  $C_T$ -values were higher than the ones of the reference samples (VM ID 3, VO ID 4, VV ID 16). This can be explained by a higher grade of processing and thus, degraded DNA. The mean  $\Delta C_T$  values for the DNA extracts of the cereal bars were lower than the mean  $\Delta C_T$  value of the chocolates. The DNA extracts of the teas investigated had the highest  $\Delta C_T$  value of the three food groups (see Table 5-21).

As for the cereal bars all the samples show a classification that matches the label “cranberry”.

Only ID 50, an organic raw bar with freeze-dried cranberries, was identified as containing *V. oxycoccus* by our method.

Out of seven chocolate products tested five were classified as containing American cranberry. ID 37 was identified as containing European cranberry (see Figure 5-59). This particular product contained poppy seeds (which were ruled out as an interference when testing matrix components), but also was the only product made with white chocolate. ID 57 were dried cranberries (and blueberries) coated with chocolate.

Regarding the teas that were investigated two (ID 39 and 41) were identified as labelled (see Figure 5-60). ID 38 (a mixed tea with American cranberry and blueberry) and ID 40 – curiously a pure organic cranberry tea – both were identified as containing lingonberry. These results are somewhat inconclusive as for ID 38 and ID 39 both the list of ingredients states “pieces of lingonberry” (see chapter 4.3).

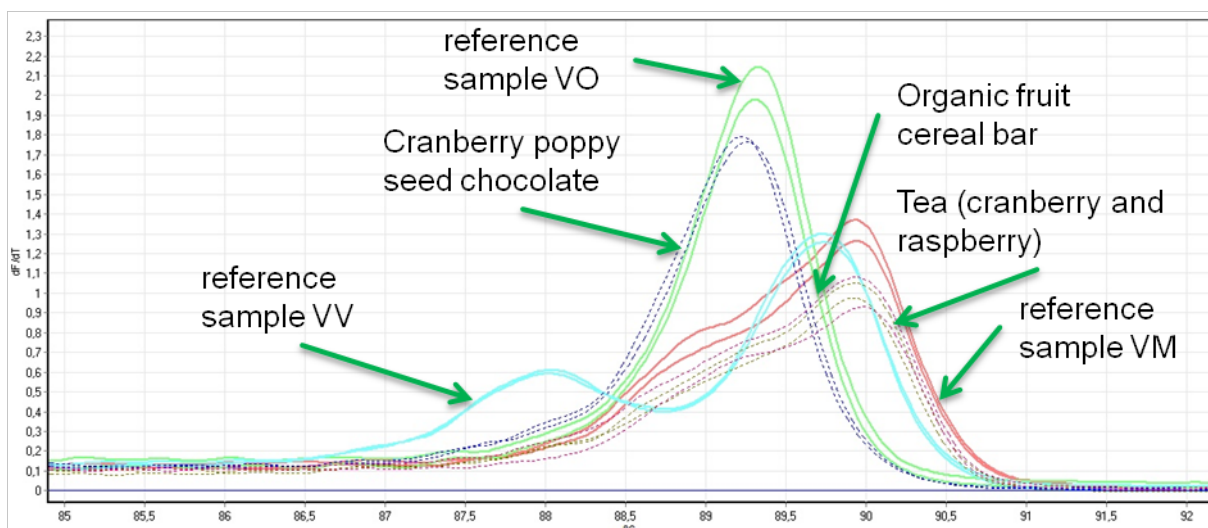


**Figure 5-59:** Melting plot of the PCR products obtained with the ITS2.1 primer set. Reference samples: red=VM (ID 3), green=VO (ID 4), blue=VV (ID 16). Olive dotted=organic fruit cereal bar (ID 21), blue dotted=cranberry poppy seed chocolate (ID 37), pink dotted=tea (cranberry and raspberry) (ID 41).

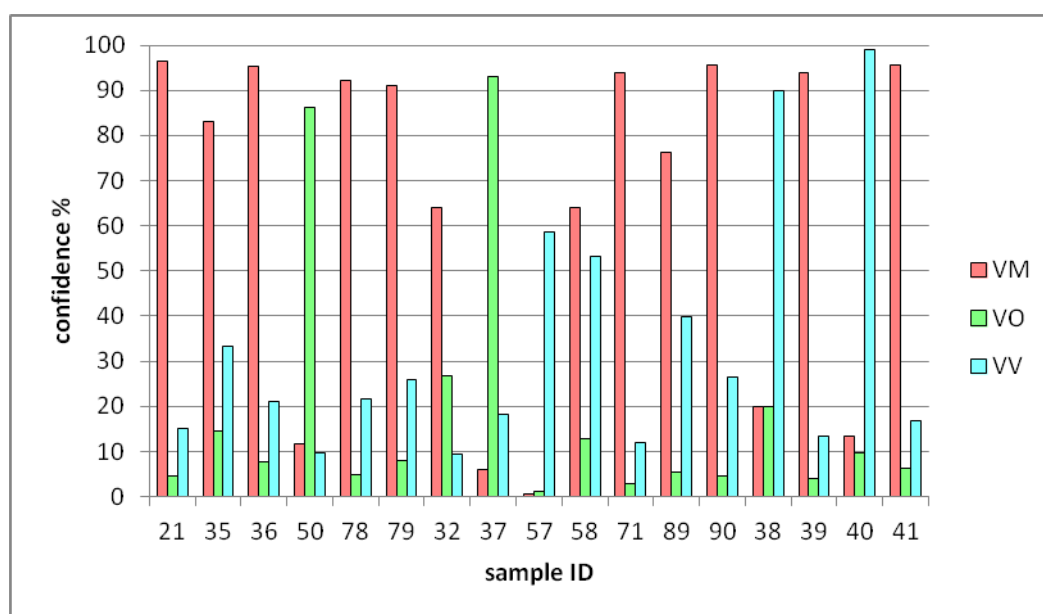


**Figure 5-60:** Confidence levels for cereal bar, chocolate, and tea samples declared as containing (American) cranberry obtained with the ITS2.1 primer set.

As shown in Table 5-22 overall 65% of the products tested were identified by our assay according to their respective label. This result though does not really reflect the power of the assay as the comparison is made between the berry advertised on the label and the berry species actually found in the product.

**Table 5-22:** Summary of the labelled and assigned *Vaccinium* species

ID	labelled	assigned	ID	labelled	assigned	ID	labelled	assigned
1	VM	VM	31	VV	VV	61	VM	VM
2	VM	VV	32	VM	VM	62	VM	VM
3	VM	VM	33	VV	VV	63	VM	VM
4	VO	VO	34	VV	VV	64	VM	VM
5	VM	VO	35	VM	VO	65	VM	VM
6	VM	VO	36	VM	VV	66	VO	VM
7	VM	VV	37	VM	VO	67	VO	VM
8	VM	VM	38	VM	VV	68	VM	VM
9	VM	VO	39	VM	VM	69	A	-
10	VM	VV	40	VM	VV	70	VM	VM
11	VO	VO	41	VM	VM	71	VM	VM
12	VV	VV	42	VM	VV	72	VM	VM
13	VM	VV	43	VV	VV	73	VM	VM
14	VM	VV	44	VV	VV	74	VM	VM
15	VM	VO	45	VV	VV	75	VM	VM
16	VV	VV	46	VV	VV	76	VM	VM
17	VM	VM	47	VM	VV	77	VV	VM
18	VM	VV	48	VV	VV	78	VM	VM
19	VV	VV	49	VM	VM	79	VM	VM
20	VM	VV	50	VM	VO	80	VM	VM
21	VM	VM	51	VV	VV	81	VM	VM
22	VM	-	52	VV	VM	82	VM	VM
23	VM	VV	53	VV	VV	83	VM	VM
24	VM	VM	54	VV	VV	84	VM	VM
25	VM	VV	55	VV	VV	85	VM	VM
26	VM	VO	56	VV	VV	86	VM	VV
27	VM	VM	57	VM	VV	87	VM	VM
28	VM	VV	58	VM	VM	88	VM	VM
29	VM	-	59	VM	VM	89	VM	VM
30	VO	VM	60	VM	VM	90	VM	VM
- ... no amplification						91	VM	VM





## 6 Conclusion

Of the primer sets investigated three primer sets designed for the MatK region, one primer set designed in the CP12 region, and the primer set designed for the ITS1 region did not show sufficient differentiation. Only the ITS2.1 primer set was found suitable for the differentiation between the three species *Vaccinium macrocarpon* (American cranberry), *Vaccinium oxycoccos* (European cranberry), and *Vaccinium vitis-idaea* (lingonberry).

Frequently used matrix-components such as different nuts (almond, cashew, walnut), different other berries (strawberry, goji, raspberry, blackberry, red/black/white currant) as well as poppy seed, raisin, grape, apple, pomegranate, and sour cherry were investigated with regards to possible interference with the three *Vaccinium* species. It could be shown, that with the ITS2.1 primer set these matrix components did not/hardly amplify, indicating a high specificity towards *V. macrocarpon* (American cranberry), *V. oxycoccos* (European cranberry), and *V. vitis-idaea* (lingonberry).

Furthermore, processed foodstuff was investigated to detect adulteration of commercial berry products. DNA could be isolated in sufficient amounts from all the products including supplements, jams, juices, dairy products, chocolates, and tea. Detection and differentiation between the three *Vaccinium* species was possible even in highly processed foodstuff. Two of the products (both of the cranberry juices) investigated could not be sufficiently amplified with the ITS2.1 primer set. With the developed assay, 65% of the products investigated were found to contain the berry species that was advertised on the label. If these findings are the result of negligent labelling or blunt adulteration was not subject of this study.

However, future research could be directed into developing a complementary assay for further validation of the results. Furthermore, the developed assay should be applied to a greater variety of plants, and processed foodstuff, especially labelled as containing *V. oxycoccos*.



## 7 Appendix

### 7.1 Abbreviations

μL	Microliter
μM	Micromolar
A	Adenine
bp	Base pairs
C	Cytosine
COI	Cytochrome c oxidase I
C <sub>T</sub>	Threshold cycle
dATP	Deoxyadenosine triphosphate
dCTP	Deoxycytidine triphosphate
dGTP	Deoxyguanosine triphosphate
DNA	Deoxyribonucleic acid
dNTP	Deoxynucleoside triphosphate
dsDNA	Double stranded DNA
dTTP	Deoxythymidine triphosphate
EDTA	Ethylenediaminetetraacetic acid
G	Guanine
g	Gram
GC	Gas chromatography
HPLC	High performance liquid chromatography
HRM	High resolution melting
ITS	Internal transcribed spacer
L	Liter
LMSVG	Food Safety and Consumer Protection Law
M	Molar
mg	Milligram
min	Minutes
mL	Milliliters
mM	Millimolar
MS	Mass spectrometry
NCBI	National Center for Biotechnology Information
ng	Nanogram
nm	Nanometer
NMR	Nuclear magnetic resonance
NTC	No template control
PCR	Polymerase chain reaction
PVP	Polyvinylpyrrolidone
rDNA	Ribosomal deoxyribonucleic acid
RNase A	Ribonuclease A
rpm	Revolutions per minute
rRNA	Ribosomal ribonucleic acid
s	Seconds
S	Svedberg unit
SPE	Solid phase extraction
ssDNA	Singlestranded DNA
T	Thymine
TAE	Tris-Acetate-EDTA
TAE-Buffer	Tris-acetate-ethylenediaminetetraacetic acid
T <sub>m</sub>	Melting temperature
VM	<i>Vaccinium macrocarpon</i>
VO	<i>Vaccinium oxycoccos</i>
VV	<i>Vaccinium vitis-idaea</i>

## 7.2 Abstract

The *Vaccinium* genus includes the species American cranberry (*Vaccinium macrocarpon* Ait.), common cranberry (*Vaccinium oxycoccos* L.) and lingonberry (*Vaccinium vitis-idaea* L.). The consumption of berries and berry products has become popular in the last years due to the phytochemicals they contain and their association with health benefits. Commercial foodstuff including berry products has to be safe and authentic to meet national and EU regulations. As far as adulteration of *Vaccinium* products is concerned, berries are often replaced by other berries of lower value and/or price.

Metabolic profiling or anthocyanin fingerprinting, as well as DNA barcoding are used for identification and differentiation of (berry) species. DNA barcoding is based on the amplification of a distinct barcoding region via polymerase chain reaction (PCR) and the subsequent analysis of the amplicons by e.g. sequencing or high resolution melting (HRM) analysis.

The aim of this research was the development of a DNA barcoding based method to differentiate between three *Vaccinium* species, *V. macrocarpon*, *V. oxycoccos*, and *V. vitis-idaea*. The first goal was to find appropriate DNA barcoding regions and to design primer sets that are capable of differentiating between the three *Vaccinium* species. The DNA barcoding regions investigated were MatK, CP12, and both ITS regions. For each primer set the PCR conditions were optimized. The selectivity was analysed by looking into cross reactions with other commonly used food ingredients. Additionally, the limit of detection (LOD) was investigated using binary mixtures. Furthermore, the application of the method to commercial food samples was investigated.

Of all the DNA barcoding regions analysed, only the ITS2 region could be used to distinguish between the three *Vaccinium* species. Neither the three primer sets designed for the MatK DNA barcoding region nor the primer sets designed for the CP12 and ITS1 barcoding region were able to distinguish between the three berry species. The melting curves of the PCR products obtained with the ITS2.1 primer set were different for each species. Frequently used matrix-components such as different nuts (almond, cashew, walnut), different other berries (strawberry, goji, raspberry, blackberry, red/black/white currant) as well as poppy seed, raisin, grape, apple, pomegranate, and sour cherry did not/hardly amplify, indicating a high selectivity towards *V. macrocarpon* (American cranberry), *V. oxycoccos* (European cranberry), and *V. vitis-idaea* (lingonberry).

Furthermore, detection and differentiation between the three *Vaccinium* species was possible even in highly processed foodstuff. With the ITS 2.1 primer set, 65% of the products investigated were found to contain the berry species that was advertised on the label.

However, future research could be directed into developing a complementary assay for further validation of the results. Furthermore, the developed assay should be applied to a greater variety of plants, and processed foodstuff, especially labelled as containing *V. oxycoccos*.

### 7.3 Zusammenfassung

Die Gattung *Vaccinium* umfasst die Arten Amerikanische Cranberry (*Vaccinium macrocarpon* Ait.), Europäische Cranberry (*Vaccinium oxycoccos* L.) und Preiselbeere (*Vaccinium vitis-idaea* L.). Auf Grund der in ihnen enthaltenen sekundären Pflanzeninhaltsstoffen hat der Konsum von Beeren und Beerenprodukten in den letzten Jahren zugenommen. Kommerzielle Lebensmittel einschließlich Beerenprodukte müssen sicher und authentisch sein, um nationale und EU-Bestimmungen zu erfüllen.

Metabolic Profiling oder Anthocyan-Fingerprinting sowie DNA Barcoding werden zur Identifizierung und Differenzierung von (Beeren-) Spezies verwendet. DNA Barcoding basiert auf der Amplifikation einer spezifischen Barcoding Sequenz mittels Polymerasekettenreaktion (PCR) mit anschließender Sequenzierung oder hochauflösender Schmelzkurvenanalyse (HRM).

Das Ziel dieser Arbeit war die Entwicklung einer DNA Barcoding basierten Methode zur Unterscheidung von drei Spezies der Gattung *Vaccinium*, nämlich der Amerikanischen Cranberry, der Europäischen Cranberry und der Preiselbeere. Zuerst sollte eine geeignete DNA Barcoding Region gefunden werden. Die untersuchten DNA Barcoding Regionen waren MatK, CP12 und beide ITS-Regionen. Für jedes Primerset wurden die PCR-Bedingungen optimiert. Die Selektivität wurde in Hinblick auf andere häufig verwendete Lebensmittelinhaltsstoffe getestet. Zusätzlich wurde die Nachweisgrenze (LOD) mit binären Mischungen untersucht, ebenso die Anwendung der Methode auf kommerzielle Lebensmittelproben.

Von allen untersuchten DNA Barcoding Regionen war nur die ITS2 Region geeignet, um zwischen den drei *Vaccinium*-Arten zu unterscheiden. Weder die drei für die MatK Regionen noch die für die CP12- und ITS1- Barcoding-Regionen entworfenen Primer-Sets konnten die drei Beerenart hinreichend unterscheiden. Die Schmelzkurven der PCR-Produkte, die mit dem ITS2.1-Primer-Set erhalten wurden, waren für jede Spezies unterschiedlich. Häufig verwendete Matrixkomponenten wie verschiedene Nüsse (Mandeln, Cashews, Walnüsse), verschiedene andere Beeren (Erdbeere, Goji, Himbeere, Brombeere, Rote/Schwarze/Weiße Johannisbeere) sowie Mohn, Rosinen, Trauben, Äpfel, Granatapfel, und Sauerkirsche

wurden nicht/kaum amplifiziert, was auf eine hohe Selektivität gegenüber *V. macrocarpon* (amerikanische Cranberry), *V. oxycoccos* (europäische Cranberry) und *V. vitis-idaea* (Preiselbeere) hindeutet.

Darüber hinaus war die Detektion und Differenzierung der drei *Vaccinium*-Arten auch in stark verarbeiteten Lebensmitteln möglich. Mit dem Primer-Set ITS 2.1 konnte 65% der untersuchten Produkte den auf dem Etikett angeführten Beerenarten zugeordnet werden. Weitere Forschungen könnten auf die Entwicklung eines komplementären Assays zur weiteren Validierung der Ergebnisse gerichtet sein. Darüber hinaus sollte die entwickelte Methode auf eine größere Zahl von Pflanzen und verarbeiteten Lebensmitteln angewendet werden, insbesondere solche, die als *V. oxycoccos* gekennzeichnet sind.

## 7.4 List of tables

Table 1-1: Scientific classification of the <i>Vaccinium</i> genus .....	4
Table 1-2: Summary of the three <i>Vaccinium</i> species and their English and German synonyms .....	5
Table 1-3: Previous research concerning <i>Vaccinium</i> species in the context of differentiation .....	6
Table 3-1: Overview over the structure of the nucleobases .....	20
Table 4-1: Herbarium samples and their origin .....	34
Table 4-2: Summary of the different commercial food groups used.....	35
Table 4-3: Primer sequences in different target regions used in this study.....	37
Table 4-4: Combinations of primer sets .....	38
Table 4-5: Pipetting scheme for the EpiTect® HRM PCR Master Mix .....	40
Table 4-6: Pipetting scheme for the MeltDoctor™ HRM Master Mix.....	41
Table 4-7: PCR parameters used on the Rotor-Gene® thermal cycler.....	41
Table 5-1: Accession numbers and definitions of the MatK sequences used .....	44
Table 5-2: Predicted melting temperatures and secondary structures of the MatK 1.2, MatK 1.4, MatK 1.5 primer sets (see Table 4-4).....	47
Table 5-3: Mean C <sub>T</sub> values (n=2) of the DNA extracts of the herbarium samples obtained with the D2 primer set.....	53
Table 5-4: Mean C <sub>T</sub> values (n=2) of the DNA extracts of the herbarium samples obtained with the M1 primer set. ....	55
Table 5-5: Primer set combinations D4-D7 .....	57
Table 5-6: Accession numbers and definitions of the CP12 sequences used .....	61
Table 5-7: Predicted melting temperatures and secondary structures of the CP12 primer set .....	62
Table 5-8: Accession numbers and definitions of the ITS sequences used.....	64
Table 5-9: Predicted melting temperatures and secondary structures of the ITS1.1 and ITS2.1 primer sets (see Table 4-4).....	65
Table 5-10: Matrix components used throughout this study.....	67
Table 5-11: Mean C <sub>T</sub> values (n=2) of the DNA extracts of the matrix components.....	69

Table 5-12: Mean $C_T$ values (n=2) and level of confidence for other <i>Vaccinium</i> species and matrix components (see chapter 7.7.3).....	72
Table 5-13: Comparison of the peak maxima of the melting plots of the reference samples with the EpiTect® and MeltDoctor™ Master Mixes. ....	90
Table 5-14: Mean $C_T$ values (n=2) and $\Delta C_T$ values for the herbarium sample DNA extracts and the reference DNA samples .....	93
Table 5-15: Mean $C_T$ values (n=2) and $\Delta C_T$ values for the sample DNA extracts labelled as <i>V. macrocarpon</i> obtained by other plant parts. ....	94
Table 5-16: Mean $C_T$ values (n=2) and $\Delta C_T$ values for samples labelled as containing <i>V. vitis-idaea</i> .....	95
Table 5-17: Mean $C_T$ values (n=2) and $\Delta C_T$ for samples labelled as containing <i>V. oxycoccos</i> .....	98
Table 5-18: Mean $C_T$ values (n=2) and $\Delta C_T$ values for samples labelled as containing (American) cranberry (juices) .....	100
Table 5-19: Mean $C_T$ values (n=2) and $\Delta C_T$ values for samples labelled as containing (American) cranberry (diverse, fruit, jam).....	102
Table 5-20: Mean $C_T$ values (n=2) and $\Delta C_T$ values for samples labelled as containing (American) cranberry (dairy, and supplements) .....	104
Table 5-21: Mean $C_T$ values (n=2) and $\Delta C_T$ values for samples labelled as containing (American) cranberry (cereal bars, chocolates, tea) .....	106
Table 5-22: Summary of the labelled and assigned <i>Vaccinium</i> species .....	108

## 7.5 List of figures

Figure 1-1: Comparison of the fruits of <i>V. macrocarpon</i> (left), <i>V. oxycoccos</i> (middle), and <i>V. vitis-idaea</i> (right) [36–38].....	4
Figure 1-2: Structure of anthocyanidines (left) and common anthocyanines found in fruits of the <i>Vaccinium</i> genus [49] .....	5
Figure 1-3: Wet harvesting Cranberries (left), and a cross section of a cranberry (right) showing the aerated cavities causing the cranberries to float [63,64].....	7
Figure 1-4: Comparison between the leaves of VM (left) and VO (right) showing the different size and shape [81]. ....	9



Figure 1-5: Alignment of a DNA section of <i>V. macrocarpon</i> (U61316.2) above, <i>V. oxycoccus</i> (LC168883.1) in the middle, and <i>V. vitis idaea</i> (AF382819.1) below. Conserved loci are denoted with an asterisk.....	10
Figure 1-6: Scheme of the MatK region and its surroundings, adapted from [93].....	11
Figure 1-7: Prokaryotic and eukaryotic ribosomes in comparison, and the subunits they are comprised of, modified from [96] .....	12
Figure 1-8: Scheme of the arrangement of the ITS region, modified from [97] .....	12
Figure 3-1: The steps to purify DNA via a commercial kit [108] .....	17
Figure 3-2: Structure of polyvinylpyrrolidone, a polymer made from the monomer N-vinylpyrrolidone .....	17
Figure 3-3: Depiction of an ideal result obtained by spectrophotometric measurement with an absorption maximum at 260 nm for DNA and an absorption maximum at 280 nm for proteins, modified from [113].....	18
Figure 3-4: DNA structure and binding structures [117]. .....	21
Figure 3-5: Scheme of a PCR cycle, modified from [121] .....	22
Figure 3-6: The mechanism of real-time PCR using fluorescent dye. The dye only binds onto dsDNA and then emits a fluorescent signal (yellow). The more dsDNA is formed during the PCR, the higher the overall fluorescent signal becomes.....	27
Figure 3-7: The kinetics of a PCR reaction. In the early cycles (E), as primers search the few template copies available, amplification is slow. During the mid cycles (M) there is almost exponential amplification until in the late cycles (L) when the reaction plateaus as primers become the limiting factor, modified from [116].....	28
Figure 3-8: Differences between non-saturating and saturating PCR dyes during the melting process, modified from [135] .....	29
Figure 3-9: Structure of the EvaGreen dye. This dye is non-toxic, non-mutagenic, and uses a “release-on-demand” mechanism while binding thus complying not only to the needs of PCR but HRM, too [143]. .....	30
Figure 3-10: Overview over different representations of the results of an HRM experiment..	31
Figure 3-11: DNA ladder showing the impact in size on the velocity of migration and leads to the formation of bands [148].....	32

Figure 3-12: Bromophenol blue (left) and xylene cyanole FF (right), two dyes used as loading dye.....	32
Figure 3-13: Structure of agarose, a disaccharide made up of D-galactose and 3,6-anhydro-L-galactopyranose [151].....	33
Figure 3-14: Structure of ethidium bromide, commonly used in nucleic acid staining. Due to health concerns other, less toxic fluorescent dyes are on the market.....	33
Figure 4-1: Default settings used for the automatic alignments with the MEGA7 software....	39
Figure 4-2: Default settings used for the automatic primer design with the PyroMark Assay Design software.....	39
Figure 4-3: Normalisation Range and Confidence Threshold used for the analysis with the Rotor-Gene Q Series Software .....	42
Figure 5-1: Alignment of the sequences of <i>V. macrocarpon</i> (above), <i>V. vitis-idaea</i> (middle), and <i>V. oxycoccos</i> (below) in the MatK barcoding region. Variable positions are labelled.....	45
<b>Figure 5-2:</b> Primer binding sites for the MatK region of <i>V. macrocarpon</i> (Accession number U61316), light blue: MatK 1.2 forward, dark blue: MatK 1.2. reverse, dark pink: MatK 1.4 forward, light pink: MatK 1.4 reverse, green: MatK 1.5 forward, dark blue MatK 1.5 reverse	46
<b>Figure 5-3:</b> Agarose gel of different samples after PCR using the MatK 1.4 primer set at different annealing temperatures. Lanes 2,3, 28, 29: NTC, lanes 4-11: VM = ID 3, lanes 12-19: VO = ID 4, lanes 20-27: VV = ID 16 (see 7.7.1 for ID information) .....	48
Figure 5-4: The influence of the annealing temperature on the melting curve of the amplicons of VM (ID 3, see chapter 7.7.1) obtained by PCR with the MatK 1.4 primer set; the lighter the colour, the higher the annealing temperature ranging from 58.1 to 52.0 °C. Typical results are shown. ....	49
Figure 5-5: The influence of Mg <sup>2+</sup> concentration on the amplification and melting plot. Typical results are shown. VM (ID 3), MatK 1.4 primer set, annealing temperature: 52°C (similar results for VO (ID 4) and VV (ID 16)). ....	50
Figure 5-6: Resulting melting plots for the PCR products obtained with the primer set MatK 1.2. Reference samples: red=VM (ID 3), green=VO (ID 4), blue=VV (ID 16).....	51
Figure 5-7: Resulting melting plots for the PCR products obtained with the primer set MatK 1.5. Reference samples: red=VM (ID 3), green=VO (ID 4), blue=VV (ID 16).....	51
Figure 5-8: Resulting melting plots for the PCR products obtained with the primer set MatK 1.4. Reference samples: red=VM (ID 3), green=VO (ID 4), blue=VV (ID 16).....	51

Figure 5-9: Melting plots for the PCR products obtained with the MatK 1.4 primer set. Reference samples: red=VM (ID 3), green=VO (ID 4), blue=VV (ID 16). Dotted teal=dried cranberries (ID 7), dotted pink=powdered cranberry (labelled *V. oxycoccos*, ID 11), dotted olive=horseradish with lingonberries (ID 33). It can be seen, that no differentiation is possible.

.....52

Figure 5-10: Melting plot for the PCR products obtained with the primer set D1. Red= VM (ID 3), green= VO (ID 4), light blue= VV (ID16), dark blue= bilberry (1A), ochre= blueberry (2B).

.....53

Figure 5-11: Melting plot for the PCR products obtained with the D2 primer set. Above: reference samples: red= VM (ID 3), green= VO (ID 4), light blue= VV (ID 16), dark blue= bilberry (1A), ochre= blueberry (2B). Below: reference samples: red= VM (ID 3), green= VO (ID 4), light blue= VV (ID 16), herbarium samples VV (H1-H3): dotted lines, VO (H4-H7): dashed lines, and VM (H13-H15): small dotted lines.

.....54

Figure 5-12: Melting plot for the PCR products obtained with the primer set M1. Red= VM (ID 3), green= VO (ID 4), light blue= VV (ID 16), dark blue= bilberry (1A) , ochre= blueberry (2B)

.....55

**Figure 5-13:** Amplification plot (above) and melting plot (below) for the PCR products obtained with the primer set M1. Reference samples: red= VM (ID 3), green= VO (ID 4), light blue= VV (ID 16), herbarium samples VV (H1-H3): dotted lines, VO (H4-H7): dashed lines, and VM (H13-H15): small dotted lines.

.....56

Figure 5-14: Melting plot for the PCR products obtained with the primer set D3. Reference samples: red=VM (ID 3), green=VO (ID 4), blue=VV (ID 16).

.....57

Figure 5-15: Melting plots for PCR products obtained with different primer sets. Reference samples: red=VM (ID 3), green=VO (ID 4), blue=VV (ID 16). Above: left: primer set D4. right: primer set D5. Below: left: primer set D6, right: primer set D7 (see Table 5-3).....

.....58

Figure 5-16: Melting plot for the PCR products obtained with the primer set D5. Reference samples: red=VM (ID 3), green=VO (ID 4), blue=VV (ID 16). Food samples: blue dotted=pure cranberry juice (ID 6), purple dotted=powdered cranberry (ID 11), olive dotted=powdered lingonberry (ID 12), (see 7.7.1 for more ID information).....

.....59

Figure 5-17: Developed agarose gel showing the size of the amplicons obtained with different primer sets. Lane 2-8: primer combination D1 (NTC, ID 1A, ID 2B, ID 3, ID 4, ID 16, ID 30). Lane 9-15: primer set D2 (NTC, ID 1A, ID 2B, ID 3, ID 4, ID 16, ID 30). Lane 17-23: primer set M1 (NTC, ID 1A, ID 2B, ID 3, ID 4, ID 16, ID 30). Lane 25-28: primer set MatK 1.4

for reference (ID 3, ID 4, ID 16, ID 30), see Table 5-3. Different ladder volumina (1.88 µl, 0.94 µL und 1.24 µL) were used (lane 1, 16, 30). .....	60
Figure 5-18: Alignment of the sequences of <i>V. macrocarpon</i> (above), <i>V. oxycoccos</i> (middle), and <i>V. vitis-idaea</i> (below) in the CP12 barcoding region. Variable positions are labelled. ....	61
Figure 5-19: Primer binding sites for the CP12 region of <i>V. macrocarpon</i> (Accession number KU710568), dark orange: CP12 forward, light orange: CP12 reverse .....	62
Figure 5-20: Melting plots for the PCR products obtained with the primer set CP12. Reference samples: red=VM (ID 3), yellow=VO (ID 4), green=VV (ID 16). Above: higher primer concentration (250nM), below: lower primer concentration (100nM). .....	63
Figure 5-21: Alignment of the sequences of <i>V. vitis-idaea</i> (above), <i>V. macrocarpon</i> (middle), and <i>V. oxycoccos</i> (below) in the ITS barcoding region. Variable positions are labelled. ....	64
Figure 5-22: Primer binding sites for the ITS regions of <i>V. macrocarpon</i> (Accession number AF382730), light green: ITS1.1 forward, dark green: ITS1.1 reverse, dark purple: ITS2.1 forward, light purple: ITS2.1 reverse .....	66
Figure 5-23: Melting plots of PCR products obtained with the ITS1.1 primer set (left) and the ITS 2.1 primer set (right), annealing temperature 67.5 °C. Reference samples: red=VM (ID 3), green=VO (ID 4), blue=VV (ID 16). .....	66
Figure 5-24: Amplification plot (above) and melting plot (below) of PCR products obtained with the ITS2.1 primer set. Reference samples: red=VM (ID 3), green=VO (ID 4), blue=VV (ID 16). Violet=cashew (ID B1), yellow= pomegranate (ID M1), magenta= sour cherry (ID N1), dark purple=apple “Gala” (ID P). The latter did not amplify. ....	68
Figure 5-25: Confidence levels of the classification of the matrix component DNA obtained with the ITS2.1 primer set (see chapter 4.5.2). See chapter 7.7.3 for ID information. ....	69
Figure 5-26: Melting plot (below) of PCR products obtained with the ITS2.1 primer set. Reference samples: red=VM (ID 3), green=VO (ID 4), blue=VV (ID 16), rosé= <i>V. myrtillus</i> (ID 1A), beige= <i>V. corymbosum</i> (ID 2B), crimson=aronia (ID 3AB), pale violet=chocolate (ID COC) no amplification, dark red=apple (ID APF), teal=beetroot (ID RET), magenta=pumpkin (ID KUE). NTC did not amplify. ....	71
Figure 5-27: Amplification plot (above) and melting plot (below) of the PCR products obtained with the ITS2.1 primer set. Reference samples: red=VM (ID 3), green=VO (ID 4), blue=VV (ID 16). Sample used for spike experiments as matrix component=cereal bar (ID BAL). ....	73

Figure 5-28: Amplification plot (above) and melting plot (below) of the PCR products obtained with the ITS2.1 primer set. Reference samples: red=VM (ID 3), green=VO (ID 4), blue=VV (ID 16). Sample used for spike experiments as matrix component=chocolate (ID COC). ....	74
Figure 5-29: Amplification plot (above) and melting plot (below) of the PCR products obtained with the ITS2.1 primer set. Reference samples: red=VM (ID 3), green=VO (ID 4), blue=VV (ID 16). Sample used for spike experiments as matrix component=apple (ID L1). ....	75
Figure 5-30: Confidence level for the DNA extracts spiked with 1% <i>Vaccinium</i> DNA extract obtained with the ITS2.1 primer set with the matrix components BAL, CO, and L1. See chapters 7.7.2 and 7.7.3 for ID information. ....	76
Figure 5-31: Confidence level for the DNA extracts spiked with 1% <i>Vaccinium</i> DNA extract obtained with the ITS2.1 primer set with the matrix components FHD, B1, K1 und M1. See chapters 7.7.2 and 7.7.3 for ID information. ....	77
Figure 5-32: Amplification plot (above) and melting plot (below) of the PCR products obtained with the ITS2.1 primer set. Reference samples: red=VM (ID 3), green=VO (ID 4), blue=VV (ID 16). Sample used for spike experiments as matrix component=bilberry jam (ID FHD). See chapters 7.7.2 and 7.7.3 for ID information. ....	78
Figure 5-33: Amplification plot (above) and melting plot (below) of the PCR products obtained with the ITS2.1 primer set. Reference samples: red=VM (ID 3), green=VO (ID 4), blue=VV (ID 16). Sample used as matrix component=Cashew (ID B1). See chapters 7.7.2 and 7.7.3 for ID information. ....	79
Figure 5-34: Amplification plot (above) and melting plot (below) of the PCR products obtained with the ITS2.1 primer set. Reference samples: red=VM (ID 3), green=VO (ID 4), blue=VV (ID 16). Sample used as matrix component=pomegranate (ID M1). See chapters 7.7.2 and 7.7.3 for ID information. ....	80
Figure 5-35: Amplification plot (above) and melting plot (below) of the PCR products obtained with the ITS2.1 primer set. Reference samples: red=VM (ID 3), green=VO (ID 4), blue=VV (ID 16). Sample used as matrix component=bilberry jam (ID FHD). See chapters 7.7.2 and 7.7.3 for ID information. ....	81
Figure 5-36: Confidence level for the DNA extracts spiked with 1% <i>Vaccinium</i> DNA extract obtained with the ITS2.1 primer set with the matrix components FHD with 5% and 10% addition of <i>Vaccinium</i> DNA, and a ternary mixture of three <i>Vaccinium</i> species VM (ID 3), VO (ID 4), and VV (ID 16), see chapters 7.7.2 and 7.7.3 for ID information. ....	82

Figure 5-37: Amplification plot (above) and melting plot (below) of the PCR products obtained with the ITS2.1 primer set. Reference samples: red=VM (ID 3), green=VO (ID 4), blue=VV (ID 16) and the ternary mixture consisting of equal parts of DNA extracts of the three reference samples.....	83
Figure 5-38: Amplification plot (above) and melting plot (below) of the PCR products for binary mixtures obtained with the ITS2.1 primer set. Reference samples: red=VM (ID 3), and green=VO (ID 4).....	84
Figure 5-39: Confidence levels for the binary mixtures of VM and VO obtained with the ITS2.1 primer set, see chapters 7.7.2 and 7.7.3 for ID information.....	85
Figure 5-40: Amplification plot (above) and melting plot (below) of the PCR products for binary mixtures obtained with the ITS2.1 primer set. Reference samples: green=VO (ID 4), and blue=VV (ID 16).....	86
Figure 5-41: Confidence levels for the binary mixtures of VV and VO obtained with the ITS2.1 primer set, see chapters 7.7.2 and 7.7.3 for ID information. ....	87
Figure 5-42: Amplification plot (above) and melting plot (below) of the PCR products for binary mixtures obtained with the ITS2.1 primer set. Reference samples: red=VM (ID 3), and blue=VV (ID 16).....	88
Figure 5-43: Confidence levels for the binary mixtures of VM and VV obtained with the ITS2.1 primer set, see chapters 7.7.2 and 7.7.3 for ID information.....	89
Figure 5-44: Amplification plot for the PCR products obtained with the ITS2.1 primer set using the MeltDoctor™ chemistry and the QuantStudio 5 cycler. Blue= VM (ID 3), green= VO (ID 4), ochre= VV (ID 16). ....	90
Figure 5-45: Melting plot for the PCR products obtained with the ITS 2.1 primer set. Blue= VM (ID 3), green= VO (ID 4), ochre= VV (ID 16), MeltDoctor™.....	91
Figure 5-46: Amplification plot (above) and melting plot (below) of the PCR products obtained with the ITS2.1 primer set. Reference samples: red=VM (ID 3), green=VO (ID 4), blue=VV (ID 16). Dotted: VV species (H1, H2, and H3), dashed: VO species (H4 – H7), and small dots: VM species (H13, H14, and H15), see Table 4.2-1.....	92
Figure 5-47: Confidence levels of the classification of herbarium sample DNA obtained with the ITS2.1 primer set. H1, H2, and H3 were VV species, H4 – H7 were VO species, and H13, H14, and H15 were VM species. (see Table 4-1). ....	93

Figure 5-48: Confidence levels of the classification of seeds (ID 68, 76), leaves (ID 61, 62), and fresh fruit (ID 27, 60, 65, 73, 74, 75) obtained with the ITS2.1 primer set.....	94
Figure 5-49: Confidence levels for samples declared as containing lingonberry obtained with the ITS2.1 primer set. Reference sample: ID 16. Samples: juices (ID 19, ID 48, ID 52), jams (ID 44, ID 45, ID 53, ID 56), supplements (ID 12, ID 43), mustard (ID 51), horseradish (ID 33), cereal bar (ID 77), plant samples – (ID 31, ID 34, and ID 46).....	96
Figure 5-50: Melting plot of the PCR products obtained with the ITS2.1 primer set. Reference samples: red=VM (ID 3), blue=VV (ID16). Above: lingonberries with red wine and cinnamon (ID 53), below: lingonberry bar (ID 77).....	97
Figure 5-51: Confidence levels for samples declared as containing European cranberry obtained with the ITS2.1 primer set. Reference sample: ID 4. Samples: other plant specimen (ID 30), supplement (ID 11), juice (ID 67), paste (ID 66).....	98
Figure 5-52: Melting plots of the PCR products obtained with the ITS2.1 primer set. Reference sample: red=VM (ID 3), green=VO (ID4). Above: powdered cranberry (ID 11). Below: juice made from European cranberries (ID 67). ....	99
Figure 5-53: Confidence levels for juice samples declared as containing (American) cranberry obtained with the ITS2.1 primer set. ....	100
Figure 5-54: Melting plot of the PCR products obtained with the ITS2.1 primer set. Reference samples: red=VM (ID 3), green=VO (ID 4), blue=VV (ID 16). Grey dotted=organic cranberry juice (ID 5), purple dotted=multivitamin juice red fruits (ID 18).....	101
Figure 5-55: Melting plot of the PCR products obtained with the ITS2.1 primer set. Reference samples: red=VM (ID 3), green=VO (ID 4), blue=VV (ID 16). rosé=cranberry superfruits (ID 2), pink=cranberry and blueberry jam (ID 17), brown= cookies chocolate and cranberries (ID 42). ....	102
Figure 5-56: Confidence levels for diverse (ID 28, ID 42, ID 49, ID 85), fruit (ID 2, 7, 8, 9, 24, 26, 63, 70, and 80), and jam (ID 17, 59, 86, 87, and 88) samples declared as containing (American) cranberry obtained with the ITS2.1 primer set.....	103
Figure 5-57: Confidence levels for dairy (ID 1, ID 91), and supplement samples (ID 10, 13, 14, and 15) declared as containing (American) cranberry obtained with the ITS2.1 primer set. ....	104
Figure 5-58: Melting plot of the PCR products obtained with the ITS2.1 primer set. Reference samples: red=VM (ID 3), green=VO (ID 4), blue=VV (ID 16). Blue dotted=organic cranberry yoghurt (ID 1), teal dotted=cranberry+Vitamin C (ID 13).....	105

Figure 5-59: Melting plot of the PCR products obtained with the ITS2.1 primer set. Reference samples: red=VM (ID 3), green=VO (ID 4), blue=VV (ID 16). Olive dotted=organic fruit cereal bar (ID 21), blue dotted=cranberry poppy seed chocolate (ID 37), pink dotted=tea (cranberry and raspberry) (ID 41). ..... 107

Figure 5-60: Confidence levels for cereal bar, chocolate, and tea samples declared as containing (American) cranberry obtained with the ITS2.1 primer set. .... 107

## 7.6 Equipment

### 7.6.1 Chemicals and kits

---

25 bp DNA Ladder (Invitrogen ThermoFisher Scientific)
Acetic acid; concentrated(Roth)
Agarose (Sigma Aldrich)
DNA-ExitusPlus™ IF(PanReac AppliChem ITW Reagents)
EDTA (Ethylenediaminetetraacetic acid) (Merck)
EpiTect® HRM PCR Kit (Qiagen)
Ethanol absolut EMSURE® (Merck)
Gel Red™ Nucleic Acid Stain (Biotium)
MgCl <sub>2</sub> (Magnesiumchloride) (Qiagen)
MeltDoctor™ HRM Master Mix (Applied Biosystems™)
Nucleic Acid Sample Loading Dye (5x) (BioRad)
PVP (Polyvinylpyrrolidone) (Sigma Aldrich)
Primer (Sigma Aldrich)
QiAamp®DNA Mini Kit (Qiagen)
Qubit™ 1xds DNA HS Assay Kit
RNase A (Ribonuclease A) ( Invitrogen ThermoFisher Scientific)
RNase free water (Qiagen)
Tris-base = 2-Amino-2-(hydroxymethyl)-1,3-propanediol (Trizma®base) (Sigma Aldrich)

---

### 7.7.2. Equipment/Instruments

Analytical balance AE 2000, Mettler		
Centrifuge Galaxy mini, VWR		
Centrifuge 5424, Eppendorf		
Electrophoresis cell Wide Mini-Sub®Cell TG, BioRad		
Fluorometer Qubit™ 2.0 Fluorometer, ThermoFisher Scientific		
Gel tray, BioRad		
Lint free laboratory wipe, Light-Duty tissue Wipers, VWR		
Magnetic mixer IKA MF® RCT, IKA®-Labortechnik		
Magnetic stir bar		
Mortar and Pestil		
PCR working station PCR Workstation PRO, VWR Peglab		
Pipettes adjustable; diverse	0.5 – 10 µL 2 – 20 µL 20 – 200 µL 100 – 1000 µL	Eppendorf
Power supply PowerPac™ HV, BioRad		



Spattle		
Spectrophotometer	NanoDrop 2000c	ThermoFisher Scientific
Thermomixer	comfort	Eppendorf
Thermal cycler	Rotor-Gene® Q	Qiagen
Thermal cycler	QuantStudio™ 5 Real-time PCR System	Applied Biosystems™
Thermal cycler for gradient PCR	iCycler iQ™5	BioRad
UV transilluminator	UVT-20 M	Herolab GmbH
Vortex	VF2	Janke & Kunkel IKA®-Labortechnik
Well comb	Sub-Cell®GT Comb	BioRad

### 7.7.3. Expendables/Consumables

Disposable serological pipettes	10 mL	VWR
Falcon tubes; diverse	15 mL 50 mL	VWR
Filter pipette tips	Biosphere® Filter Tips 0,1 – 20 µL	Sarstedt
Filter pipette tips; diverse	TipBox BIO-CERT® 0.5 – 20 µL 5 - 200 µL 50 - 1000 µL	VWR
Microcentrifuge tubes; diverse	0.65 mL 1.5 mL 2 mL	VWR
PCR tubes	200 µL	VWR
Qubit™ Assay tube		Invitrogen ThermoFisher Scientific
Strip tubes + caps	100 µL	Qiagen

### 7.7.4. Software

- MEGA7.0.21
- PyroMark Assay Design version 2.0.1.15
- RotorGene Q – Pure Detection Version 2.3.1

## 7.7 Sample-list

### 7.7.1 Samples

#### Positive controls

ID	Name	Food group	labelled as
3	<i>V. macrocarpon</i> leaves	Positive control	VM
4	<i>V. oxycoccos</i> leaves	Positive control	VO
16	<i>V. vitis-idaea</i> leaves	Positive control	VV
27	American Cranberry fresh fruit	Positive control	VM
30	<i>V. oxycoccos</i> leaves	Positive control	VO
31	<i>V. vitis-idaea</i> fruits	Positive control	VV
34	<i>V. vitis-idaea</i> "Fireballs" fruits	Positive control	VV
46	<i>V. vitis-idaea</i> leaves	Positive control	VV
60	Cranberry "Stevens" fresh fruit	Positive control	VM
61	Cranberry "Stevens" leaves	Positive control	VM
62	Cranberry "Pilgrim" leaves	Positive control	VM
65	fresh cranberries	Positive control	VM
68	<i>V. macrocarpon</i> seeds	Positive control	VM
73	Cranberry "Stevens" fresh fruit	Positive control	VM
74	Cranberry "Stevens" leaves	Positive control	VM
75	Cranberry fresh fruit	Positive control	VM
76	<i>V. macrocarpon</i> seeds	Positive control	VM

#### Herbarium samples

ID	Species
H1	
H2	<i>V. vitis-idaea</i>
H3	
H4	
H5	<i>V. oxycoccos</i>
H6	
H7	
H13	
H14	<i>V. macrocarpon</i>
H15	

## Commercial food samples

ID	Name	Foodgroup	labelled ingredients
21	organic fruit-Cereal bar	Cereal bar	Cranberries; 6% dried cranberries
35	Cereal Bar Cranberry	Cereal bar	Cranberries; 3% dried cranberries
36	FlapJack Cranberry	Cereal bar	Cranberries; 1% dried cranberries
50	Raw Cereal bar Acai Banana	Cereal bar	Cranberries; freeze dried cranberry powder
77	wild lingonberry bar with fruits	Cereal bar	Lingonberries; 8.2% lingonberry concentrate
78	Flapjack Cashew Cranberry	Cereal bar	Cranberries; 9% cranberries
79	Cereal bar forrest fruits	Cereal bar	Cranberries; cranberries in pineapple juice
32	Cranberry Chocolate	Chocolate	Cranberries; 3.5% cranberry granulate
37	Cranberry Poppy seed Chocolate	Chocolate	Cranberries; 3% dried cranberries
57	dried Bluberries & Cranberries coated with Chocolate	Chocolate	Cranberries
58	Cranberry chocolate	Chocolate	Cranberries; 7.7% cranberries
71	dark Cranberry chocolate	Chocolate	Cranberries; 2.5% cranberries
89	Cranberries coated with Chocolate	Chocolate	Cranberries; 40% cranberries
90	Dark Chocolate with Cranberry	Chocolate	Cranberries; 7% cranberries
1	rosehip & branberry organic yoghurt mild	Dairy product	Cranberries; 4% cranberries
91	Skyr Raspberry-Cranberry	Dairy product	Cranberries; 4% cranberries
28	Jellied Cranberry Sauce	Div	Cranberries
33	Horseradish with Lingonberries	Div	Lingonberries; 11% lingonberries
42	Cookies White Chocolate & Cranberry	Div	Cranberries; 8% cranberries
49	Cranberry BBQ Sauce	Div	Cranberries; 12% cranberries
51	Mustard with wild lingonberries	Div	Lingonberries
66	Paste made from european cranberries	Div	VO; 100% Moosbeeren (V. oxycoccos)
85	Grape Cranberry Vinegar	Div	Cranberries; 2% cranberry juice concentrate
2	Superfruits	Fruit	Cranberries

7	dried Cranberrys	Fruit	Cranberries; 74% dried cranberries
8	Cranberry Nut	Fruit	Cranberries; 25% dried cranberries
9	Cashew cranberry Mix	Fruit	Cranberries; 30% dried cranberries
24	dried Cranberry Medley	Fruit	Cranberries; dried cranberries
25	dried Cranberries	Fruit	Cranberries; 60% dried cranberries
26	Craisins Dried Cranberries	Fruit	Cranberries; dried cranberries
63	Cranberry Kokos Snack	Fruit	Cranberries; 7% dried cranberries
70	Organic Pumpkin Seeds Cranberry Kokos	Fruit	Cranberries; 24% dried cranberries
80	Cranberries	Fruit	Cranberries
17	cranberry and blueberry jam	Jam	Cranberries; 25,5% cranberries
44	wild lingonberries jam	Jam	Lingonberries; 50% lingonberries
45	lingonberry jam	Jam	Lingonberries; 70% lingonberries
53	Lingonberries with Red Wine and Cinnamon	Jam	Lingonberries
54	Lingonberries with Cassis and Vanilla	Jam	Lingonberries
55	Wild Lingonberries	Jam	Lingonberries
56	Wild Lingonberries	Jam	Lingonberries; 50% lingonberries
59	Strawberry Cranberry jam	Jam	Cranberries; 23% cranberries
86	Cranberry jam extra	Jam	Cranberries; cranberries
87	Cranberry jam	Jam	Cranberries; 45% cranberries
88	Cranberry (European Cranberry)	Jam	Cranberries; 45% cranberries
5	Organic CranberryJuice	Juice	Cranberries; 100% cranberry juice
6	Pure CranberryJuice	Juice	Cranberries; 100% cranberry juice
18	Multivitamin juice red fruits	Juice	Cranberries; juice from concentrate
19	pure lingonberry Juice	Juice	Lingonberries; 100% lingonberries
20	Syrup Cranberry-Aronia	Juice	Cranberries; 42% cranberry juice from concentrate
22	Cranberry juice	Juice	Cranberries; 26% cranberry juice from concentrate
23	Kombucha Cranberry	Juice	Cranberries; 5.1% cranberry juice
29	Aloe vera Cranberry Juice	Juice	Cranberries; 1% cranberry juice
47	Organic Cranberry Nectar	Juice	Cranberries; cranberry juice

48	Scandinavian Lingonberry Juice	Juice	
52	Lingonberry Syrup	Juice	Lingonberries
64	Organic Cranberry juice	Juice	Cranberries; 12.5% cranberry juice
67	Juice made from european cranberries	Juice	VO; 100% Moosbeeren (V. oxycoccos)
69	Aronia Juice	Juice	
72	Cranberry Juice	Juice	Cranberries; 100% cranberry juice
81	Rosehip Cranberry juice	Juice	Cranberries
82	Cranberry Premium Nectar	Juice	Cranberries
83	Organic Cranberry juice	Juice	Cranberries
84	Cranberry juice	Juice	Cranberries; 27% cranberry juice from concentrate
10	Cranberry 1000 + Vitamin C	Supplements	Cranberries; pulverised cranberryjuice
11	powdered Cranberry	Supplements	VO; 100% Moosbeeren (V. oxycoccos)
12	powdered Lingonberry	Supplements	Lingonberries; 100% lingonberries
13	Cranberry + Vitamin C	Supplements	Cranberries; 50% pulverised cranberry juice
14	Cranberry capsule	Supplements	Cranberries; pulverised cranberry juice
15	Super strength Cranberry	Supplements	Cranberries
43	Lingonberry Granulate+Vitamin C	Supplements	Lingonberries; lingonberry extract
38	Tea (Blueberry and cranberry)	Tea	Cranberries; 1% lingonberries
39	Tea (Cranberry and Raspberry)	Tea	Cranberries; 1% lingonberries
40	Cranberry fruit Tea organic	Tea	Cranberries; 20% cranberries
41	Tea (Cranberry and Raspberry)	Tea	Cranberries; 3% cranberry pomace

**7.7.2 Concentration and purity of the DNA extracts of the positive controls, herbarium samples, and commercial food samples**

ID	DNA [ng/μl] Qubit	DNA [ng/μl] Nanodrop	A260/280	A260/230
1	0.472	2.00	2.14	0.59
2	0.042	1.60	0.78	0.09
3	4.960	11.25	1.72	0.40
4	1.300	14.75	1.44	0.27
5	< LOD	< LOD	1.63	< LOD
6	< LOD	< LOD	1.40	< LOD
7	0.010	0.40	0.27	0.04
8	0.081	0.60	0.57	0.05
9	0.013	0.05	0.58	0.01
10	< LOD	< LOD	1.15	0.82
11	0.070	15.15	1.45	0.18
12	0.043	6.05	1.12	0.10
13	< LOD	< LOD	1.67	0.70
14	< LOD	1.10	2.03	0.22
15	0.037	24.80	1.22	0.55
16	1.250	16.25	1.16	0.29
17	0.000	7.40	1.00	0.17
18	< LOD	< LOD	1.36	0.51
19	0.005	< LOD	1.65	0.80
20	< LOD	< LOD	1.54	0.40
21	0.298	5.80	2.94	0.11
22	< LOD	< LOD	1.89	0.57
23	0.006	< LOD	1.41	0.71
24	0.059	< LOD	< LOD	< LOD
25	0.016	0.60	0.66	0.04
26	0.011	0.75	0.60	0.05
27	0.360	0.95	0.60	0.04
28	0.008	0.70	0.45	0.06
29	0.006	< LOD	1.29	0.95
30	5.530	21.20	1.54	0.38
31	0.596	9.55	1.25	0.22
32	0.032	< LOD	1.44	3.85
33	0.118	4.72	0.82	< LOD
34	0.326	< LOD	1.35	< LOD
35	0.604	7.35	2.18	0.27
36	0.700	8.75	2.38	0.24
37	0.660	0.10	1.13	0.01
38	0.345	44.15	1.41	0.55
39	0.390	86.05	1.28	0.46

40	0.436	28.55	0.80	0.13
41	0.198	25.00	1.49	0.44
42	0.848	6.60	1.34	0.13
43	0.005	< LOD	1.58	0.52
44	0.025	< LOD	< LOD	< LOD
45	0.022	9.40	0.63	0.10
46	0.314	2.15	0.37	0.06
47	< LOD	< LOD	1.62	0.57
48	< LOD	< LOD	1.59	0.52
49	0.012	< LOD	1.28	< LOD
50	3.500	4.25	2.30	0.12
51	0.040	8.50	0.75	0.10
52	< LOD	< LOD	1.46	0.54
53	0.039	< LOD	1.98	< LOD
54	0.032	< LOD	4.41	< LOD
55	0.018	11.65	0.67	0.12
56	0.017	< LOD	3.40	< LOD
57	0.034	< LOD	3.44	< LOD
58	0.015	< LOD	1.81	< LOD
59	0.008	< LOD	2.05	< LOD
60	0.056	< LOD	1.40	< LOD
61	1.170	< LOD	1.60	3.62
62	0.792	< LOD	1.77	0.69
63	0.350	0.25	< LOD	0.01
64	< LOD	< LOD	1.48	0.50
65	0.193	< LOD	1.48	0.73
66	0.013	< LOD	3.77	< LOD
67	0.006	< LOD	1.52	0.72
68	0.754	< LOD	1.49	0.87
69	0.007	< LOD	1.55	< LOD
70	0.122	< LOD	1.63	3.08
71	0.200	4.25	0.77	0.08
72	< LOD	< LOD	1.40	0.74
73	0.119	< LOD	1.47	< LOD
74	1.890	21.10	1.48	0.18
75	0.088	< LOD	1.37	< LOD
76	1.050	23.00	1.15	0.12
77	0.688	3.95	3.86	0.06
78	0.768	< LOD	1.14	< LOD
79	0.358	< LOD	1.22	< LOD
80	0.010	< LOD	1.74	3.54
81	0.005	< LOD	1.59	0.54
82	0.005	< LOD	1.52	0.60
83	0.006	< LOD	1.61	0.54
84	0.007	< LOD	1.59	0.57

85	0.005	< LOD	1.56	0.54
86	0.011	< LOD	< LOD	< LOD
87	0.009	< LOD	< LOD	< LOD
88	0.028	24.20	0.94	0.13
89	0.047	< LOD	< LOD	< LOD
90	0.030	< LOD	< LOD	< LOD
91	0.148	< LOD	1.35	< LOD

ID	DNA [ng/μl] Nanodrop	260/280	260/230
H1	12.7	1.08	0.28
H2	11.8		
H3	7.3	1.02	0.23
H4	3.5	1.73	0.33
H5	6.1		
H6	5.9	1.48	0.29
H7	7.1	1.62	0.37
H13	4.9	1.44	0.39
H14	4.45		
H15	7.9	1.33	0.28



### 7.7.3 Concentration and purity of the Matrix-components DNA extracts

ID	Name	DNA		A260/280	A260/230
		DNA [ng/μl] Qubit	[ng/μl] Nanodrop		
A	almond	2.440	<LOD	0.94	0.63
A1	almond	3.140	<LOD	1.07	0.99
B	cashew	1.860	11.55	2.30	0.29
B1	cashew	0.840	1.70	<LOD	0.09
C	walnut	4.300	12.45	1.28	0.25
C1	walnut	3.920	1.10	1.22	0.11
D	poppy seed	14.700	23.55	1.94	1.63
D1	poppy seed	16.900	21.10	2.06	1.76
E	raisin	0.074	0.10	0.08	0.01
E1	raisin	0.284	<LOD	1.54	39.63
F	grape	0.101	<LOD	1.57	0.62
F1	grape	0.177	<LOD	1.55	1.44
G	strawberry	0.490	9.90	1.01	0.15
G1	strawberry	0.642	7.35	1.12	0.11
H	goji	5.340	2.20	3.05	0.54
H1	goji	5.040	<LOD	0.90	0.27
I	raspberry	0.836	10.50	1.15	0.22
I1	raspberry	0.298	1.80	0.81	0.07
J	blackberry	0.184	<LOD	1.69	1.26
J1	blackberry	0.214	<LOD	1.74	3.42
K	red currant	0.103	<LOD	1.44	0.82
K1	red currant	0.151	<LOD	1.37	0.69
K2	red currant	0.390	<LOD	1.35	0.57
L	apple	0.034	<LOD	1.44	0.70
L1	apple	0.036	<LOD	1.45	0.93
M	pomegranate	0.023	<LOD	1.51	0.65
M1	pomegranate	0.294	1.10	0.41	0.03
N	sour cherry	0.066	2.40	0.53	0.06
N1	sour cherry	0.020	<LOD	3.85	<LOD
O	apple Evelina	0.032	<LOD	1.32	0.75
P	apple Gala	0.021	<LOD	1.32	0.99
Q	apple Granny Smith	0.054	<LOD	1.37	0.80
	apple Golden				
R	delicious	0.036	<LOD	1.22	0.89
S	white currant leaves	13.600	22.4	1.95	0.75
T	red currant leaves	18.700	25.25	1.94	0.80
U	black currant leaves	11.200	18.65	1.95	0.56
V	black currant leaves	5.800	9.6	2.00	0.33

## Other Samples

ID	Name	DNA [ng/μl] Qubit	DNA [ng/μl] Nanodrop	A260/280	A260/230
1A	Bilberry	0.448	< LOD	< LOD	< LOD
2B	Blueberry	0.172	< LOD	1.68	1.22
A3B	Aronia	0.051	5.20		
APF	Apple	0.057	< LOD	1.15	< LOD
	Cereal				
BAL	bar	0.484	11	3.81	0.1
	Chocolate				
	75%				
COC	cacao	0.596	6.75	0.94	0.14
	Bilberry				
FHD	jam	0.099	< LOD	2.59	< LOD
	Raw				
	muscat				
KUE	pumpkin	1.210	< LOD	1.12	< LOD
RET	Beetroot	0.117	< LOD	1.34	0.9

## 7.8 References

1. Sumar, S.; Ismail, H. Adulteration of foods – past and present. *Nutr. Food Sci.* **1995**, *95*, 11–15.
2. Shears, P. Food fraud – a current issue but an old problem. *Br. Food J.* **2010**, *112*, 198–213.
3. RIS - Lebensmittelsicherheits- und Verbraucherschutzgesetz - Bundesrecht konsolidiert, Fassung vom 02.07.2018 Available online: <https://www.ris.bka.gv.at/GeltendeFassung.wxe?Abfrage=Bundesnormen&Gesetzesnummer=20004546> (accessed on Jul 2, 2018).
4. Oostvogels, R.; Kemperman, H.; Hubeek, I.; ter Braak, E.W. The importance of the osmolality gap in ethylene glycol intoxication. *BMJ* **2013**, *347*, f6904–f6904.
5. Beccaria, F.; Herring, R.; Thom, B.; Kolind, T.; Moskalewicz, J. Alcohol harm reduction in Europe. In *Harm reduction: evidence, impacts and challenges*; Rhodes, T., Hedrich, D., Eds.; 2010; pp. 275–301 ISBN 978-92-9168-419-9.
6. Skinner, P. The Utilisation of a Central Wine Marketing Organisation in The Re-Marketing of Austrian Wine — Post - 1985. *Int. J. Wine Mark.* **1993**, *5*, 4–14.
7. Pei, X.; Tandon, A.; Alldrick, A.; Giorgi, L.; Huang, W.; Yang, R. The China melamine milk scandal and its implications for food safety regulation. *Food Policy* **2011**, *36*, 412–420.
8. EFSA Panel on Dietetic Products, Nutrition and Allergies (NDA) Statement of EFSA on risks for public health due to the presences of melamine in infant milk and other milk products in China. *EFSA J.* **2008**, *807*, 1–10.
9. Langman, C.B. Melamine, Powdered Milk, and Nephrolithiasis in Chinese Infants. *N. Engl. J. Med.* **2009**, *360*, 1139–1141.
10. Gossner, C.M.-E.; Schlundt, J.; Ben Embarek, P.; Hird, S.; Lo-Fo-Wong, D.; Beltran, J.J.O.; Teoh, K.N.; Tritscher, A. The Melamine Incident: Implications for International Food and Feed Safety. *Environ. Health Perspect.* **2009**, *117*, 1803–1808.
11. Chen, J.-R.; Shiau, Y.-J. Application of internal transcribed spacers and maturase K markers for identifying *Anoectochilus*, *Ludisia*, and *Ludochilus*. *Biol. Plant.* **2015**, *59*, 485–490.
12. Lawrence, F. Findus beef lasagne withdrawn after tests show high level of horsemeat. *The Guardian* 2013.
13. Collins, D. Ring of steel, high chimneys and few windows: Horse meat lasagne factory revealed Available online: <http://www.mirror.co.uk/news/uk-news/horse-meat-lasagne-factory-revealed-1595234> (accessed on Jul 30, 2018).
14. Premanandh, J. Horse meat scandal – A wake-up call for regulatory authorities. *Food Control* **2013**, *34*, 568–569.
15. Galimberti, A.; De Mattia, F.; Losa, A.; Bruni, I.; Federici, S.; Casiraghi, M.; Martellos, S.; Labra, M. DNA barcoding as a new tool for food traceability. *Food Res. Int.* **2013**, *50*, 55–63.
16. Konczak, I.; Roulle, P. Nutritional properties of commercially grown native Australian fruits: Lipophilic antioxidants and minerals. *Food Res. Int.* **2011**, *44*, 2339–2344.
17. Pereira, C.; Barros, L.; Carvalho, A.M.; Ferreira, I.C.F.R. Nutritional composition and bioactive properties of commonly consumed wild greens: Potential sources for new trends in modern diets. *Food Res. Int.* **2011**, *44*, 2634–2640.
18. Shelton, A.M.; Zhao, J.-Z.; Roush, R.T. Economic, Ecological, Food Safety, and Social Consequences of the Deployment of Bt Transgenic Plants. *Annu. Rev. Entomol.* **2002**, *47*, 845–881.
19. Pritchard, L.; Glover, R.H.; Humphris, S.; Elphinstone, J.G.; Toth, I.K. Genomics and taxonomy in diagnostics for food security: soft-rotting enterobacterial plant pathogens. *Anal. Methods* **2016**, *8*, 12–24.
20. Ramarathnam, N.; Osawa, T.; Ochi, H.; Kawakishi, S. The contribution of plant food antioxidants to human health. *Trends Food Sci. Technol.* **1995**, *6*, 75–82.

21. Utsumi, S. Plant Food Protein Engineering. In *Advances in Food and Nutrition Research*; Kinsella, J.E., Ed.; Elsevier, 1992; Vol. 36, pp. 89–208 ISBN 978-0-12-016436-3.
22. Radauer, C.; Breiteneder, H. Evolutionary biology of plant food allergens. *J. Allergy Clin. Immunol.* **2007**, *120*, 518–525.
23. Spink, J.; Moyer, D.C. Defining the Public Health Threat of Food Fraud. *J. Food Sci.* **2011**, *76*, R157–R163.
24. Moore, J.C.; Spink, J.; Lipp, M. Development and Application of a Database of Food Ingredient Fraud and Economically Motivated Adulteration from 1980 to 2010. *J. Food Sci.* **2012**, *77*, R118–R126.
25. Francis, F.J. Detection of Enocyanin in Cranberry Juice Cocktail by Color and Pigment Profile. *J. Food Sci.* **1985**, *50*, 1640–1642.
26. Hale, M.L.; Francis, F.J.; Fagerson, I.S. Detection of Enocyanin in Cranberry Juice Cocktail by HPLC Anthocyanin Profile. *J. Food Sci.* **1986**, *51*, 1511–1513.
27. Wrolstad, R.E.; Culbertson, J.D.; Cornwell, C.J.; Mattick, L.R. Detection of adulteration in blackberry juice concentrates and wines. *J. - Assoc. Off. Anal. Chem.* **1982**, *65*, 1417–1423.
28. Lee, J. Analysis of bokbunja products show they contain *Rubus occidentalis* L. fruit. *J. Funct. Foods* **2015**, *12*, 144–149.
29. Lee, J. Anthocyanin analyses of *Vaccinium* fruit dietary supplements. *Food Sci. Nutr.* **2016**, *4*, 742–752.
30. Marieschi, M.; Torelli, A.; Beghé, D.; Bruni, R. Authentication of *Punica granatum* L.: Development of SCAR markers for the detection of 10 fruits potentially used in economically motivated adulteration. *Food Chem.* **2016**, *202*, 438–444.
31. Foster, S.; Blumenthal, M. The Adulteration of Commercial Bilberry Extracts. *HerbalGram* **96**, 64–73.
32. Natho, G. D. J. Mabberley: The Plant-Book. A portable dictionary of the vascular plants. *Feddes Repert.* **2008**, *109*, 378–378.
33. Hyam, R.; Pankhurst, R.J. *Plants and their names: a concise dictionary*; Oxford University Press; Royal Botanic Gardens: Oxford [England]; New York: Edinburgh [England], 1995; ISBN 978-0-19-866189-4.
34. Powell, E.A.; Kron, K.A. Hawaiian Blueberries and Their Relatives: A Phylogenetic Analysis of *Vaccinium* Sections *Macropelma*, *Myrtillus*, and *Hemimyrtillus* (Ericaceae). *Syst. Bot.* **2002**, *27*, 768–779.
35. Kalt, W.; Dufour, D. Health Functionality of Blueberries. *HortTechnology* **1997**, *7*, 216–221.
36. File:CDC\_cranberry1.jpg - Wikimedia Commons Available online: [https://commons.wikimedia.org/wiki/File:CDC\\_cranberry1.jpg](https://commons.wikimedia.org/wiki/File:CDC_cranberry1.jpg) (accessed on Jan 6, 2019).
37. *Vaccinium\_oxycoccos.\_(1).jpg* Available online: [https://upload.wikimedia.org/wikipedia/commons/0/01/VACCINIUM\\_OXYCOCCOS.\\_%281%29.jpg](https://upload.wikimedia.org/wikipedia/commons/0/01/VACCINIUM_OXYCOCCOS._%281%29.jpg) (accessed on Jan 6, 2019).
38. English: Lingonberry (*Vaccinium vitis-idaea*) by Arto J. Available online: [https://commons.wikimedia.org/wiki/File:Lingonberry\\_\(Vaccinium\\_vitis-idaea\)\\_-\\_panoramio.jpg](https://commons.wikimedia.org/wiki/File:Lingonberry_(Vaccinium_vitis-idaea)_-_panoramio.jpg) (accessed on Jan 6, 2019).
39. Neto, C.C. Cranberry and blueberry: Evidence for protective effects against cancer and vascular diseases. *Mol. Nutr. Food Res.* **2007**, *51*, 652–664.
40. Vvedenskaya, I.O.; Vorsa, N. Flavonoid composition over fruit development and maturation in American cranberry, *Vaccinium macrocarpon* Ait. *Plant Sci.* **2004**, *167*, 1043–1054.
41. Camire, M.E. Phytochemicals in the *Vaccinium* Family: Billberries, Blueberries, and Cranberries. In *Phytochemicals in Nutrition and Health*; Meskin, M.S., Bidlack, W.R., Davies, A.J., Omaye, S.T., Eds.; CRC Press: Boca Raton, 2002, pp. 29–35 ISBN 1-58716-083-8.

42. Vinson, J.A.; Su, X.; Zubik, L.; Bose, P. Phenol antioxidant quantity and quality in foods: fruits. *J. Agric. Food Chem.* **2001**, *49*, 5315–5321.
43. Prior, R.L.; Lazarus, S.A.; Cao, G.; Muccitelli, H.; Hammerstone, J.F. Identification of procyanidins and anthocyanins in blueberries and cranberries (*Vaccinium* spp.) using high-performance liquid chromatography/mass spectrometry. *J. Agric. Food Chem.* **2001**, *49*, 1270–1276.
44. Wang, S.Y.; Stretch, A.W. Antioxidant capacity in cranberry is influenced by cultivar and storage temperature. *J. Agric. Food Chem.* **2001**, *49*, 969–974.
45. Wu, X.; Prior, R.L. Systematic identification and characterization of anthocyanins by HPLC-ESI-MS/MS in common foods in the United States: fruits and berries. *J. Agric. Food Chem.* **2005**, *53*, 2589–2599.
46. Riihinen, K.; Jaakola, L.; Kärenlampi, S.; Hohtola, A. Organ-specific distribution of phenolic compounds in bilberry (*Vaccinium myrtillus*) and 'northblue' blueberry (*Vaccinium corymbosum* x *V. angustifolium*). *Food Chem.* **2008**, *110*, 156–160.
47. Sapers, G.; Hargrave, D. Proportions of individual anthocyanins in fruits of cranberry cultivars. *J. Am. Soc. Hortic. Sci.* **1987**, *112*, 100–104.
48. Hong, V.; Wrolstad, R.E. Use of HPLC separation/photodiode array detection for characterization of anthocyanins. *J. Agric. Food Chem.* **1990**, *38*, 708–715.
49. Forney, C.F.; Kalt, W. Blueberry and Cranberry. In *Health-promoting Properties of Fruit and Vegetables*; Terry, L.A., Ed.; CABI: Wallingford, Oxfordshire, UK; Cambridge, MA, USA, 2011; pp. 51-65 ISBN 978-1-84593-528-3.
50. Fajardo, D.; Morales, J.; Zhu, H.; Steffan, S.; Harbut, R.; Bassil, N.; Hummer, K.; Polashock, J.; Vorsa, N.; Zalapa, J. Discrimination of American Cranberry Cultivars and Assessment of Clonal Heterogeneity Using Microsatellite Markers. *Plant Mol. Biol. Report.* **2013**, *31*, 264–271.
51. Zhu, H.; Senalik, D.; McCown, B.H.; Zeldin, E.L.; Speers, J.; Hyman, J.; Bassil, N.; Hummer, K.; Simon, P.W.; Zalapa, J.E. Mining and validation of pyrosequenced simple sequence repeats (SSRs) from American cranberry (*Vaccinium macrocarpon* Ait.). *Theor. Appl. Genet.* **2012**, *124*, 87–96.
52. Bassil, N.V. Microsatellite Markers: Valuable in *Vaccinium* L. *Int. J. Fruit Sci.* **2012**, *12*, 288–293.
53. Kylli, P.; Nohynek, L.; Puupponen-Pimiä, R.; Westerlund-Wikström, B.; Leppänen, T.; Welling, J.; Moilanen, E.; Heinonen, M. Lingonberry ( *Vaccinium vitis-idaea* ) and European Cranberry ( *Vaccinium microcarpon* ) Proanthocyanidins: Isolation, Identification, and Bioactivities. *J. Agric. Food Chem.* **2011**, *59*, 3373–3384.
54. Jungfer, E.; Zimmermann, B.F.; Ruttkat, A.; Galensa, R. Comparing Procyanidins in Selected *Vaccinium* Species by UHPLC-MS<sup>2</sup> with Regard to Authenticity and Health Effects. *J. Agric. Food Chem.* **2012**, *60*, 9688–9696.
55. Jaakola, L.; Suokas, M.; Häggman, H. Novel approaches based on DNA barcoding and high-resolution melting of amplicons for authenticity analyses of berry species. *Food Chem.* **2010**, *123*, 494–500.
56. Vander Kloet, S.P. *The genus Vaccinium in North America*; Canadian Government Publishing Centre: Ottawa, Canada, 1988; pp. 1-38 ISBN 978-0-660-13037-8.
57. Trehane, J. *Blueberries, Cranberries and Other Vacciniums.*; Timber Press, Incorporated Workman Publishing Company, Incorporated [distributor: Portland; New York, 2009; ISBN 978-1-60469-072-9.
58. Kuhnlein, H.V.; Turner, N.J. *Traditional plant foods of Canadian indigenous peoples: nutrition, botany, and use*; Food and nutrition in history and anthropology; Gordon and Breach: Philadelphia, 1991; pp. 173-174 ISBN 978-2-88124-465-0.
59. Litz, R.E.; *Biotechnology of fruit and nut crops*; Biotechnology in agriculture series; CABI Pub: Wallingford, Oxfordshire, UK; Cambridge, MA, 2005; pp. 247-261 ISBN 978-0-85199-662-2.

60. Song, G.-Q.; Hancock, J.F. *Vaccinium*. In *Wild Crop Relatives: Genomic and Breeding Resources*; Kole, C., Ed.; Springer Berlin Heidelberg: Berlin, Heidelberg, 2011; pp. 197–221 ISBN 978-3-642-16056-1.
61. Camp, W.H. A Preliminary Consideration of the Biosystematy of *Oxycoccus*. *Bull. Torrey Bot. Club* **1944**, *71*, 426.
62. Terry, L.A.; *Health-promoting properties of fruit and vegetables*; CABI: Wallingford, Oxfordshire, UK : Cambridge, MA, USA, 2011; p 52 ISBN 978-1-84593-528-3.
63. Moosbeeren-Ernte in New Jersey./Cranberry harvest in New Jersey. by Keith Weller Available online: [https://commons.wikimedia.org/wiki/File:Cranberrys\\_beim\\_Ernten.jpeg](https://commons.wikimedia.org/wiki/File:Cranberrys_beim_Ernten.jpeg) (accessed on Jan 6, 2019).
64. Bild: STEM: All Hands on Tech - The Season's Science Packed Berry ... Available online: [https://www.google.com/imgres?imgurl=http%3A%2F%2Ffarmhousefruit.com%2Fwp-content%2Fuploads%2F2015%2F10%2FCranberry-Single.jpg&imgrefurl=https%3A%2F%2Fwww.carnegielibrary.org%2Fcranberry%2F&docid=dWyzHsdAfaF9kM&tbid=W6u8v-LHIDUk5M%3A&vet=10ahUKEwjw5PXzqpzcAhVJZVAKHfcPD\\_4QMwg0KAewAQ.i&w=500&h=375&client=firefox-b-ab&bih=593&biw=1348&q=cranberry%20inside&ved=0ahUKEwjw5PXzqpzcAhVJZVAKHfcPD\\_4QMwg0KAewAQ&iact=mrc&uact=8](https://www.google.com/imgres?imgurl=http%3A%2F%2Ffarmhousefruit.com%2Fwp-content%2Fuploads%2F2015%2F10%2FCranberry-Single.jpg&imgrefurl=https%3A%2F%2Fwww.carnegielibrary.org%2Fcranberry%2F&docid=dWyzHsdAfaF9kM&tbid=W6u8v-LHIDUk5M%3A&vet=10ahUKEwjw5PXzqpzcAhVJZVAKHfcPD_4QMwg0KAewAQ.i&w=500&h=375&client=firefox-b-ab&bih=593&biw=1348&q=cranberry%20inside&ved=0ahUKEwjw5PXzqpzcAhVJZVAKHfcPD_4QMwg0KAewAQ&iact=mrc&uact=8) (accessed on Jul 30, 2018).
65. Hooper, S.N.; Chandler, R.F. Herbal remedies of the maritime Indians: Phytosterols and triterpenes of 67 plants. *J. Ethnopharmacol.* **1984**, *10*, 181–194.
66. Eck, P. *The American cranberry*; Rutgers University Press: New Brunswick, 1990; ISBN 978-0-8135-1491-8.
67. Weiss, E.I.; Lev-Dor, R.; Kashamn, Y.; Goldhar, J.; Sharon, N.; Ofek, I. Inhibition of interspecies coaggregation of plaque bacteria with cranberry juice constituent. *J. Am. Dent. Assoc.* **1998**, *129*, 1719–1723.
68. Weiss, E.I.; Lev-Dor, R.; Sharon, N.; Ofek, I. Inhibitory Effect of a High-Molecular-Weight Constituent of Cranberry on Adhesion of Oral Bacteria. *Crit. Rev. Food Sci. Nutr.* **2002**, *42*, 285–292.
69. Bodet, C.; Grenier, D.; Chandad, F.; Ofek, I.; Steinberg, D.; Weiss, E.I. Potential Oral Health Benefits of Cranberry. *Crit. Rev. Food Sci. Nutr.* **2008**, *48*, 672–680.
70. Ruel, G.; Pomerleau, S.; Couture, P.; Lemieux, S.; Lamarche, B.; Couillard, C. Low-calorie cranberry juice supplementation reduces plasma oxidized LDL and cell adhesion molecule concentrations in men. *Br. J. Nutr.* **2008**, *99*.
71. McKay, D.L.; Blumberg, J.B. Cranberries (*Vaccinium macrocarpon*) and Cardiovascular Disease Risk Factors. *Nutr. Rev.* **2008**, *65*, 490–502.
72. Yan, X.; Murphy, B.T.; Hammond, G.B.; Vinson, J.A.; Neto, C.C. Antioxidant Activities and Antitumor Screening of Extracts from Cranberry Fruit ( *Vaccinium macrocarpon* ). *J. Agric. Food Chem.* **2002**, *50*, 5844–5849.
73. Liu, Y.; Black, M.A.; Caron, L.; Camesano, T.A. Role of cranberry juice on molecular-scale surface characteristics and adhesion behavior of *Escherichia coli*. *Biotechnol. Bioeng.* **2006**, *93*, 297–305.
74. Kontiokari, T.; Sundqvist, K.; Nuutinen, M.; Pokka, T.; Koskela, M.; Uhari, M. Randomised trial of cranberry-lingonberry juice and Lactobacillus GG drink for the prevention of urinary tract infections in women. *BMJ* **2001**, *322*, 1571.
75. EFSA Panel on Dietetic Products, Nutrition and Allergies (NDA) Scientific Opinion on the substantiation of health claims related to: a combination of millet seed extract, L-cystine and pantothenic acid (ID 1514), amino acids (ID 1711), carbohydrate and protein combination (ID 461), *Ribes nigrum* L. (ID 2191), *Vitis vi*: Health claims related to not sufficiently characterised foods/food constituents. *EFSA J.* **2011**, *9*, 2244.
76. European Food Safety Authority (EFSA) Ocean Spray Cranberry Products® and urinary tract infection in women - Scientific substantiation of a health claim related to Ocean Spray Cranberry Products® and urinary tract infection in women pursuant to Article 14

- of Regulation (EC) No 1924/2006: Ocean Spray Cranberry Products® and urinary tract infection in women - Scientific substantiation of a health claim related to Ocean Spray Cranberry Pr. *EFSA J.* **2009**, 7, 943.
77. EFSA Panel on Dietetic Products, Nutrition and Allergies (NDA) Scientific Opinion on the substantiation of health claims related to proanthocyanidins from cranberry (*Vaccinium macrocarpon* Aiton) fruit and defence against bacterial pathogens in the lower urinary tract (ID 1841, 2153, 2770, 3328), “powerful protectors: Proanthocyanidins from cranberry (*Vaccinium macrocarpon* Aiton) fruit related health claims. *EFSA J.* **2011**, 9, 2215.
  78. Česonienė, L.; Daubaras, R.; Jasutienė, I. Selection of the European cranberry in Lithuania. *Latv. J. Agron. Vestis* **2009**.
  79. Suda, J. Sympatric occurrences of various cytotypes of *Vaccinium* sect. *Oxycoccus* (Ericaceae). *Nord. J. Bot.* **2002**, 22, 593–601.
  80. Suda, J.; Lysák, M.A. A taxonomic study of the *Vaccinium* sect. *Oxycoccus* (Hill) W.D.J. Kock (Ericaceae) in the Czech Republic and adjacent territories. *Folia Geobot.* **2001**, 36, 303–320.
  81. *vaccinium\_GaultheriaLeafComparison01gf400.jpg* (JPEG-Grafik, 541 × 400 Pixel) Available online: [https://www.uwgb.edu/biodiversity/herbarium/shrubs/vaccinium\\_GaultheriaLeafComparison01gf400.jpg](https://www.uwgb.edu/biodiversity/herbarium/shrubs/vaccinium_GaultheriaLeafComparison01gf400.jpg) (accessed on Jul 30, 2018).
  82. Gafner, S. on Bilberry (*Vaccinium myrtillus*) Extracts. *Bot. Adulterants Bull.* **2016**, 6.
  83. Kole, C.; *Wild Crop Relatives: Genomic and Breeding Resources* Springer Berlin Heidelberg: Berlin, Heidelberg, 2011; p 202 ISBN 978-3-642-16056-1.
  84. Janick, J., Moore, J.N., *Fruit breeding* Wiley: New York, 1996; pp. 1-107 ISBN 978-0-471-12675-1.
  85. Gustavsson, B. Breeding Strategies in Lingonberry Culture (*Vaccinium vitis-idaea*). *Acta Hortic.* **1997**, 129–138.
  86. Wang, S.Y.; Feng, R.; Bowman, L.; Penhallegon, R.; Ding, M.; Lu, Y. Antioxidant Activity in Lingonberries (*Vaccinium vitis-idaea* L.) and Its Inhibitory Effect on Activator Protein-1, Nuclear Factor-κB, and Mitogen-Activated Protein Kinases Activation. *J. Agric. Food Chem.* **2005**, 53, 3156–3166.
  87. Kress, W.J.; Wurdack, K.J.; Zimmer, E.A.; Weigt, L.A.; Janzen, D.H. Use of DNA barcodes to identify flowering plants. *Proc. Natl. Acad. Sci. U. S. A.* **2005**, 102, 8369–8374.
  88. Savolainen, V.; Cowan, R.S.; Vogler, A.P.; Roderick, G.K.; Lane, R. Towards writing the encyclopaedia of life: an introduction to DNA barcoding. *Philos. Trans. R. Soc. B Biol. Sci.* **2005**, 360, 1805–1811.
  89. Hebert, P.D.N.; Ratnasingham, S.; de Waard, J.R. Barcoding animal life: cytochrome c oxidase subunit 1 divergences among closely related species. *Proc. R. Soc. B Biol. Sci.* **2003**, 270, S96–S99.
  90. Group, C.P.W.; Hollingsworth, P.M.; Forrest, L.L.; Spouge, J.L.; Hajibabaei, M.; Ratnasingham, S.; van der Bank, M.; Chase, M.W.; Cowan, R.S.; Erickson, D.L. A DNA barcode for land plants. *Proc. Natl. Acad. Sci.* **2009**, 106, 12794–12797.
  91. Mohr, G.; Perlman, P.S.; Lambowitz, A.M. Evolutionary relationships among group II intron-encoded proteins and identification of a conserved domain that may be related to maturase function. *Nucleic Acids Res.* **1993**, 21, 4991–4997.
  92. Zoschke, R.; Nakamura, M.; Liere, K.; Sugiura, M.; Börner, T.; Schmitz-Linneweber, C. An organellar maturase associates with multiple group II introns. *Proc. Natl. Acad. Sci.* **2010**, 107, 3245–3250.
  93. Wilson, C.A. Phylogeny of Iris based on chloroplast *matK* gene and *trnK* intron sequence data. *Mol. Phylogenet. Evol.* **2004**, 33, 402–412.
  94. Staats, M.; Arulandhu, A.J.; Gravendeel, B.; Holst-Jensen, A.; Scholtens, I.; Peelen, T.; Prins, T.W.; Kok, E. Advances in DNA metabarcoding for food and wildlife forensic species identification. *Anal. Bioanal. Chem.* **2016**, 408, 4615–4630.

95. Baldwin, B.G. Phylogenetic utility of the internal transcribed spacers of nuclear ribosomal DNA in plants: an example from the compositae. *Mol. Phylogenet. Evol.* **1992**, *1*, 3–16.
96. nF3kE.jpg (JPEG-Grafik, 570 × 400 Pixel) Available online: <https://i.stack.imgur.com/nF3kE.jpg> (accessed on Jul 30, 2018).
97. Lafontaine, D.L.; Tollervey, D. The function and synthesis of ribosomes. *Nat. Rev. Mol. Cell Biol.* **2001**, *2*, 514.
98. Loomis, W.D. [54] Overcoming problems of phenolics and quinones in the isolation of plant enzymes and organelles. In *Methods in Enzymology*; Fleischer, S., Packer, L., Eds.; Elsevier, 1974; Vol. 31, pp. 528–544 ISBN 978-0-12-181894-4.
99. Demeke, T.; Adams, R.P. The effects of plant polysaccharides and buffer additives on PCR. *BioTechniques* **1992**, *12*, 332–334.
100. John, M.E. An efficient method for isolation of RNA and DNA from plants containing polyphenolics. *Nucleic Acids Res.* **1992**, *20*, 2381.
101. Seeram, N.P.; Adams, L.S.; Zhang, Y.; Lee, R.; Sand, D.; Scheuller, H.S.; Heber, D. Blackberry, Black Raspberry, Blueberry, Cranberry, Red Raspberry, and Strawberry Extracts Inhibit Growth and Stimulate Apoptosis of Human Cancer Cells In Vitro. *J. Agric. Food Chem.* **2006**, *54*, 9329–9339.
102. Wei, T.; Lu, G.; Clover, G. Novel approaches to mitigate primer interaction and eliminate inhibitors in multiplex PCR, demonstrated using an assay for detection of three strawberry viruses. *J. Virol. Methods* **2008**, *151*, 132–139.
103. Hennion, M.-C. Solid-phase extraction: method development, sorbents, and coupling with liquid chromatography. *J. Chromatogr. A* **1999**, *856*, 3–54.
104. Augusto, F.; Hantao, L.W.; Mogollón, N.G.S.; Braga, S.C.G.N. New materials and trends in sorbents for solid-phase extraction. *TrAC Trends Anal. Chem.* **2013**, *43*, 14–23.
105. Vogelstein, B.; Gillespie, D. Preparative and analytical purification of DNA from agarose. *Proc. Natl. Acad. Sci. U. S. A.* **1979**, *76*, 615–619.
106. Boom, R.; Sol, C.J.; Salimans, M.M.; Jansen, C.L.; Wertheim-van Dillen, P.M.; van der Noordaa, J. Rapid and simple method for purification of nucleic acids. *J. Clin. Microbiol.* **1990**, *28*, 495–503.
107. Butler, J.M. DNA Extraction Methods. In *Advanced Topics in Forensic DNA Typing*; Butler, J.M., Ed.; Elsevier, 2012; pp. 29–47 ISBN 978-0-12-374513-2.
108. Blood DNA Extraction: QIAamp DNA Blood Mini Kit - QIAGEN Online Shop Available online: <https://www.qiagen.com/us/shop/sample-technologies/dna/genomic-dna/qiaamp-dna-blood-mini-kit/#orderinginformation> (accessed on Jul 30, 2018).
109. Henson, J.M.; French, R. The Polymerase Chain Reaction and Plant Disease Diagnosis. *Annu. Rev. Phytopathol.* **1993**, *31*, 81–109.
110. Sipahioglu, H.M.; Usta, M.; Ocak, M. Use of dried high-phenolic laden host leaves for virus and viroid preservation and detection by PCR methods. *J. Virol. Methods* **2006**, *137*, 120–124.
111. Japelaghi, R.H.; Haddad, R.; Garoosi, G.-A. Rapid and Efficient Isolation of High Quality Nucleic Acids from Plant Tissues Rich in Polyphenols and Polysaccharides. *Mol. Biotechnol.* **2011**, *49*, 129–137.
112. Kim, C.S.; Lee, C.H.; Shin, J.S.; Chung, Y.S.; Hyung, N.I. A Simple and Rapid Method for Isolation of High Quality Genomic DNA from Fruit Trees and Conifers Using PVP. *Nucleic Acids Res.* **1997**, *25*, 1085–1086.
113. 280nm\_260nm\_A260\_A280\_ratio.png (PNG-Grafik, 579 × 388 Pixel) Available online: [http://gecko-instruments.de/media/Kemtrak/Protein\\_280nm/280nm\\_260nm\\_A260\\_A280\\_ratio.png](http://gecko-instruments.de/media/Kemtrak/Protein_280nm/280nm_260nm_A260_A280_ratio.png) (accessed on Jul 30, 2018).
114. Elliott, W.H.; Elliott, D.C. *Biochemistry and molecular biology*, 3rd ed.; Oxford University Press: Oxford ; New York, 2005; pp. 482-508 ISBN 978-0-19-927199-3.



115. Matissek, R.; Steiner, G.; Fischer, M. *Lebensmittelanalytik*; Springer-Lehrbuch; Springer Berlin Heidelberg: Berlin, Heidelberg, 2014; pp. 137-158 ISBN 978-3-642-34828-0.
116. Mcpherson, M.; Moller, S. *PCR: the Basics*; Taylor & Francis Ltd.: Hoboken, 2006; pp. 9-20 ISBN 978-0-203-00267-4.
117. Nucleobase Available online: <https://en.wikipedia.org/w/index.php?title=Nucleobase&oldid=851098518> (accessed on Jan 10, 2019).
118. Berg, J.M.; Tymoczko, J.L.; Stryer, L. *Biochemie*; Spektrum-Lehrbuch; 5. Aufl.; Spektrum Akad. Verl: Heidelberg, 2003; pp. 129-158 ISBN 978-3-8274-1303-1.
119. Alberts, B.; Jaenicke, L., *Molekularbiologie der Zelle: mit Cell biology interactive*; 4. Aufl.; Wiley-VCH: Weinheim, 2004; pp. 221-270 ISBN 978-3-527-30492-9.
120. Bartlett, J.M.S.; Stirling, D. A Short History of the Polymerase Chain Reaction. In *PCR Protocols*; Bartlett, J.M.S., Stirling, D., Eds.; Humana Press: New Jersey, 2003; Vol. 226, pp. 3–6 ISBN 978-1-59259-384-2.
121. Bild: Polymerase Chain Reaction (PCR): Steps, Types and Applications - Available online: [https://www.google.com/imgres?imgurl=https%3A%2F%2Fmicrobeonline.com%2Fwp-content%2Fuploads%2F2016%2F07%2FPolymerase\\_chain\\_reaction.svg\\_.png&imgrefurl=https%3A%2F%2Fmicrobeonline.com%2Fpolymerase-chain-reaction-pcr-steps-types-applications%2F&docid=k0nuM8YSWCLiSM&tbnid=pn\\_Na6BX23gROM%3A&vet=10ahUKEwj4syDuKPcAhUH3aQKHe0CCWwQMwg6KAAwAA..i&w=2000&h=1043&client=firefox-b-ab&bih=611&biw=1366&q=polymerase%20chain%20reaction&ved=0ahUKEwj4syDuKPcAhUH3aQKHe0CCWwQMwg6KAAwAA&iact=mrc&uact=8](https://www.google.com/imgres?imgurl=https%3A%2F%2Fmicrobeonline.com%2Fwp-content%2Fuploads%2F2016%2F07%2FPolymerase_chain_reaction.svg_.png&imgrefurl=https%3A%2F%2Fmicrobeonline.com%2Fpolymerase-chain-reaction-pcr-steps-types-applications%2F&docid=k0nuM8YSWCLiSM&tbnid=pn_Na6BX23gROM%3A&vet=10ahUKEwj4syDuKPcAhUH3aQKHe0CCWwQMwg6KAAwAA..i&w=2000&h=1043&client=firefox-b-ab&bih=611&biw=1366&q=polymerase%20chain%20reaction&ved=0ahUKEwj4syDuKPcAhUH3aQKHe0CCWwQMwg6KAAwAA&iact=mrc&uact=8) (accessed on Jul 30, 2018).
122. Li, M.; Palais, R.A.; Zhou, L.; Wittwer, C.T. Quantifying variant differences in DNA melting curves: Effects of length, melting rate, and curve overlay. *Anal. Biochem.* **2017**, *539*, 90–95.
123. Jansohn, M., Rothhämel, S., Aigner, A. *Gentechnische Methoden: eine Sammlung von Arbeitsanleitungen für das molekularbiologische Labor*; 5. Aufl.; Spektrum Akad. Verl: Heidelberg, 2012; pp. 137-171 ISBN 978-3-8274-2429-7.
124. Wartell, R.M.; Benight, A.S. Thermal denaturation of DNA molecules: A comparison of theory with experiment. *Phys. Rep.* **1985**, *126*, 67–107.
125. Chien, A.; Edgar, D.B.; Trela, J.M. Deoxyribonucleic acid polymerase from the extreme thermophile *Thermus aquaticus*. *J. Bacteriol.* **1976**, *127*, 1550–1557.
126. Lawyer, F.C.; Stoffel, S.; Saiki, R.K.; Chang, S.Y.; Landre, P.A.; Abramson, R.D.; Gelfand, D.H. High-level expression, purification, and enzymatic characterization of full-length *Thermus aquaticus* DNA polymerase and a truncated form deficient in 5' to 3' exonuclease activity. *PCR Methods Appl.* **1993**, *2*, 275–287.
127. Saiki, R.K.; Gelfand, D.H.; Stoffel, S.; Scharf, S.J.; Higuchi, R.; Horn, G.T.; Mullis, K.B.; Erlich, H.A. Primer-directed enzymatic amplification of DNA with a thermostable DNA polymerase. *Science* **1988**, *239*, 487–491.
128. Lewin, B. *Molekularbiologie der Gene*; Spektrum Lehrbuch; Studienausgabe.; Spektrum Akademischer Verlag: Heidelberg Berlin, 2002; pp. 381-408 ISBN 978-3-8274-1349-9.
129. Cline, J.; Braman, J.C.; Hogrefe, H.H. PCR fidelity of pfu DNA polymerase and other thermostable DNA polymerases. *Nucleic Acids Res.* **1996**, *24*, 3546–3551.
130. *PCR technology: principles and applications for DNA amplification*; Erlich, H.A., Ed.; Breakthroughs in molecular biology; Stockton Press [u.a.]: New York, 1989; pp. 17-22 ISBN 978-0-333-48948-2.
131. Lottspeich, F., Engels, J.W., *Bioanalytik*, 2., [aktualisierte und erw.] Aufl., [Nachdr.]; Spektrum, Akad. Verl: Heidelberg, 2009; pp. 743-776 ISBN 978-3-8274-1520-2.

132. Müller, H.-J.; Prange, D.R. *PCR - Polymerase-Kettenreaktion*; Springer Berlin Heidelberg: Berlin, Heidelberg, 2016; pp. 6-8 ISBN 978-3-662-48235-3.
133. Heid, C.A.; Stevens, J.; Livak, K.J.; Williams, P.M. Real time quantitative PCR. *Genome Res.* **1996**, *6*, 986–994.
134. Mao, F.; Leung, W.-Y.; Xin, X. Characterization of EvaGreen and the implication of its physicochemical properties for qPCR applications. *BMC Biotechnol.* **2007**, *7*, 76.
135. Ruskova, L.; Raclavsky, V. The Potential of High Resolution Melting Analysis (HRMA) to streamline, facilitate and enrich Routine Diagnostics in Medical Microbiology. *Biomed. Pap.* **2011**, *155*, 239–252.
136. Wittwer, C.T.; Herrmann, M.G.; Moss, A.A.; Rasmussen, R.P. Continuous fluorescence monitoring of rapid cycle DNA amplification. *BioTechniques* **1997**, *22*, 130–131, 134–138.
137. Ririe, K.M.; Rasmussen, R.P.; Wittwer, C.T. Product Differentiation by Analysis of DNA Melting Curves during the Polymerase Chain Reaction. *Anal. Biochem.* **1997**, *245*, 154–160.
138. Liew, M. Genotyping of Single-Nucleotide Polymorphisms by High-Resolution Melting of Small Amplicons. *Clin. Chem.* **2004**, *50*, 1156–1164.
139. Palais, R.; Wittwer, C.T. Chapter 13 Mathematical Algorithms for High-Resolution DNA Melting Analysis. In *Methods in Enzymology*; Elsevier, 2009; Vol. 454, pp. 323–343 ISBN 978-0-12-374552-1.
140. Reed, G.H.; Kent, J.O.; Wittwer, C.T. High-resolution DNA melting analysis for simple and efficient molecular diagnostics. *Pharmacogenomics* **2007**, *8*, 597–608.
141. Erali, M.; Wittwer, C.T. High resolution melting analysis for gene scanning. *Methods* **2010**, *50*, 250–261.
142. Herrmann, M.G. Amplicon DNA Melting Analysis for Mutation Scanning and Genotyping: Cross-Platform Comparison of Instruments and Dyes. *Clin. Chem.* **2006**, *52*, 494–503.
143. EvaGreen® Dye for qPCR & Other Applications. *Biotium*.
144. Overbergh, L.; Vig, S.; Coun, F.; Mathieu, C. Quantitative Polymerase Chain Reaction. In *Molecular Diagnostics*; Patrinos, G.P., Danielson, P.B., Ansorge, W., Eds.; Elsevier, 2017; pp. 41–58 ISBN 978-0-12-802971-8.
145. Farrar, J.S.; Wittwer, C.T. High-Resolution Melting Curve Analysis for Molecular Diagnostics. In *Molecular Diagnostics*; Patrinos, G.P., Danielson, P.B., Ansorge, W., Eds.; Elsevier, 2017; pp. 79–102 ISBN 978-0-12-802971-8.
146. Wittwer, C.T. High-Resolution Genotyping by Amplicon Melting Analysis Using LCGreen. *Clin. Chem.* **2003**, *49*, 853–860.
147. Garritano, S.; Gemignani, F.; Voegelé, C.; Nguyen-Dumont, T.; Le Calvez-Kelm, F.; De Silva, D.; Lesueur, F.; Landi, S.; Tavtigian, S.V. Determining the effectiveness of High Resolution Melting analysis for SNP genotyping and mutation scanning at the TP53 locus. *BMC Genet.* **2009**, *10*, 5.
148. Invitrogen™ 25 bp DNA Ladder Available online: [https://www.fishersci.de/shop/products/invitrogen-25-bp-dna-ladder/11598626?change\\_lang=true](https://www.fishersci.de/shop/products/invitrogen-25-bp-dna-ladder/11598626?change_lang=true).
149. Michov, B. *Elektrophorese: Theorie und Praxis*; 2011; pp. 339 ISBN 978-3-11-081942-7.
150. Jeppsson, J.O.; Laurell, C.B.; Franzén, B. Agarose gel electrophoresis. *Clin. Chem.* **1979**, *25*, 629–638.
151. Yikrazuul Agarose Available online: [https://commons.wikimedia.org/wiki/File:Agarose\\_polymere.svg](https://commons.wikimedia.org/wiki/File:Agarose_polymere.svg) (accessed on Jan 12, 2019).
152. Mülhardt, C. *Der Experimentator Molekularbiologie/Genomics*; Springer Berlin Heidelberg: Berlin, Heidelberg, 2013; pp. 58-72 ISBN 978-3-642-34635-4.
153. GelRed® & GelGreen® - DNA Stains | EtBr Alternatives | Biotium, Inc. *Biotium*.